



GUIDANCE NOTES
GD 09-2013

CHINA CLASSIFICATION SOCIETY

**GUIDELINES FOR FATIGUE STRENGTH
ASSESSMENT OF OFFSHORE
ENGINEERING STRUCTURES**

2013

Effective from October 1 2013

Beijing

CONTENTS

CHAPTER 1	GENERAL.....	1
Section 1	General.....	1
Section 2	Definitions.....	1
Section 3	S-N Curve Approach.....	4
Section 4	Fracture Mechanics Method.....	4
Section 5	Structural Detail Types.....	4
CHAPTER 2	FATIGUE ANALYSIS BASED ON S-N CURVES.....	5
Section 1	General.....	5
Section 2	Cumulative Fatigue Damage.....	6
Section 3	Fatigue Analysis Method Based on Nominal Stress.....	7
Section 4	Fatigue Analysis Method Based on Hot Spot Stress.....	10
Section 5	S-N Curves.....	11
CHAPTER 3	STRESS CONCENTRATION FACTORS AND HOT SPOT STRESS CALCULATION.....	20
Section 1	General.....	20
Section 2	Stress Concentration Factors for Plated Structures.....	20
Section 3	Stress Concentration Factors for Tubular Butt Weld Connections.....	24
Section 4	Stress Concentration Factors for Ship Structure.....	29
Section 5	Stress Concentration Factors for Tubular Joints.....	29
Section 6	Direct Calculation of Hot Spot Stress.....	33
CHAPTER 4	SAFETY FACTOR OF FATIGUE.....	39
Section 1	General Provisions.....	39
CHAPTER 5	SIMPLIFIED FATIGUE ANALYSIS METHOD.....	41
Section 1	General Provisions.....	41
Section 2	Mathematical Development.....	41
Section 3	Application of Simplified Fatigue Method to Jacket Type Fixed Offshore Installations.....	44
CHAPTER 6	SPECTRAL-BASED FATIGUE ANALYSIS METHOD.....	46
Section 1	General Provisions.....	46
Section 2	Spectral-based Fatigue Analysis for Offshore Engineering Structures.....	47
Section 3	Combined Method of Low-frequency and Wave-frequency Fatigue Damage.....	51

Section 4	Fatigue Damage due to Loading and Offloading of Produced Fluids.....	52
Section 5	Time-Domain Analysis Fatigue Assessment Methods.....	53
CHAPTER 7	FATIGUE ANALYSIS METHOD BASED ON FRACTURE MECHANICS.....	55
Section 1	General.....	55
Section 2	Crack Growth Model.....	55
Section 3	Crack Growth Life Prediction.....	56
Section 4	Possible Failure Modes of Fatigue Assessment Based on Fracture Mechanics.....	57
Section 5	Determination of Geometry Function.....	57
CHAPTER 8	IMPROVEMENT METHODS OF FATIGUE LIFE.....	58
Section 1	General.....	58
Section 2	Weld Profiling.....	58
Section 3	Weld Toe Grinding.....	59
Section 4	Tungsten Inert Gas (TIG) Dressing.....	60
Section 5	Hammer Peening.....	60
CHAPTER 9	EXTENDED FATIGUE LIFE.....	62
Section 1	General.....	62
APPENDIX 1	STRUCTURAL DETAIL CLASSIFICATION CORRESPONDING TO S-N CURVE FATIGUE ASSESSMENT.....	63
Section 1	Structural Detail Classification Used in This Appendix.....	63
APPENDIX 2	PARAMETRIC FORMULAE OF STRESS CONCENTRATION FACTORS OF TUBULAR JOINTS.....	72
Section 1	General.....	72
Section 2	Simple Tubular Joints.....	72
Section 3	Multi Planar Tubular Joints.....	73
Section 4	Overlapped Tubular Joints.....	73
Section 5	Stiffened Tubular Joints.....	73
Section 6	Efthymiou Equations and Validity Ranges.....	73
APPENDIX 3	STRESS CONCENTRATION FACTORS FOR PENETRATIONS WITH REINFORCEMENTS.....	79
Section 1	Stress Concentration Factors for Circular Penetrations with Reinforcements.....	79

CHAPTER 1 GENERAL

Section 1 General

1.1.1 The Guidelines are applicable to welded steel offshore engineering structures, e.g. jacket units, mobile units, offshore floating production units, etc.

1.1.2 The fatigue strength assessment of offshore engineering structures of special types and using novel structural types is to be specially considered and subject to agreement of CCS.

1.1.3 With regard to the S-N curves of welded and casted tubular joints of the Guidelines, the curves given in American Petroleum Institute (API) RP 2A-WSD 2007 edition are used. The curves apply to steels of less than 500 N/mm² in minimum yield strength.

1.1.4 With regard to the S-N curves of non-tubular details of the Guidelines, 8 curves given in IACS Common Structural Rules for Double Hull Oil Tankers (CSR-OT) are used. The curves apply to steel welded connection of less than 400 N/mm² in minimum yield strength.

1.1.5 Where the yield strength of steel exceeds that specified in 1.1.3 and 1.1.4 of this Section, the S-N curves of such material may be obtained in accordance with the relevant requirements of 2.5.11, Chapter 2 of the Guidelines or the S-N curves given in 1.1.3 and 1.1.4 of this Section may be used as a reference.

1.1.6 Designers and Analysts are advised that a cognizant Regulatory Authority for the offshore engineering structure may have required technical criteria that could be different from those in the Guidelines. CCS will consider the use of such alternative criteria as a basis of classification where it is shown that the use of the alternative criteria produces a level of safety that is not less than that produced by the criteria in the Guidelines.

Section 2 Definitions

1.2.1 Classified structural detail

A structural detail containing a structural discontinuity including a weld or welds, for which the nominal stress approach is applicable to fatigue life calculation, and which appear in the tables of Appendix 1 of the Guidelines, also referred to as standard structural detail.

1.2.2 Fatigue damage ratio

Ratio of number of cycles of fatigue alternating stress under consideration and corresponding number of cycles to failure (fatigue life) at constant amplitude loading of such stress level.

1.2.3 Fatigue life

Number of stress cycles at an alternating stress of particular magnitude required to cause fatigue failure of the structural detail. For practical purpose of offshore engineering, generally the fatigue life is calculated in years. Under the assumption of Miner cumulative damage and the assumption that the same damage is caused by environmental loads in each basic calculation time (generally one year), the basic time (in seconds) for fatigue damage calculation is divided by the maximum damage ratio of structure within such basic time, and then divided by 31,536,000 seconds (i.e. 365 days × 24 h/day × 3,600 seconds/h) in order to obtain the fatigue life.

1.2.4 Fatigue strength

Magnitude of alternating stress range leading to particular fatigue life.

1.2.5 Fatigue resistance

Structural detail's resistance against fatigue actions in terms of S-N curve or crack propagation properties.

1.2.6 Safety factor of fatigue

A safety factor used for fatigue life in design (≥ 1.0) that is applied to individual structural details which accounts for the influence of some important elements, e.g. the consequences of failure (i.e. criticality), and the relative difficulty of survey and repair.

1.2.7 Nominal stress

Stress calculated in a structure, only taking into account the macro-geometric effect, but disregarding the stress concentration due to the structural detail's discontinuity and welds (see Figures 2.1.5, 2.3.1(1) and (2)). The nominal stress may either be obtained by using classical theories such as beam theory, or by FEM such as coarse mesh or fine mesh.

1.2.8 Structural discontinuity

A geometric discontinuity due to the type of welded joint, usually found in tables of classified structural details. The effects of a structural discontinuity are (i) concentration of the membrane stress and (ii) formation of secondary bending stress.

1.2.9 Structural stress

A stress in a component, resolved taking into account the effects of a structural discontinuity, and consisting of membrane and shell bending stress components, also referred to as geometric stress (see Figure 2.1.5).

1.2.10 Hot spot

The spot where a fatigue crack is likely to initiate in a structure under the alternating stress. The hot spot may be located at weld toe, fillet weld or weld root of partial penetration weld or the free edge of plates/sections.

1.2.11 Hot spot stress

The value of structural stress on the surface at the hot spot (also known as geometric stress or structural stress). The hot spot stress includes all stress raising effects of discontinuity or existing attachment in a structural detail excluding the non-linear peak stress caused by the local notch, i.e. the weld toe (see Figures 3.6.4(1) and 2.4.1). The hot spot stress may either be obtained by means of multiplying the nominal stress by the hot spot stress concentration factor (SCF), or by means of refined FE analysis.

1.2.12 Hot spot stress concentration factor

The ratio of hot spot stress to nominal stress. Such nominal stress includes stress raising due to macro-geometric effects. In the Guidelines it is referred to as "stress concentration factor" (SCF) where no confusion is caused.

1.2.13 Notch stress

Total stress at the root of a notch taking into account the stress concentration caused by the local notch. Thus the notch stress consists of the sum of structural stress and non-linear stress peak (see Figure 2.1.5).

1.2.14 Notch stress concentration factor

The ratio of notch stress to structural stress.

1.2.15 Effective notch stress

Notch stress calculated for a notch with a certain effective notch radius.

1.2.16 S-N curve

Graphical presentation of the dependence of fatigue life (N) on fatigue stress range (S).

1.2.17 Stress cycle

A part of a stress history containing a stress maximum and a stress minimum.

1.2.18 Stress range

The difference between stress maximum and stress minimum in a stress cycle.

1.2.19 Rainflow counting

A standardised procedure for stress range counting.

1.2.20 Nonlinear stress peak

The stress component of a notch stress which exceeds the linearly distributed structural stress at a local notch.

1.2.21 Eccentricity

Misalignment of plates at welded connections measured transverse to the plates.

1.2.22 Misalignment

Axial and angular misalignments caused either by detail design or by fabrication.

1.2.23 Fracture mechanics

A branch of mechanics dealing with the behaviour and strength of components or details containing cracks.

1.2.24 Stress intensity factor

Factor used in fracture mechanics to characterise the stress at the vicinity of a crack tip.

1.2.25 Paris' law

An experimentally determined relation between crack growth rate and stress intensity factor range.

Section 3 S-N Curve Approach

1.3.1 In the S-N curve approach the fatigue strength of commonly occurring (generic) structural details is presented as a curve or equation. The horizontal coordinate of the curve is in general the life or number of cycles (N) and the longitudinal coordinate is stress range (S). Each data pair (N_i, S_i) represents the life or number of cycles (N_i) of a constant stress range (S_i) that will cause fatigue failure for such structural detail.

1.3.2 The data used to construct published S-N curves are assembled from collections of experimental data. The S-N curves used in the Guidelines are based on the mean-minus-two-standard-deviation curves for relevant experimental data. The S-N curves are thus associated with a 97.6% probability of survival.

1.3.3 The user is to ensure that the stresses are calculated in agreement with the definition of the stresses to be used together with a particular S-N curve. At present the following two S-N curves of different concepts are commonly used in offshore engineering:

- nominal stress S-N curve;
- hot spot stress S-N curve.

1.3.4 Based on the difference between specific calculation process of stress and life, three methods are in general called the simplified fatigue analysis method, deterministic fatigue analysis method and spectral-based fatigue analysis method.

Section 4 Fracture Mechanics Method

1.4.1 Fracture mechanics establishes quantitative relationships between mechanical property of material, geometric size of details and cracks, and the load applied to details, while recognizing that cracks/defects exist on the surface or in the interior of structural members (especially welds), in order to draw a conclusion on the fracture resistant capability of details based on fracture mechanics test data of small specimen.

1.4.2 In view of the wide application and dominant position of S-N curve approach in the offshore engineering, the fracture mechanics method is generally used as a supplementary and supporting method of fatigue strength calculation, especially in cases where cracks are identified in structures in service.

1.4.3 Fracture mechanics method is of great engineering significance for evaluating crack growth and to revise and refine inspection programs.

Section 5 Structural Detail Types

1.5.1 In general the fatigue strength assessment of offshore engineering structures are based on two major categories of structural details. These are referred to as Tubular Joints and Non-Tubular Details; the latter (also referred to as Plate Details or Plate Connections) includes welded and non-welded connection details, see classification of common non-tubular details in Appendix 1. The calculation of fatigue strength of offshore engineering is mainly carried out for steel tubular and non-tubular details.

CHAPTER 2 FATIGUE ANALYSIS BASED ON S-N CURVES

Section 1 General

2.1.1 The main principles for fatigue analysis based on S-N curves are described in this Chapter.

2.1.2 Suitable curve is to be selected for fatigue analysis based on S-N curves according to the scope of application of each curve.

2.1.3 The fatigue analysis of plated structures may be based on nominal S-N curves, see S-N curves of non-tubular details in Section 5 of this Chapter.

2.1.4 The nominal stress approach and hot spot stress approach are mainly used in this Chapter. Fatigue analysis using notch stress approach will be specially considered by CCS.

2.1.5 Corresponding stress value is to be obtained by means of different calculation methods of fatigue life, see Table 2.1.5 and Figures 2.1.5 and 3.6.4(1).

**Stress Concentration Factor, Stress Range and
Corresponding Calculation Method of Fatigue Life**

Table 2.1.5

Type	Stress concentration factor	Stress range	Calculation method of fatigue life
A	Stress obtained by analysis using classical theory, e.g. beam theory, not considering stress concentration	Range of general nominal stress	Not applicable for fatigue analysis of welded joints
B	A + stress concentration due to macro-geometrical effects, but disregarding the stress concentration due to the structural discontinuity and welds	Range of modified nominal stress	Fatigue analysis method based on nominal stress
C	A + B + stress concentration due to the structural discontinuity, but disregarding the stress concentration due to the weld notch	Range of hot spot stress	Fatigue analysis method based on hot spot stress
D	A + B + C + stress concentration due to the weld notch a) actual notch stress b) effective notch stress	Range of notch stress	a) Fracture mechanics method b) Fatigue analysis method based on effective notch stress

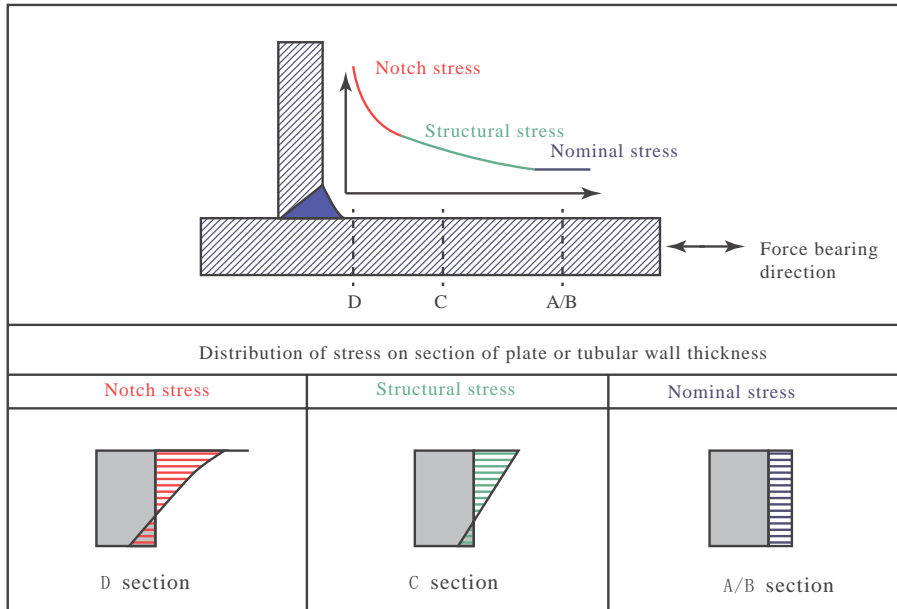


Figure 2.1.5 Stress Distribution of Weld Toe Area

Section 2 Cumulative Fatigue Damage

2.2.1 The cumulative fatigue damage is calculated under the assumption of linear cumulative damage (Palmgren-Miner rule). Such rule assumes that under any given stress level, the speed of cumulative damage is irrelevant to previous load history and the sequence of loading does not affect the calculated fatigue life.

2.2.2 When the long-term stress range distribution is expressed by a stress histogram, consisting of a constant stress range S_i and number of stress cycles n_i for each block, the fatigue criterion reads:

$$D = \sum_{i=1}^k \frac{n_i}{N_i} \leq \frac{1}{S_{fg}} \quad (2.1)$$

where: D — cumulative fatigue damage;

k — number of stress blocks;

n_i — number of stress cycles in stress block i ;

N_i — number of cycles to failure at constant stress range S_i ;

S_{fg} — safety factor of fatigue, see Section 1 of Chapter 4.

2.2.3 Applying a histogram to express the stress distribution, the number of stress blocks, k , is to be large enough to ensure reasonable numerical accuracy, and is not to be less than 20. In addition, the blocks are to be distributed in a reasonable way, i.e. they are to be densely distributed in way of peak value of stress distribution and may be appropriately sparse in other areas of low stress value.

2.2.4 For the calculation of fatigue life of offshore engineering structures, as structures normally have multiple load cases and each case accounts for different time proportion during service life, the damage is to be calculated respectively for each considered load case. And then the total damage is obtained by the weighted summation of damages in each load case, according to the proportion of each case during the service life of the assessed structure:

$$D = \sum_{i=1}^m p_i D_i \quad (2.2)$$

where: D — total cumulative fatigue damage of a calculation point in the structure;

m — number of cases of fatigue damage calculation during the service life of the structure;

D_i — fatigue damage of a calculation point in the structure if the whole service life is case i only;

p_i — time proportion of case i during the service life.

2.2.5 For different purposes the structure is intended for during the service life, consideration is to be given to cumulative fatigue damage caused by those purposes. For example, where the offshore floating production unit is converted from an oil tanker, the fatigue damage caused by the ship as an oil tanker is to be considered for the assessment of residual fatigue life of the offshore floating production unit and attention is to be given to the following requirements:

- (1) When calculating the fatigue damage for past services, the wave conditions of specific routes the vessel has experienced in past service can be employed, instead of using the wave condition representing unrestricted service as may have been done for classification as a tanker.
- (2) When calculating the fatigue damage accumulated during the “trading tanker” phase, the effects of vessel speed is be included, i.e. using encounter frequency for the calculation of stress response amplitude operator (RAO) and number of stress cycles.

Section 3 Fatigue Analysis Method Based on Nominal Stress

2.3.1 Nominal stress for fatigue assessment is the stress calculated in the sectional area under consideration, which can be in general obtained by classical elastic theory. It disregards the stress concentration due to structural discontinuity and welds, but needs to take into account the stress concentration due to macro-geometric shape of the component in the vicinity of the point of fatigue assessment. Macro-geometric effects may cause a significant redistribution of the nominal stresses across the section, see Figure 2.3.1(1). Similar effects occur in the vicinity of concentrated loads or reaction forces, see Figure 2.3.1(2).

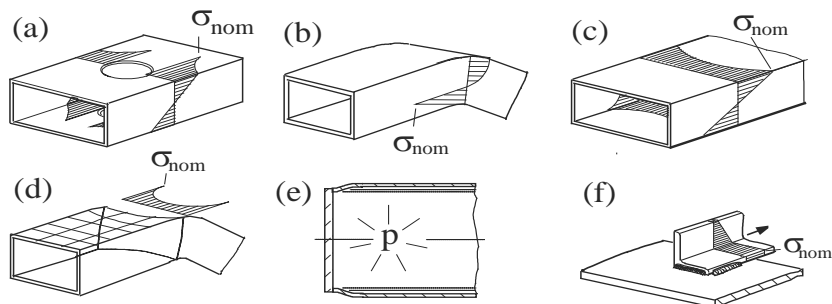


Figure 2.3.1(1) Examples of Change of Nominal Stress due to Macro-geometric Effects

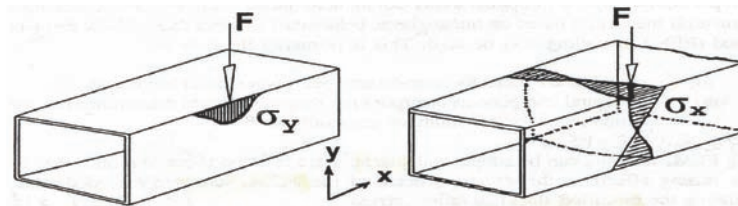


Figure 2.3.1(2) Change of Nominal Stress due to Concentrated Loads

2.3.2 Different nominal stress components may have different stress concentration factors as appropriate.

2.3.3 In general, the following two methods may be used to obtain the nominal stress used for the assessment of fatigue strength:

- (1) direct use of formulae or figures of stress concentration factors recognized by the industry, see Sections 2 to 4 of Chapter 3;
- (2) for structures with complicated geometric shape or bearing complicated stress, the stress concentration factor may be obtained by means of FE direct calculation methods. Generally it is obtained by applying unit stress, but attention is to be given to the following:
 - (1) The nominal stress only takes into account the effect the macro-geometric change has on the stress (e.g. change of opening, taper, camber, bracket, size etc.). Consideration is also to be given if the misalignment of the weld exceeds the amount which is inherent in the S-N curve.
 - (2) The S-N curve corresponding to certain structural detail generally has already reflected the stress concentration effects due to abrupt change of geometry, and as a result the stress due to such abrupt change of geometry is not considered, as it is inherent in the relevant S-N curve.
 - (3) The stress concentration due to weld shape is not to be considered, as it is already covered by the selected S-N curve.
 - (4) Where the actual stress field is more complicated than the uniaxial stress, the principal stress in way of where cracking is most likely to initiate is selected as local nominal stress. When the principal stress direction is different from that of the normal to the weld toe, it becomes conservative to use the S-N curve of such type of detail obtained from test for principal stress normal to the weld toe. As the angle between the principal stress direction and the normal to the weld, φ , is increased further, fatigue cracking may no longer initiate along the weld toe, but may initiate in the weld and grow normal to the principal stress direction as shown in Figure 2.3.3. This means that the notch at the weld toe no longer significantly influences the fatigue capacity and a higher S-N curve applies for this stress direction.
 - (5) When the FE mode is established, a uniform mesh is to be used with smooth transition and avoidance of abrupt changes in mesh size. Sometime it is not necessary and even not suitable to use finer mesh to obtain required local nominal stress.

- ⑥ When fatigue assessment is carried out to the area where the weld is subjected to transverse loads so that cracking may initiate at the weld throat (see joint W in Appendix 1), the nominal stress is to be the nominal shear stress passing the minimum cross section of weld throat.

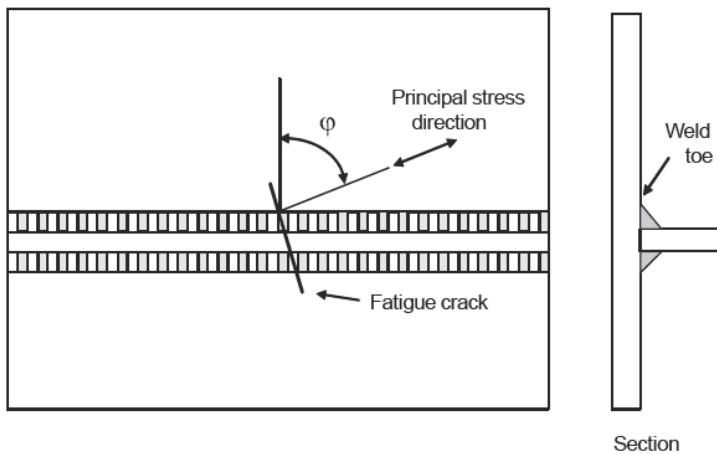


Figure 2.3.3 Fatigue Cracking When Principal Stress Direction is More Parallel with Weld Toe

2.3.4 In addition to nominal stress raising due to macro-geometric shape as specified in 2.3.1 above, where another small welding component exists in the local area subject to fatigue assessment, such small welding component will further raise the nominal stress, so as to increase the uncertainty of selection of S-N curves and calculation of local stress.

2.3.5 Classified structural details are generally given in Appendix 1. The details and corresponding S-N curves are obtained according to the nominal stress of test and thus include the effects of:

- (1) structural hot spot stress concentrations due to the structural discontinuity of the detail;
- (2) non-linear stress raising due to the geometric shape of weld;
- (3) weld imperfections consistent with normal fabrication standards;
- (4) stress direction;
- (5) welding residual stresses;
- (6) metallurgical conditions of weld zone and heat affected zone;
- (7) NDT, if applicable;
- (8) post-weld heat treatment, if specified in the table.

2.3.6 For more complicated situations or uncertainties, the hot spot stress approach of Section 4 of this Chapter is to be used. In that case, subparagraphs ② and ⑤ of 2.3.3(2) above do not apply. As structural discontinuity is no longer covered by the S-N curve corresponding to the hot spot stress approach, the stress concentration due to structural discontinuity is to be accurately obtained by means of structural analysis. In most cases, a refined FE model is needed (modeling by using refined mesh in the vicinity of hot spot, the element size of refined mesh area is to be approximately equal to plate thickness of assessment area, and the aspect ratio is to be close to 1.0).

Section 4 Fatigue Analysis Method Based on Hot Spot Stress

2.4.1 General

(1) Hot spot stress is the value of structural stress on the surface at the hot spot (also known as geometric stress or structural stress). The hot spot stress includes all stress raising effects of discontinuity or existing attachment in a structural detail excluding the non-linear peak stress caused by the local notch, i.e. the weld toe.

(2) For welded joints, the hot spot is generally located at weld toe, see Figure 2.4.1.

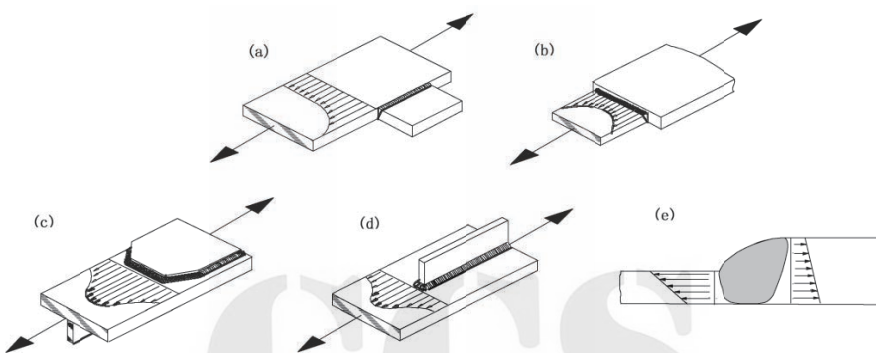


Figure 2.4.1 Hot Spot Stress of Non-tubular Details

(3) The hot spot stress approach may be considered where the geometric type and stress of a structural detail are difficult to be classified according to the existing structural detail in Appendix 1.

2.4.2 Tubular joints

(1) The hot spot stress approach and its associated S-N curves are generally used for the fatigue analysis of tubular joints.

(2) The positions of hot spot stress of tubular joints during fatigue analysis are in way of several weld toes on the side of chords and braces around the circumference of the weld of tubular joints.

(3) The hot spot stress may be obtained based on appropriate and detailed FE analysis which has been verified. For non-strengthened simple tubular joints, the hot spot stress may be obtained by means of multiplying tubular nominal stress by its hot spot stress concentration factor (SCF). It is recommended to calculate such SCF according to Efthymiou hot spot SCF equation, see Appendix 2.

2.4.3 Non-tubular details

(1) For plated structures with complicated structure or bearing complicated stress where it is difficult to carry out fatigue analysis based on nominal stress according to Appendix 1, it is recommended to use the hot spot stress approach and its associated S-N curves.

(2) For welded structure, the hot spot is generally located at weld toe. The hot spot stress may be obtained by various methods but in generally it is obtained based on appropriate and detailed FE analysis which has been verified.

(3) As many factors in the FE analysis of local refined mesh will cause stress result fluctuations and such stress result is very sensitive to fatigue analysis result, it is recommended to follow the FE analysis principles in Section 6, Chapter 3 of the Guidelines when FE method is used to calculate the hot spot stress.

2.4.4 Selection of S-N curves in hot spot stress approach

(1) For non-tubular details where the hot spot stress approach is used for fatigue assessment, unless otherwise provided by the Guidelines, curve D in Section 5 of this Chapter is to be used to carry out fatigue calculation for welded joints and curve C is to be used for those other than welded joints.

(2) For casted or welded tubular joints where the hot spot stress approach is used for fatigue assessment, the S-N curves of tubular joints in Section 5 of this Chapter may be used.

Section 5 S-N Curves

2.5.1 The S-N curves used in the Guidelines are based on the mean-minus-two-standard-deviation curves for relevant experimental data. The S-N curves are thus associated with a 97.6% probability of survival.

2.5.2 Failure criterion inherent in the S-N curves

(1) For structural details with the same calculated damage, the initiation period of a fatigue crack takes longer time for a notch in base material than at a weld toe or weld throat. This also means that with a higher fatigue resistance of the base material as compared with welded details, the crack growth will be faster in base material when fatigue cracks are growing.

(2) For practical purpose of offshore engineering, one defines these failures as being crack growth through the thickness. When this failure criterion is transferred into a crack size in a real structure where some redistribution of stress is more likely, this means that this failure criterion corresponds to a crack size that is somewhat less than the plate thickness.

(3) The tests with tubular joints are normally of a larger size. These joints also show larger possibility for redistribution of stresses as a crack is growing. Thus a crack can grow through the thickness and also along a part of the joint before a fracture occur during the testing. The number of cycles at a crack size through the thickness is used when the S-N curves are derived. As these tests are not very different from that of the actual behaviour in a structure, this failure criterion for S-N curves for tubular joints corresponds approximately to the number of cycles at a crack size through the thickness at the hot spot (chord or brace as relevant).

2.5.3 S-N curves and structural detail classification

(1) Structural details are divided into several classes, each with a corresponding design S-N curve according to the geometry of the structural detail and other considerations such as the direction of loading and expected fabrication/ inspection methods.

(2) S-N curves for non-tubular details are composed of Curves B, C, D, E, F, F2, G and W and each curve shows a kind of relationship of structural details bearing alternating stress range values S and the number of stress cycles N.

(3) In any welded joint, there are several locations at which fatigue cracks may develop, e. g. at the weld toe in each of the parts joined, at the weld ends, and in the weld itself. Each location is to be classified separately.

(4) All tubular joints are assumed to be class CJ or WJ, which is taken from the Recommended Practice for Planning, Designing and Constructing Fixed Offshore Platforms—Working Stress Design (API RP 2A-WSD) 2007 edition.

(5) The design S-N curves generally consist of one or two segments in the double logarithmic coordinate, see Figure 2.5.3. For S-N curves consisting of two segments, when the number of cycles to failure N is less than or equal to N_q , the relationship between number of cycles to failure N and stress range S may be expressed as follows:

$$\log(N) = \log(K_i) - m_i \log(S) \quad (2.3)$$

When the number of cycles to failure N is greater than N_q , the relationship between number of cycles to failure N and stress range S may be expressed as follows:

$$\log(N) = \log(K_2) - m_2 \log(S) \quad (2.4)$$

where: N — predicted number of cycles to failure for stress range S ;

S — stress range;

m_i — negative inverse slope of S-N curve ($i = 1, 2$), generally referred to as the slope of S-N curve where no confusion is caused;

$\log(K_i)$ — intercept of $\log N$ axis by S-N curve ($i=1, 2$), $\log(K_i) = \log(\bar{K}) - 2\sigma_{\log N}$;

$\log(\bar{K})$ — intercept of mean S-N curve with the $\log N$ axis corresponding to each segment;

$\sigma_{\log N}$ — standard deviation of $\log N$.

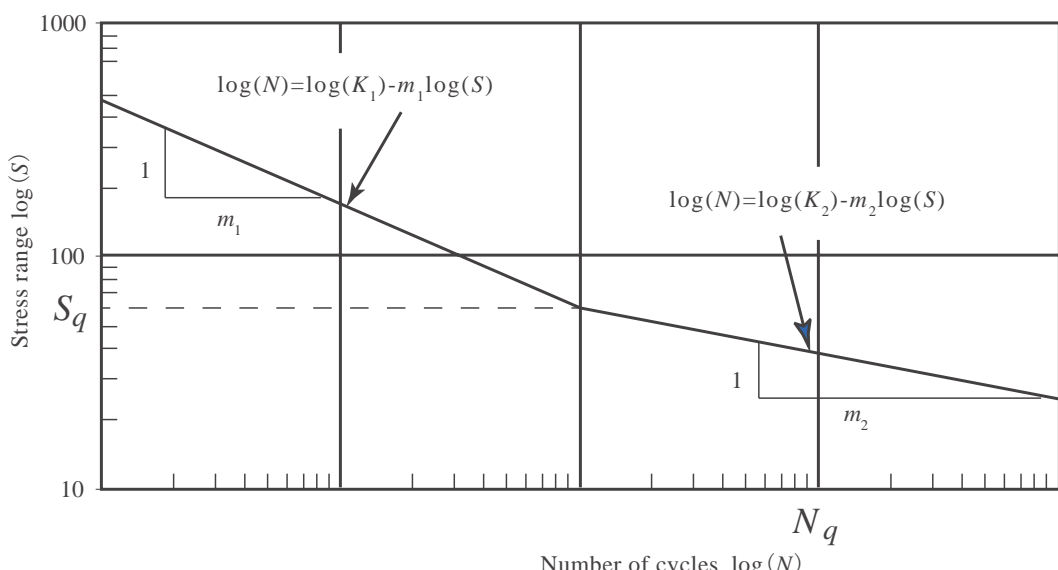


Figure 2.5.3 Two-segment S-N Curves

2.5.4 Design S-N curves for non-tubular details in air

Design S-N curves for non-tubular details in air are given in Figure 2.5.4 and Table 2.5.4. The two segments may be expressed as follows:

$$\begin{aligned}\log(N) &= \log(K_1) - m_1 \log(S) \\ \log(N) &= \log(K_2) - m_2 \log(S)\end{aligned}\quad (2.5)$$

where: K_1, K_2 — constant before and after $N = 10^7$ respectively, see Table 2.5.4;
 m_1, m_2 — slope of S-N curve before and after $N = 10^7$ respectively, see Table 2.5.4;
 N, S — see 2.5.3.

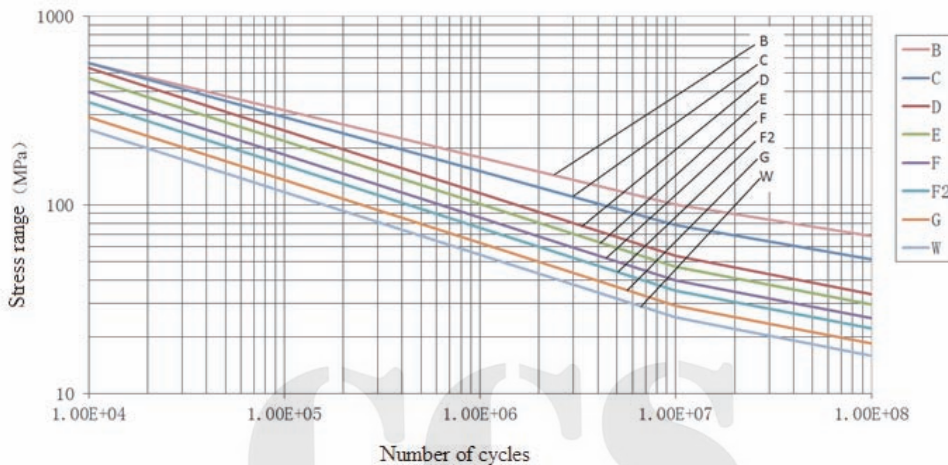


Figure 2.5.4 Design S-N Curves for Non-tubular Details in Air

Design S-N Curves for Non-tubular Details in Air

Table 2.5.4

Class	K_1	K_2	m_1	m_2	N_q	S_q (MPa)
B	1.01×10^{15}	1.02×10^{19}	4.0	6.0	1.0×10^7	100.2
C	4.23×10^{13}	2.59×10^{17}	3.5	5.5	1.0×10^7	78.2
D	1.52×10^{12}	4.33×10^{15}	3.0	5.0	1.0×10^7	53.4
E	1.04×10^{12}	2.30×10^{15}	3.0	5.0	1.0×10^7	47.0
F	6.30×10^{11}	9.97×10^{14}	3.0	5.0	1.0×10^7	39.8
F ₂	4.30×10^{11}	5.28×10^{14}	3.0	5.0	1.0×10^7	35.0
G	2.50×10^{11}	2.14×10^{14}	3.0	5.0	1.0×10^7	29.2
W	1.60×10^{11}	1.02×10^{14}	3.0	5.0	1.0×10^7	25.2

2.5.5 Design S-N curves for non-tubular details in seawater with effective cathodic protection

Design S-N curves for non-tubular details in seawater with effective cathodic protection are given in Figure 2.5.5 and Table 2.5.5. As compared to design S-N curves in air, the fatigue life in low cycle segment is reduced to 40% of fatigue life in air. The number of cycles N corresponding to stress range S is 2/5 of that in air and N_q is moved from 10^7 in air to around 10^6 . The high cycle segment of fatigue life remains unchanged.

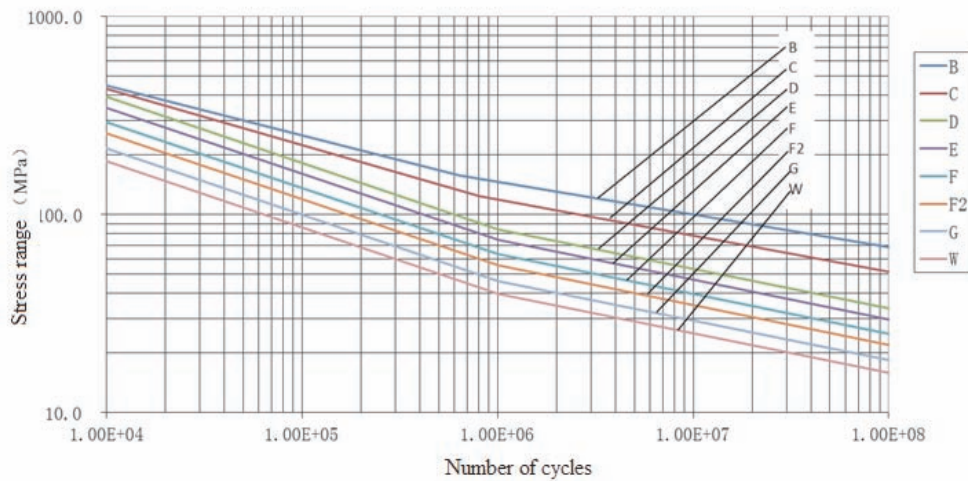


Figure 2.5.5 Design S-N Curves for Non-tubular details in Seawater with Effective Cathodic Protection

Design S-N Curves for Non-tubular Details in Seawater with Effective Cathodic Protection

Table 2.5.5

Class	K_1	K_2	m_1	m_2	N_q	S_q (MPa)
B	4.04×10^{14}	1.02×10^{19}	4.0	6.0	6.4×10^5	158.5
C	1.69×10^{13}	2.59×10^{17}	3.5	5.5	8.1×10^5	123.7
D	6.08×10^{11}	4.33×10^{15}	3.0	5.0	1.01×10^6	84.4
E	4.16×10^{11}	2.30×10^{15}	3.0	5.0	1.01×10^6	74.4
F	2.52×10^{11}	9.97×10^{14}	3.0	5.0	1.01×10^6	62.9
F ₂	1.72×10^{11}	5.28×10^{14}	3.0	5.0	1.01×10^6	55.4
G	1.00×10^{11}	2.14×10^{14}	3.0	5.0	1.01×10^6	46.2
W	6.40×10^{10}	1.02×10^{14}	3.0	5.0	1.01×10^6	39.8

2.5.6 Design S-N curves for non-tubular details in seawater for free corrosion

Design S-N curves for non-tubular details in seawater for free corrosion are given in Figure 2.5.6 and Table 2.5.6. As compared to design S-N curves in air, the fatigue life in low cycle segment is reduced to 33.33% of fatigue life in air. The number of cycles N corresponding to stress range S is 1/3 of that in air, and the low cycle segment is directly extended to the high cycle segment.

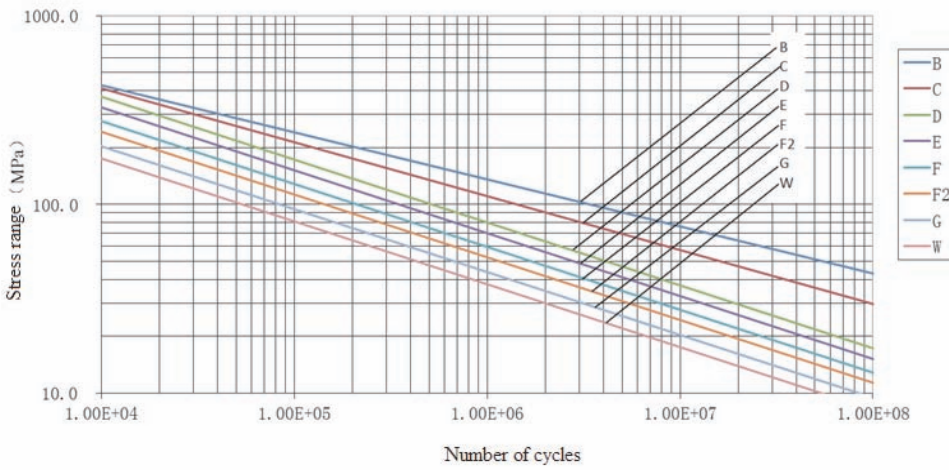


Figure 2.5.6 Design S-N Curves for Non-tubular Details in Seawater for Free Corrosion

Design S-N Curves for Non-tubular Details in Seawater for Free Corrosion Table 2.5.6

Class	K	m
B	3.37×10^{14}	4.0
C	1.41×10^{13}	3.5
D	5.07×10^{11}	3.0
E	3.47×10^{11}	3.0
F	2.10×10^{11}	3.0
F ₂	1.43×10^{11}	3.0
G	8.33×10^{10}	3.0
W	5.33×10^{10}	3.0

2.5.7 Classified structural detail

For the calculation of fatigue strength of structural details, suitable S-N curves are to be selected in accordance with the general principles and type of structural details given in Appendix 1, force-bearing direction and construction techniques.

2.5.8 S-N curves for tubular joints

(1) Design S-N curves for tubular joints in air

Design S-N curves for tubular joints in air are given in Figure 2.5.8(1). Parameter selection is given in Table 2.5.8(1).

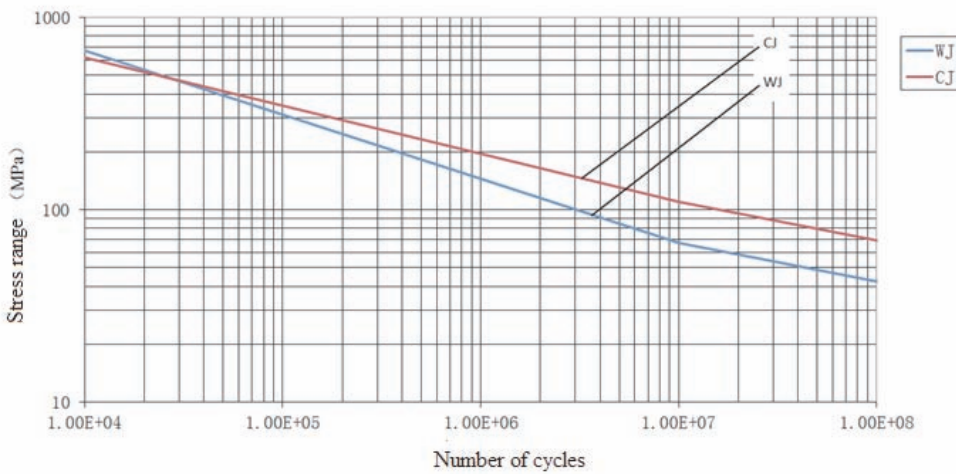


Figure 2.5.8(1) Design S-N Curves for Tubular Joints in Air

Design S-N Curves for Tubular Joints in Air

Table 2.5.8(1)

Class	K_1	$\log(K_1)$	K_2	$\log(K_2)$	m_1	m_2	N_q	S_q (MPa)
WJ	3.02×10^{12}	12.48	1.36×10^{16}	16.13	3.0	5.0	1.0×10^7	67.1
CJ	1.48×10^{15}	15.17	1.62×10^{17}	17.21	4.0	5.0	1.0×10^7	110.3

Note: WJ means welded joint and CJ means casted joint.

(2) Design S-N curves for tubular joints in seawater with cathodic protection

Design S-N curves for tubular joints in seawater with cathodic protection are given in Figure 2.5.8(2) and Table 2.5.8(2). As compared to S-N curves in air, the fatigue life in low cycle segment is reduced to 50% of fatigue life in air. The number of cycles N corresponding to stress range S is 1/2 of that in air and N_q is moved from 10^7 in air to around 10^6 . The high cycle segment of fatigue life remains unchanged.

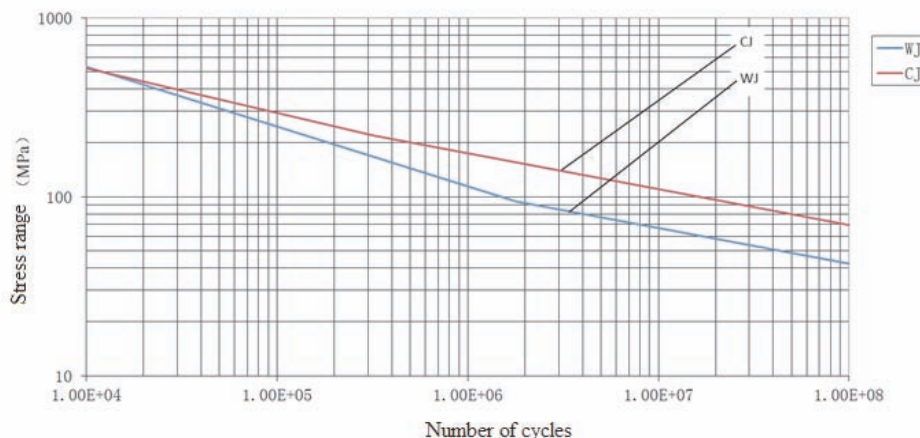


Figure 2.5.8(2) Design S-N Curves for Tubular Joints in Seawater with Effective Cathodic Protection

Design S-N Curves for Tubular Joints in Seawater with Effective Cathodic Protection

Table 2.5.8(2)

Class	K_1	$\log(K_1)$	K_2	$\log(K_2)$	m_1	m_2	N_q	S_q (MPa)
WJ	1.51×10^{12}	12.18	1.36×10^{16}	16.13	3.0	5.0	1.78×10^6	94.52
CJ	7.39×10^{14}	14.87	1.62×10^{17}	17.21	4.0	5.0	3.20×10^5	219.30

Note: WJ means welded joint and CJ means casted joint.

(3) Design S-N curves for tubular joints in seawater for free corrosion

Design S-N curves for tubular joints in seawater for free corrosion are given in Figure 2.5.8(3) and Table 2.5.8(3). As compared to S-N curves in air, the fatigue life in low cycle segment is reduced to 33.33% of fatigue life in air. The number of cycles N corresponding to stress range S is 1/3 of that in air, and the low cycle segment is directly extended to the high cycle segment.

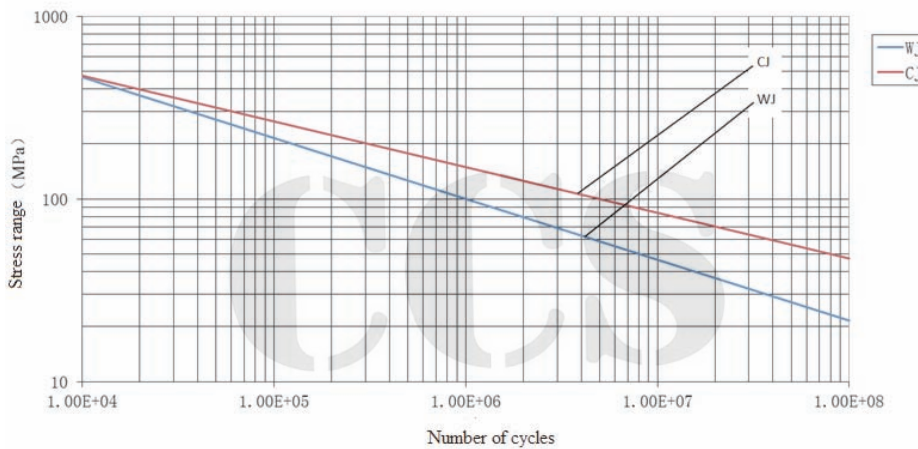


Figure 2.5.8(3) Design S-N Curves for Tubular Joints in Seawater for Free Corrosion

Design S-N Curves for Tubular Joints in Seawater for Free Corrosion Table 2.5.8(3)

Class	K	m
WJ	1.01×10^{12}	3.0
CJ	4.93×10^{14}	4.0

Note: WJ means welded joint and CJ means casted joint.

2.5.9 Thickness correction

The fatigue performance of structural detail is dependent on thickness of structural member. For the same stress range, as the thickness of structural member is increased, the fatigue resistant performance of joint is reduced. The thickness effect is accounted for by a modification on stress such that the design S-N curve for thickness larger than the reference thickness reads:

$$\log(N) = \log(K) - m \log \left(S \left(\frac{t}{t_{ref}} \right)^r \right) \quad (2.6)$$

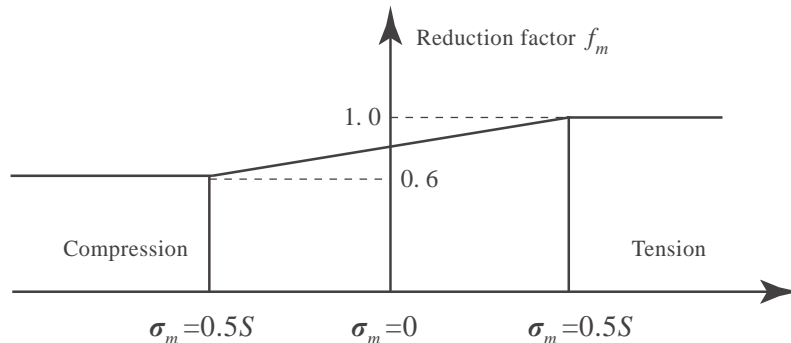
where: m — negative inverse slope of S-N curve;
 $\log(K)$ — intercept of $\log N$ axis by S-N curve;
 t_{ref} — reference thickness, to be taken as 22 mm for S-N curves of non-tubular details in 2.5.4 to 2.5.7, 16 mm for S-N curves of welded tubular joints in 2.5.8 and 38 mm for S-N curves of casted tubular joints in 2.5.8;
 t — thickness through which a crack will most likely grow. $t = t_{ref}$ is used for thickness less than t_{ref} ;
 r — thickness correction exponent, to be taken as 0.25 for non-tubular details or welded tubular joints not applying fatigue strength enhancement technique, 0.2 for welded tubular joints with satisfactory profile control which are approved by CCS, 0.15 for welded tubular joints applying grinding or hammer peening technique which are approved by CCS and 0.15 for casted tubular joints.

2.5.10 Mean stress influence for non-welded structures

For fatigue analysis of regions in the base material (corners of cut-outs in the base material) not significantly affected by residual stresses due to welding, the stress range may be reduced appropriately if part of the stress cycle is in compression.

$$f_m = \begin{cases} 0.6 & \text{when } \sigma_t \leq 0 \\ \frac{\sigma_t - 0.6\sigma_c}{\sigma_t - \sigma_c} & \text{when } \sigma_t > 0 \text{ and when } \sigma_c < 0 \\ 1.0 & \text{when } \sigma_c \geq 0 \end{cases} \quad (2.7)$$

where: σ_t — maximum stress value of stress cycle, negative for compression stress;
 σ_c — minimum stress value of stress cycle, negative for compression stress;



$$\sigma_m = 0.5(\sigma_t + \sigma_c); S \text{ is stress range}$$

Figure 2.5.10 Reduction Factor of Mean Stress to Stress Range in Fatigue Life Calculation

2.5.11 Qualification of new S-N curves based on fatigue test data

- (1) For qualification of new S-N curves to be used in a project it is important that the test specimens are representative for the actual fabrication and construction. This includes possibility for relevant production defects as well as fabrication tolerances. The sensitivity to defects may also be assessed by fracture mechanics.

(2) For new types of connections it is recommended to perform testing of at least 15 specimens in order to establish a new S-N curve. At least three different stress ranges are to be selected in the relevant S-N region such that a representative slope of the S-N curve can be determined. It is recommended to follow the mature methods used by existing S-N curves on how to derive S-N curves from few fatigue test data. Reference is made to IIW document No.IIW-XIII-WG1-114-03 (Best Practice Guide on Statistical Analysis of Fatigue Data).

(3) Normally fatigue test data are derived for number of cycles less than 10^7 . Thus it is important as to how to extrapolate the fatigue test data into the high cycle region of $N \geq 10^7$ cycles based on test data and engineering experience. High cycle fatigue test is to be added as necessary in order to verify the extrapolation results of the high cycle region.

(4) It is well known that good details where fatigue initiation contribute significantly to the fatigue life show a more horizontal S-N curve than for less good details where the fatigue life consists mainly of crack growth.

(5) The residual stresses at weld toes of small scale test specimens are normally small as compared with that actual full size structures due to different restraints during fabrication. This is an item that is of importance when planning fatigue testing and for assessment of design S-N curves.

(6) It is also to be remembered that for $N \geq 10^7$ cycles there is additional uncertainty due to variable amplitude loading. This is an issue that is to be kept in mind if less conservative S-N curves than given in the Guidelines are aimed for by qualifying a new S-N curve.

(7) It is to be noted that the defects that normally can be detected in a steel structure by an acceptable probability are normally larger than that inherent in the test specimens.

CHAPTER 3 STRESS CONCENTRATION FACTORS AND HOT SPOT STRESS CALCULATION

Section 1 General

3.1.1 For practical purpose of ships and offshore engineering, the nominal stress approach may be generally used for the calculation of fatigue life with regard to butt welds, T joints and cruciform joints of plated structures and tubular butt welds.

3.1.2 For the calculation of fatigue life based on nominal stress S-N curves, additional stresses resulting from fabrication tolerances are to be considered when the fabrication tolerances exceed that inherent in the S-N curves, see Sections 2, 3 and 4 of this Chapter.

3.1.3 The hot spot stress approach may be considered where the geometric type and stress of a structural detail are difficult to be classified according to the existing structural detail. However, the hot spot stress approach is in general limited to the calculation of fatigue life of the weld toe. Such approach is applicable to cases a) ~ e) as shown in Figure 3.1.3. It is not applicable in cases where crack will grow from the weld root, i.e. cases f) ~ j) in Figure 3.1.3. In such case, analysis may be carried out by referring to relevant documents, e.g. Recommendations for Fatigue Design of Welded Joints and Components (IIW document XIII-1965-03 / XV-1127-03).

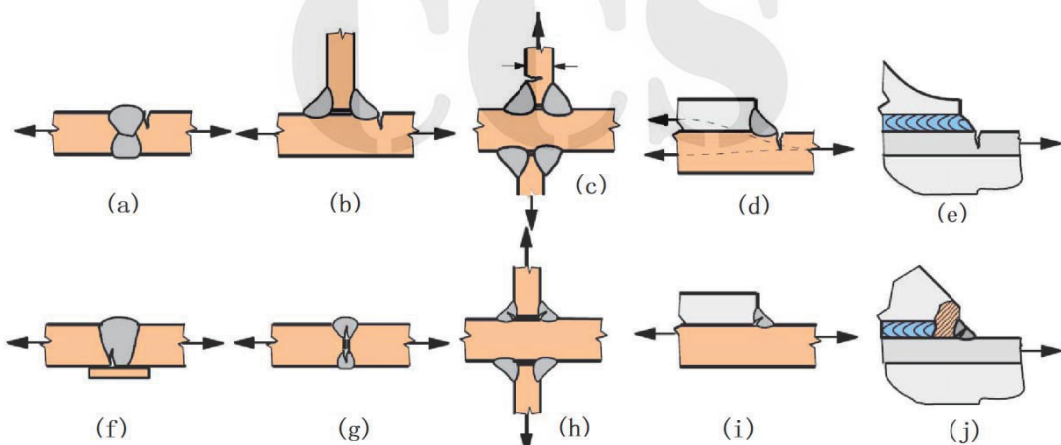


Figure 3.1.3 Various Locations of Crack Propagation in Welded Joints

Section 2 Stress Concentration Factors for Plated Structures

3.2.1 For the calculation of fatigue life of butt welds of plated structures by means of the nominal stress approach, when the fabrication tolerances exceed that inherent in the S-N curve, the nominal stress is to be multiplied by the corresponding stress concentration factor.

3.2.2 Stress concentration factors for butt welds

For plates with same thickness or for a pipe butt weld with a large radius, the stress concentration factor may be derived from the following formula:

$$SCF = 1 + \frac{3(\delta_m - \delta_0)}{t} \quad (3.1)$$

where: δ_m — maximum misalignment;
 δ_0 — $0.1t$ is eccentricity inherent in the S-N curve for butt welds;
 t — plate thickness.

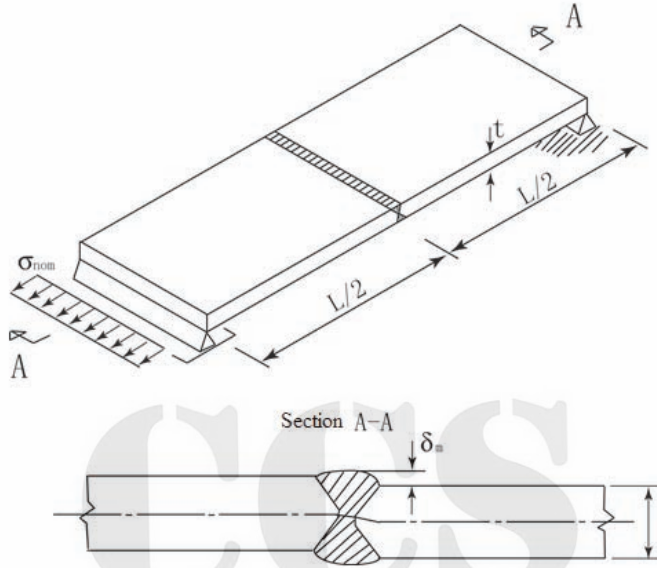


Figure 3.2.2 Eccentricity of Plates with Same Thickness

The stress concentration factor for the weld between plates with different thickness in a plate field may be derived from the following formula:

$$SCF = 1 + \frac{6(\delta_m + \delta_t - \delta_0)}{t \left[1 + \frac{T^{1.5}}{t^{1.5}} \right]} \quad (3.2)$$

where: δ_m — maximum misalignment;
 δ_t — $0.5(T-t)$ eccentricity due to change in thickness;
 δ_0 — $0.1t$ is eccentricity inherent in the S-N curve for butt welds;
 t — thickness of thinner plate;
 T — thickness of thicker plate.

3.2.3 Stress concentration factors for cruciform joints

For cruciform joint at plate thickness t_1, t_2, t_3 and t_4 , when the stress concentration factor of the weld on one side is calculated, it may be derived from following formula:

$$SCF_i = 1 + \frac{6t_i^2 (\delta_m + \delta_t - \delta_0)}{l_i \left[\frac{t_1^3}{l_1} + \frac{t_2^3}{l_2} + \frac{t_3^3}{l_3} + \frac{t_4^3}{l_4} \right]} \quad (3.3)$$

where: δ_m — maximum misalignment;
 δ_t — $0.5(t_1 - t_2)$ eccentricity due to change in thickness;
 δ_0 — $0.3 t_i$ eccentricity embedded in S-N curve for cruciform joints;
 t_i — thickness of the considered plate ($i = 1, 2$);
 l_i — length of the considered plate ($i = 1, 2$).

The other symbols are defined in Figure 3.2.3.

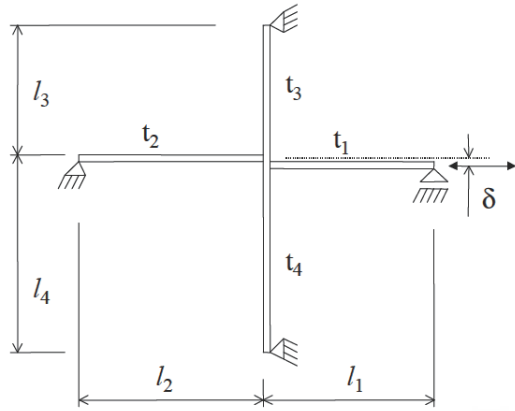


Figure 3.2.3 Parameters of Cruciform Joint

3.2.4 Stress concentration factors for rounded rectangular holes

Stress concentration factors for rounded rectangular holes are given in Figure 3.2.4, where a is the length of opening, b is the width of opening and r is the radius of corner of opening.

Stress concentration factors for elliptic opening corners may be determined by means of finite element calculations. Stress concentration factors for elliptic opening corners may be estimated by means of approximate calculation according to Figure 3.2.4, where radius r of the corner is the one of short axis of ellipse.

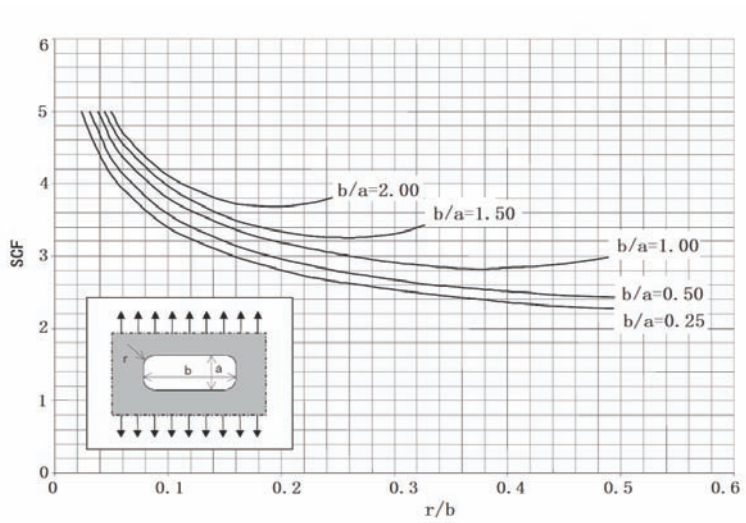


Figure 3.2.4 Stress Concentration Factors for Rounded Rectangular Holes

3.2.5 Stress concentration factors for holes with edge reinforcement

Stress concentration factors for holes with reinforcement are given in Appendix 3.

Fatigue cracking around a circumferential weld may occur at several locations at reinforced rings in plates depending on geometry of ring and weld size:

- ① for reinforced rings with smaller stiffness, fatigue cracking transverse to the weld toe in a region with a large stress concentration giving large stress parallel to the weld (equivalent to fatigue calculation of opening of parent material). See Figure 3.2.5(a). Then $S = \Delta\sigma_p$, where S is the stress range and σ_p is the tangential stress of hole circumference. The local stress obtained with SCF from Appendix 3 together with the C curve is to be used for the calculation of fatigue life;
- ② for reinforced rings with large stiffness and large weld size, fatigue cracking is likely parallel to the weld toe. See Figure 3.2.5(b):

for fatigue crack initiating from the weld toe, then $S = \Delta\sigma_i$, where σ_i is the principal stress and S is the stress range;

when the region at crown position is to be checked, then $S = \Delta\sigma_n$;

the above local stress obtained with SCF from Appendix 3 together with the D curve is to be used for the calculation of fatigue life;

- ③ for reinforced rings with large stiffness and small fillet weld size, fatigue cracking is likely from the weld root. See Figure 3.2.5(c). At some locations of the welds there are normal stresses in the plate transverse to the fillet weld σ_n , and shear stress in the plate parallel with the weld $\tau_{//p}$ see Figure 3.2.5(c). Then the fillet weld is designed for a combined stress obtained as:

$$S_w = \frac{t}{2a} \sqrt{\Delta\sigma_n^2 + 0.2\Delta\tau_{//p}^2} \quad (3.4)$$

where: t — plate thickness;

a — throat thickness for a double sided continuous fillet weld;

S_w — stress range used for the calculation of fatigue life of fillet weld;

$\Delta\sigma_n$ — range of normal stress transverse to the weld;

$\Delta\tau_{//p}$ — range of shear stress parallel with the weld.

The total stress range (i.e. maximum compression and maximum tension) is to be considered to be transmitted through the welds for fatigue assessments.

The stress component in the formula is to be obtained from Appendix 3 and used together with the S-N curve W.

For fillet welds all the cases, i.e. ①, ② and ③ are to be assessed with respect to fatigue. For full penetration welds the first two cases, i.e. ① and ② are to be assessed.

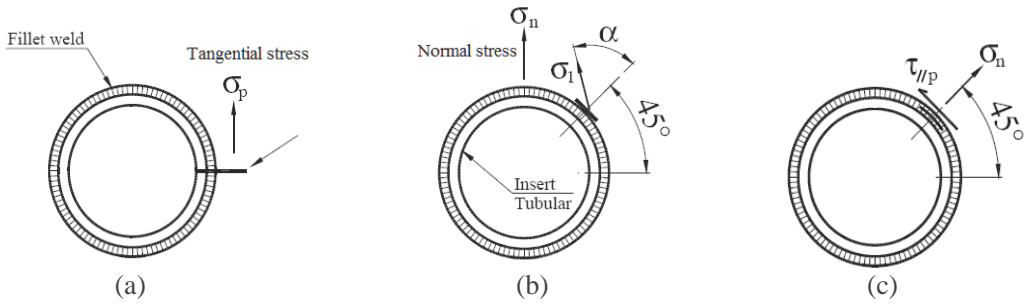


Figure 3.2.5 Potential Fatigue Crack Locations around a Circumferential Weld

3.2.6 Stress concentration factors for scallops

Reference is made to Figure 3.2.6 for stress concentration factors for scallops. The stress concentration factors are applicable to stiffeners subject to axial loads. For significant dynamic pressure loads on the plate these details are susceptible to fatigue cracking and appropriate solutions are to be adopted to improve the fatigue performance.

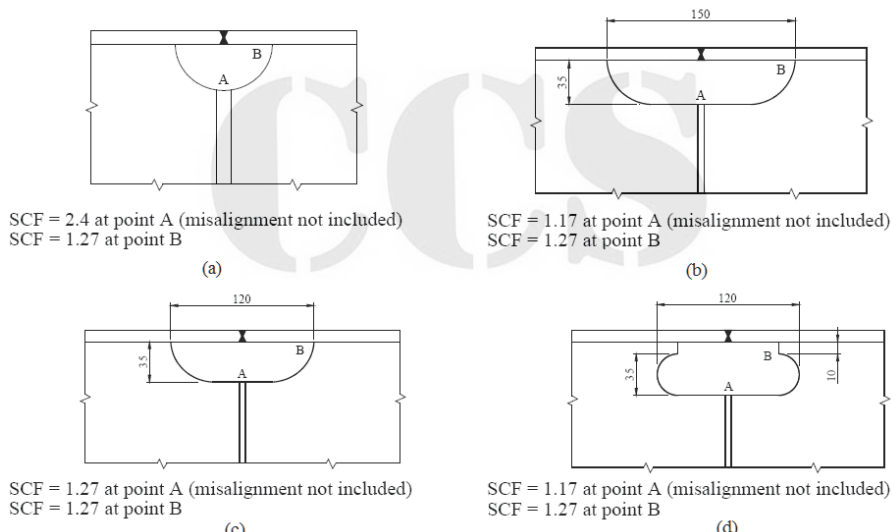


Figure 3.2.6 Stress Concentration Factors for Scallops (For Scallops without Transverse Welds, the SCF at Point B will be Governing for the Design)

Section 3 Stress Concentration Factors for Tubular Butt Weld Connections

3.3.1 Tubular butt welds with same nominal thickness and diameter

For tubular butt welds with same nominal thickness and diameter, the tolerances of eccentricity are in general required to be less than $0.1t$ or maximum 3 mm (t = wall thickness). NDE of the root area where defects are most critical is to be carried out. Provided that the same acceptance criteria are used for pipelines with larger wall thickness as for that used as reference thickness (25 mm), a thickness exponent r as specified in 2.5.9, Chapter 2 of the Guidelines may be taken as 0 for hot spot at the root and 0.15 for the weld toe. Provided that these requirements are fulfilled, the detail at the root side may be classified as F2 with SCF = 1.0. The F-curve and SCF = 1.0 may be used for the detail at the root side of welding on temporary backing.

Where the weld eccentricity does not comply with the above requirements, a stress concentration for the weld root due to maximum allowable eccentricity is to be included. This stress concentration factor may be calculated from the following formula:

$$SCF = 1 + \frac{3(\delta_m - \delta_0)}{t} \cdot \exp(-\sqrt{t/D}) \quad (3.5)$$

where: D — diameter of pipe;

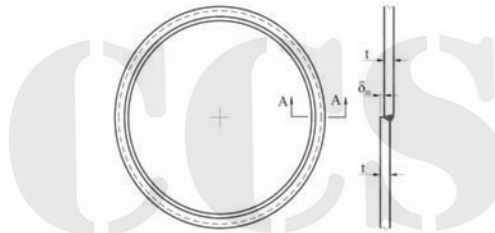
T — wall thickness of pipe;

δ_m — maximum misalignment, see Figure 3.3.1;

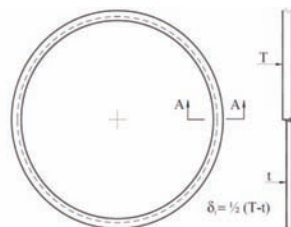
δ_0 — $0.1t$ is eccentricity inherent in the butt welds.

This stress concentration factor above can also be used for fatigue assessments of the weld toes, see Table 3.3.1.

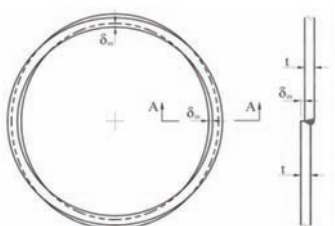
The nominal stress on the outside of the pipe is to be used for fatigue assessment of the outside and the nominal stress on the inside of the pipe is to be used for fatigue assessment of the inside. The membrane stress in the considered section is to be used for calculation of local bending stress due to misalignment over the thickness together with the stress concentration factor above.



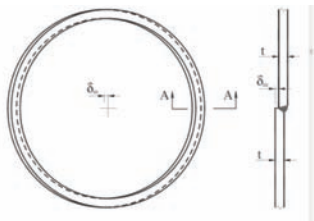
(a) Concentricity and same wall thickness,
but different diameter Section A-A



(b) Concentricity and same diameter,
but different wall thickness Section A-A



(c) Concentricity and same diameter,
but different out of roundness Section A-A



(d) Same diameter and wall thickness, but center eccentricity

Figure 3.3.1 Geometric Sources of Local Stress Concentrations in Tubular Butt Welds

**Classification of Connections of Tubular Butt Welds with
Same Wall thickness and Diameter**

Table 3.3.1

Welding	Geometry and hot spot	Tolerance requirement	S-N curve	Thickness exponent	SCF
Single side		$\delta \leq \min(0.15t, 3\text{mm})$	F2	0.00	1.0
Single side on backing		$\delta \leq \min(0.15t, 2\text{mm})$	F	0.00	1.0
Single side			D or E ^①	0.15	Formula
Double side			D or E ^①	0.15	Formula

Note: ① The transition of the weld to base material on the outside of the tubular may normally be classified to S-N curve E. If welding is performed in a horizontal position it may be classified as D. This means that the pipe would have to be rotated during welding.

3.3.2 Tubular butt welds with different nominal thickness and diameter

For tubular butt welds with different nominal thickness and diameter, stress concentrations at tubular butt weld connections are due to eccentricities resulting from different sources. These may be classified as difference in tubular diameters, differences in thickness of joined tubulars, out of roundness and centre eccentricity, see Figure 3.3.1. The resulting eccentricity may be conservatively evaluated by a direct summation of the contribution from the different sources. The eccentricity due to out of roundness normally gives the largest contribution to the resulting eccentricity δ .

It is conservative to use the formula for plate eccentricities for calculation of SCF at tubular butt welds. The effect of the diameter in relation to thickness may be included by use of the following formula, provided that $T/t \leq 2$:

$$SCF = 1 + \frac{6(\delta_t + \delta_m - \delta_0)}{t} \cdot \frac{e^{-\alpha}}{1 + (T/t)^\beta} \quad (3.6)$$

$$\alpha = \frac{1.82L}{\sqrt{Dt}} \cdot \frac{1}{1 + (T/t)^\beta}; \quad \beta = 1.5 - \frac{1.0}{\log(D/t)} + \frac{3.0}{[\log(D/t)]^2}$$

where: δ_m — maximum misalignment;

δ_t — $0.5(T-t)$ eccentricity due to change in thickness;

δ_0 — $0.1t$ is eccentricity inherent in the butt welds;

t — thickness of thinner plate;

T — thickness of thicker plate;

L — length over which the eccentricity is distributed, see Figures 3.3.2(1) and (2).

The stress concentration is reduced as L is increased and/or D is reduced. It is noted that for small L and large D the above formula provides stress concentration factors that are close to but lower than that of the simpler formula for plates given in Section 2 of this Chapter.

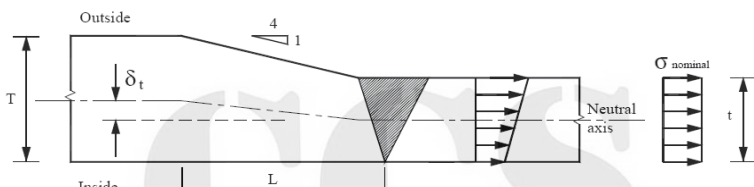


Figure 3.3.2(1) Preferred Transition in Thickness is on Outside of Tubular Butt Weld

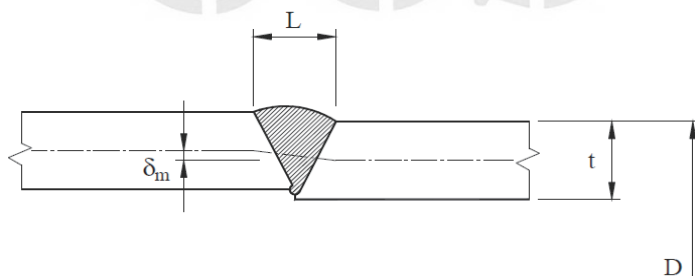


Figure 3.3.2(2) Local Diagram of Welds of Tubular Butt Weld on Wall Thickness

Due to less severe S-N curve for the outside weld toe than the inside weld root, it is strongly recommended that tubular butt weld connections are designed such that any thickness transitions are placed on the outside (see Figure 3.3.2(1)). For this geometry, the SCF for the transition applies to the outside. On the inside it is then conservative to use $SCF = 1.0$. Thickness transitions are normally to be fabricated with slope 1:4.

The transition of the weld to base material on the outside of the tubular can normally be classified to S-N curve E. If welding is performed in a horizontal position it can be classified as D. This means that the pipe would have to be rotated during welding.

The formula (3.6) above applies for calculation of stress concentration factors for the outside tubular side shown in Figure 3.3.2(3) a) when the thickness transition is on the outside. For the inside of connections with transitions in thickness on the outside as shown in Figure 3.3.2(3) b) the following formula may be used:

$$SCF = 1 - \frac{6(\delta_t - \delta_m)}{t} \cdot \frac{e^{-\alpha}}{1 + (T/t)^\beta} \quad (3.7)$$

If the transition in thickness is on the inside of the tubular and the weld is made from both sides, formula (3.6) may be applied for the inside weld toe and formula (3.7) for the outside weld toe.

If the transition in thickness is on the inside of the tubular and the weld is made from the outside only, as shown in Figure 3.3.2(3) c), formula (3.7) may be used for calculation of stress concentration for the outside weld toe.

If the transition in thickness is on the inside of the tubular and the weld is made from the outside only, as shown in Figure 3.3.2(3) d), formula (3.6) may be used for calculation of stress concentration for the inside weld toe.

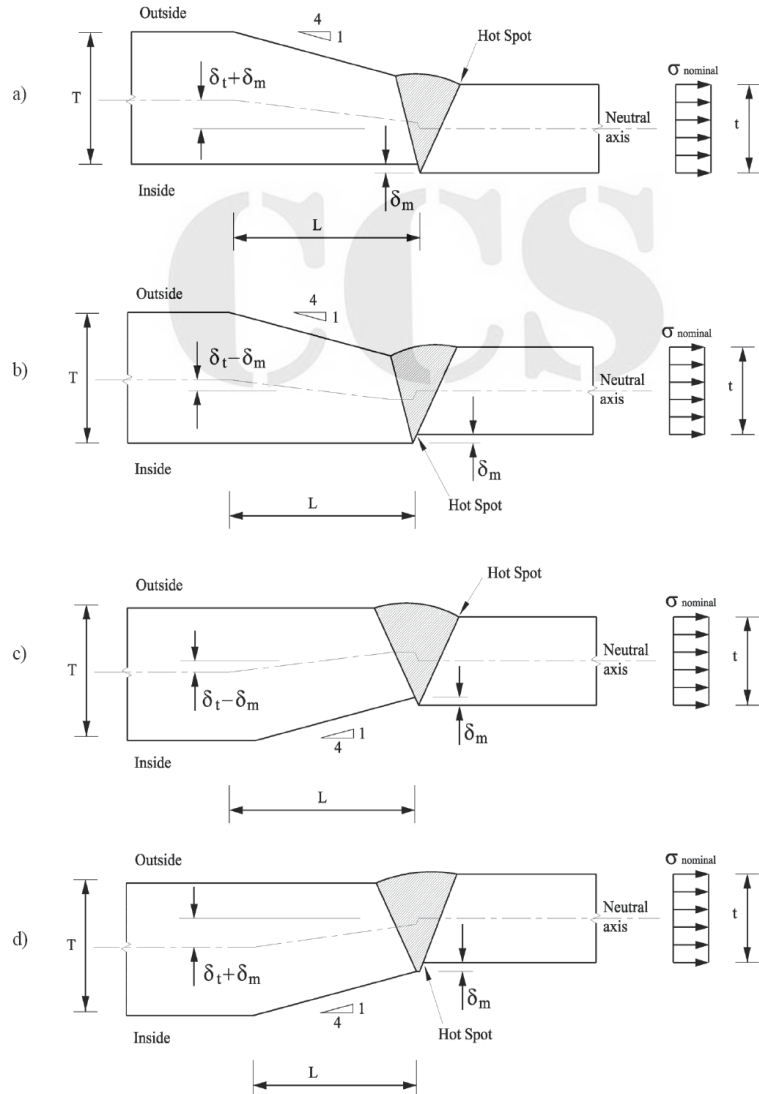


Figure 3.3.2(3) Influence of Transition Type of Tubulars with Different Thickness and Fabrication Tolerances on SCF of Weld Toe

In tubulars, the root side of welds made from one side is normally classified as F2. This requires good workmanship during construction, in order to ensure full penetration welds, and that work is checked by nondestructive examination. It may be difficult to document a full penetration weld in most cases due to limitations in the non-destructive examination technique to detect defects in the root area. The F2 curve may be considered to account for some lack of penetration, but it is to be noted that a major part of the fatigue life is associated with the initial crack growth while the defects are small. This may be evaluated by fracture mechanics such as described in BS 7910 “Guidance on Methods for Assessing the Acceptability of Flaws in Fusion Welded Structures”. Therefore, if a fabrication method is used where lack of penetration is to be expected, the design S-N curves is to be adjusted to account for this by use of fracture mechanics.

For global moments over the tubular section it is the nominal stress derived at the outside that is to be used together with an SCF from formula (3.6) for calculation of hot spot stress for fatigue assessment of the outside weld toe. The nominal stress on the inside is to be used together with an SCF from formula (3.6) for calculation of hot spot stress for fatigue assessment of the inside weld toe.

Section 4 Stress Concentration Factors for Ship Structure

3.4.1 For the calculation of fatigue life of typical details in ship structure, reference may be made to CCS Guidelines for Fatigue Strength of Ship Structure for stress concentration factors.

Section 5 Stress Concentration Factors for Tubular Joints

3.5.1 Hot spot stress in tubular joints

The stresses are calculated at the crown and the saddle points, see Figure 3.5.1(1). Then the hot spot stress at these points is derived by summation of the single stress components from axial load, in-plane and out-of -plane bending moment. The hot spot stress at the intermediate points between the saddle and the crown may be derived by interpolation of the values at the saddle and crown. The hot spot stress at these points is derived by a linear interpolation of the stress due to the axial action at the crown and saddle and a sinusoidal variation of the bending stress resulting from in-plane and out of plane bending. Thus the hot spot stress may be calculated from the following formulae (see number 1 to 8 in Figure 3.5.1(2)):

$$\begin{aligned}
 \sigma_1 &= \text{SCF}_{AC} \sigma_x + \text{SCF}_{MIP} \sigma_{my} \\
 \sigma_2 &= \frac{1}{2} (\text{SCF}_{AC} + \text{SCF}_{AS}) \sigma_x + \frac{\sqrt{2}}{2} \text{SCF}_{MIP} \sigma_{my} - \frac{\sqrt{2}}{2} \text{SCF}_{MOP} \sigma_{mz} \\
 \sigma_3 &= \text{SCF}_{AS} \sigma_x - \text{SCF}_{MOP} \sigma_{mz} \\
 \sigma_4 &= \frac{1}{2} (\text{SCF}_{AC} + \text{SCF}_{AS}) \sigma_x - \frac{\sqrt{2}}{2} \text{SCF}_{MIP} \sigma_{my} - \frac{\sqrt{2}}{2} \text{SCF}_{MOP} \sigma_{mz} \\
 \sigma_5 &= \text{SCF}_{AC} \sigma_x - \text{SCF}_{MIP} \sigma_{my} \\
 \sigma_6 &= \frac{1}{2} (\text{SCF}_{AC} + \text{SCF}_{AS}) \sigma_x - \frac{\sqrt{2}}{2} \text{SCF}_{MIP} \sigma_{my} + \frac{\sqrt{2}}{2} \text{SCF}_{MOP} \sigma_{mz} \\
 \sigma_7 &= \text{SCF}_{AS} \sigma_x + \text{SCF}_{MOP} \sigma_{mz} \\
 \sigma_8 &= \frac{1}{2} (\text{SCF}_{AC} + \text{SCF}_{AS}) \sigma_x + \frac{\sqrt{2}}{2} \text{SCF}_{MIP} \sigma_{my} + \frac{\sqrt{2}}{2} \text{SCF}_{MOP} \sigma_{mz}
 \end{aligned} \tag{3.8}$$

where: σ_x — maximum nominal stresses due to axial load;
 σ_{my} — maximum nominal stresses due to in-plane bending moment;
 σ_{mz} — maximum nominal stresses due to out-of-plane bending moment;
 SCF_{AS} — stress concentration factor at the saddle for axial load;
 SCF_{AC} — stress concentration factor at the crown for axial load;
 SCF_{MIP} — stress concentration factor for in-plane bending moment;
 SCF_{MOP} — stress concentration factor for out-of-plane bending moment.

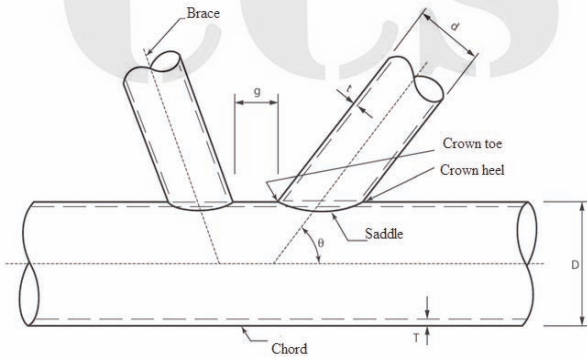
The hot spot stress may be obtained by using other recognized and reasonable methods subject to approval by CCS. For multi planar joints SCFs are usually determined assuming there is no interaction between joints in different planes so that they are treated as simple tubular joints. However, in certain load cases, significant interaction can occur between joints in different planes. These effects, which can result in significantly different SCFs, are to be assessed using appropriate methods, e.g. expressions used in Efthymiou, see Appendix 2.

3.5.2 Stress concentration factors for simple tubular joints

Stress concentration factors for simple tubular joints are given in Appendix 2.

3.5.3 Stress concentration factors for overlapped tubular joints

Special consideration is to be given to the formula of stress concentration factors for overlapped tubular joints.



θ — brace angle (measure from the chord);
 g — gap between braces;
 t — brace thickness;
 T — chord thickness;
 D — chord diameter;
 d — brace diameter;
 $\alpha = L / D$ — ratio of chord length to chord outer diameter, reflecting the flexibility of chord;
 $\beta = d / D$ — ratio of brace outer diameter to chord outer diameter, reflecting the transfer of load and distribution of stress;
 $\gamma = R / T$ — ratio of chord outer radius to chord wall thickness, reflecting the radial rigidity of chord;
 $\tau = t / T$ — ratio of brace wall thickness to chord wall thickness, reflecting the bending rigidity of brace relative to chord.

Figure 3.5.1(1) Geometrical Definitions for Tubular Joints

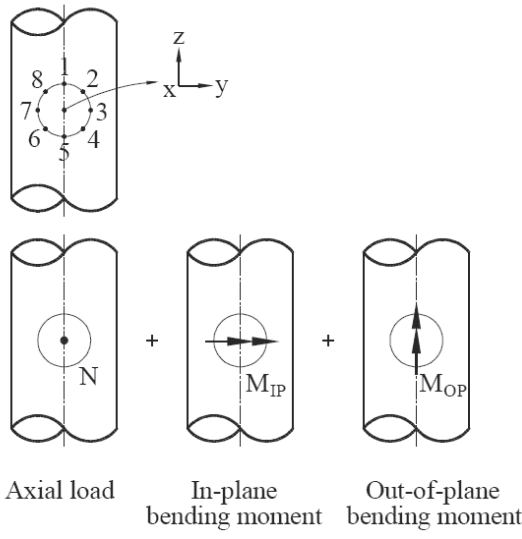


Figure 3.5.1(2) Superposition of Stresses

3.5.4 Stiffened tubular joints

(1) Stress concentration factors for joints for ring stiffened tubular joints are given in relevant references, e.g. “Stress Concentration Factors for Ring-Stiffened Tubular Joints” (1991) (reference [14] of Appendix 2) published by SMEDLEY, P.A. and FISHER, P. at the Fourth International Symposium on Tubular Structures. The following points are to be noted regarding the equations:

- ① The derived SCF ratios for the brace/chord intersection and the SCFs for the ring edge are mean values, although the degree of scatter and proposed design factors are given.
 - ② Short chord effects are to be taken into account where relevant.
 - ③ For joints with diameter ratio $\beta \geq 0.8$, the effect of stiffening is uncertain. It may even increase the SCF.
 - ④ The maximum of the saddle and crown stress concentration factor values is to be applied around the whole brace/chord intersection.
- (2) The following points can be made about the use of ring stiffeners in general:

- ① Thin shell FE analysis is to be avoided for calculating the SCF if the maximum stress is expected to be near the brace-ring crossing point in the fatigue analysis. An alternative is to use a three-dimensional solid element analysis model.
- ② Ring stiffeners have a marked effect on the circumferential stress in the chord, but have little or no effect on the longitudinal stress.
- ③ Ring stiffeners outside the brace footprint have little effect on the SCF, but may be of help for the static strength.

- ④ Failures in the ring inner edge or brace ring interface occur internally, and will probably only be detected after through thickness cracking, at which the majority of the fatigue life will have been expired. These areas are therefore to be considered as non-inspectable unless more sophisticated inspection methods are used.

3.5.5 Grouted tubular joints

Grouted tubular joints have either the chord completely filled with grout (single skin grouted joints) or the annulus between the chord and an inner member filled with grout (double skin grouted joints). The grouted joints are to be treated as simple joints, except that the chord thickness in the γ term for saddle SCF calculation for brace and chord is to be substituted with an equivalent chord wall thickness given by:

$$T_e = (5D + 134T)/144 \quad (3.9)$$

where: D — chord diameter;

T — chord thickness.

Joints with high β or low γ ratios have little effect of grouting. The benefits of grouting are to be neglected for joints with $\beta > 0.90$ or $\gamma \leq 12.0$ unless documented otherwise.

3.5.6 Cast tubular joints

It is recommended that finite element analysis is to be used to determine the magnitude and location of the maximum stress range in castings sensitive to fatigue. The finite element model is to use volume elements at the critical areas and properly model the shape of the joint. The brace to casting circumferential butt weld may be the most critical location for fatigue.

3.5.7 Tubular joints welded from one side

The root area of single-sided welded tubular joints may be more critical with respect to fatigue cracks than the outside region connecting the brace to the chord. In such cases, it is recommended that stubs are provided for tubular joints where high fatigue strength is required, such that welding from the backside can be performed.

Failure from the root has been observed at the saddle position of tubular joints where the brace diameter is equal the chord diameter, both in laboratory tests and in service. It is likely that fatigue cracking from the root might occur for rather low stress concentrations. Thus, special attention is to be given to joints other than simple joints, such as ring-stiffened joints and joints where weld profiling or grinding on the surface is required to achieve sufficient fatigue life. It is to be remembered that surface improvement does not increase the fatigue life at the root.

Based on experience it is not likely that fatigue cracking from the inside will occur earlier than from the outside for simple T and Y joints and K type tubular joints. The same consideration may be made for X-joints with diameter ratio $\beta \leq 0.90$. For other joints and for simple tubular X-joints with $\beta > 0.90$ it is recommended that a fatigue assessment of the root area is performed.

Due to limited accessibility for in service survey a higher safety factor of fatigue is to be used for the weld root than for the outside weld toe hot spot.

Section 6 Direct Calculation of Hot Spot Stress

3.6.1 General provisions

Fatigue strength assessment of complicated structure requires the use of fatigue hot spot stress approach. But generally the hot spot stress of structural details cannot be obtained by theoretical method and the parametric formulae of hot spot stress are very limited. As a result the fatigue hot spot stress is predominantly determined by means of fine finite element direct calculation.

The mesh is to be refined in the vicinity of hot spots for finite element model used for obtaining each hot spot of the structure, so as to obtain the correct stress gradient from low stress region to high stress region (hot spot position). However, the mesh is not to be refined too much, leading to overestimation of peak value stress due to abrupt change of geometry and other discontinuities.

3.6.2 Structural modeling

The fine finite element model is to be based on the following principles:

- (1) The fatigue hot spot stress may be calculated by means of a separate fine finite element model, with boundary conditions being obtained from analysis of a coarse mesh finite element model; alternatively, direct calculation may be performed via a fine finite element model fitted into a coarse mesh finite element model.
- (2) Where a separate local finite element model is used, the extent of the local model is to be such that the calculated stresses are not significantly affected by the imposed boundary conditions and application of loads. The boundary of the fine mesh model is to coincide with the primary support members, such as girders and floors.
- (3) The types of elements are generally recommended to be linear rectangular plate or shell elements. The mesh is to be developed at the neutral surface, disregarding welds. In special cases where the analysis is focused on the effects of weld shape, three-dimensional solid elements may be considered for modelling and generally hexahedron elements are used. Triangular elements are to be avoided in the hot spot region.
- (4) In the hot spot stress region (including the region for interpolation), the mesh size is not to be greater than the thickness t of force bearing structural members (t is the plate thickness where the weld toe to be assessed is located). Mesh size of $t \times t$ is recommended. The fine mesh zone is to be such as to extend over at least $10t$ in all directions leading to the fatigue hot spot position.
- (5) The 1:1 aspect ratio of element is ideally to be used in the hot spot region and those regions very close to the hot spot. Away from the hot spot region, the aspect ratio is to be ideally limited to 1:3, and any element exceeding this ratio is to be well away from the area of interest and then is not to exceed 1:5. The corner angles of the quadrilateral plate or shell elements is to be confined to the range 50 to 130 degrees.
- (6) The change in mesh size from the finest at the hot spot to coarser gradations away from the hot spot region is to be accomplished in a smooth and uniform fashion. Immediately adjacent to the hot spot, it is suggested that several of the elements leading into the hot spot location is to be the same size of $t \times t$.

3.6.3 Tubular joints

The stress range at the hot spot of tubular joints is to be combined with the S-N curve of tubular joints in Section 5, Chapter 2.

Analysis based on shell elements may be used. In this case, the weld is not included in the model. The hot spot stress may be determined as for welded connections of non-tubular details.

More reliable results are obtained by including the weld in the model. This implies use of three-dimensional elements. Here the Gaussian points, where stresses are calculated, may be placed $0.1\sqrt{rt}$ from the weld toe (r = radius of considered tubular and t = thickness of tubular for the weld toe). The stress at this point may be used directly in the fatigue assessment.

The hot spot stress or geometric stress at tubular joints can also be obtained by a linear extrapolation of the stresses obtained from analysis at positions at distances a and b from the weld toe as indicated in Figure 3.6.3.

For extrapolation of stress along the brace surface normal to the weld toe: $a=0.2\sqrt{rt}$ and $b=0.65\sqrt{rt}$;
 For extrapolation of stress along the chord surface normal to the weld toe at the crown position:
 $a=0.2\sqrt{RT}$ and $b=0.4\sqrt{rtRT}$; For extrapolation of stress along the chord surface normal to the weld toe at the saddle position: $a=0.2\sqrt{RT}$ and $b=\pi R/36$; where r , t , R and T are defined in Figure 3.6.3.

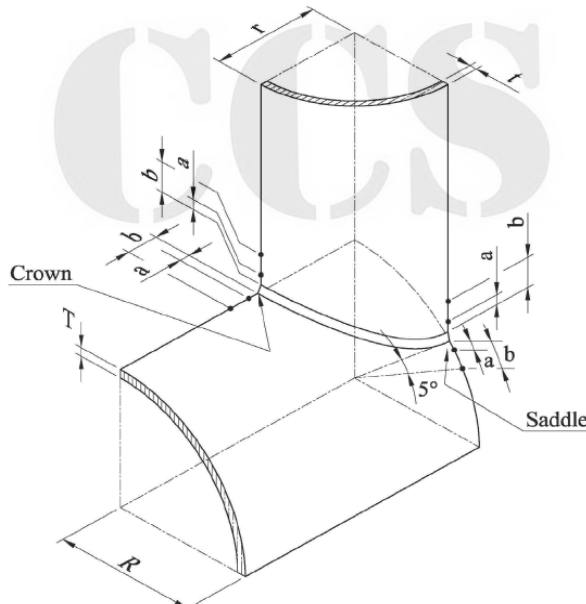


Figure 3.6.3 Extrapolation of Hot Spot Stress in Tubular Joints

3.6.4 Welded connections other than tubular joints

(1) Stress field at a welded detail

Due to the complexity of the stress field at a hot spot region, the hot spot stress is to be established by developing certain regulations, see Figure 3.6.4(1). The notch effect due to the weld is included in the S-N curve and the hot spot stress is derived by linear extrapolation of the structural stress to the specific point as indicated in Figure 3.6.4(1). It is observed that the stress used as basis for such an extrapolation is to be outside that affected by the weld notch, but close enough to pick up the accurate stress gradient.

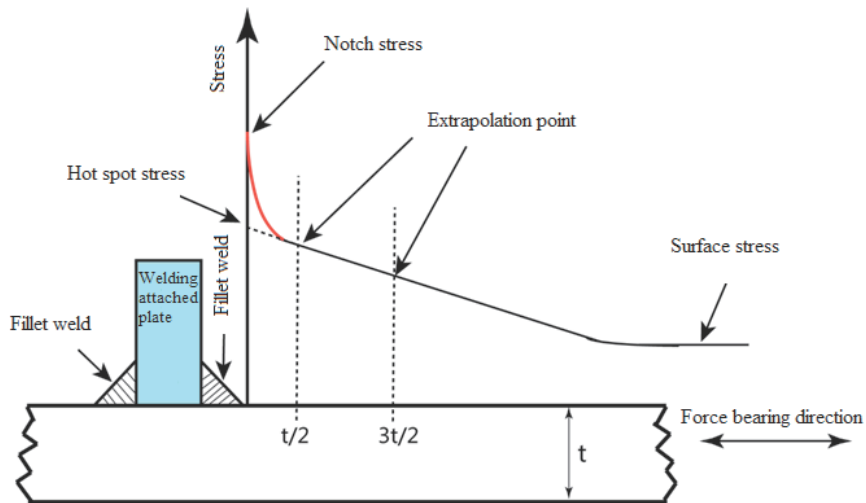


Figure 3.6.4(1) Hot Spot Stress Extrapolation in Weld Toe Area

(2) FE modeling

In plate structures, three types of hot spots at weld toes can be identified as exemplified in Figure 3.6.4(2):

- ① at the weld toe on the plate surface at an ending attachment (on the plate surface) (type a in Figure 3.6.4(2));
- ② at the weld toe on the plate surface at an ending attachment (on the attachment surface) (type b in Figure 3.6.4(2));
- ③ along the weld of an attached plate (weld toes on both the plate and attachment surface) (type c in Figure 3.6.4(2)).

Models with thin plate or shell elements or alternatively with solid elements are normally used. It is to be noted that on the one hand the arrangement and type of elements have to allow for steep stress gradients as well as for the formation of plate bending, and on the other hand, only the linear stress distribution in the plate thickness direction needs to be evaluated with respect to the definition of hot spot stress. Attention is to be given to the following points in addition to complying with the principles of modelling in 3.6.2:

- ① The simplest way of modeling is offered by thin plate and shell elements which have to be arranged in the mid-plane of the structural components, see (a) of Figure 3.6.4(3).
- ② 8-noded elements are recommended particularly in case of steep stress gradients. Care is to be given to possible stress underestimation especially at type b in Figure 3.6.4(2) when 4-noded elements are used. Use of 4-noded elements with improved in-plane bending modes is a good alternative.
- ③ The welds are usually not modelled except for special cases where the results are affected by high local bending, e. g. due to an offset between plates or due to a small free plate length between adjacent welds such as at lug (or collar) plates. Here, the weld may be included by transverse plate elements having appropriate stiffness or by introducing constrained equations for coupled node displacements.

- ④ A thickness equal 2 times the thickness of the plates may be used for modeling of the welds by transverse plates.
- ⑤ An alternative particularly for complex cases is offered by solid elements which need to have a displacement function allowing steep stress gradients as well as plate bending with linear stress distribution in the plate thickness direction. This is offered, e.g., by isoparametric 20-node elements (with mid-side nodes at the edges) which mean that only one element in plate thickness direction is required. An easy evaluation of the membrane and bending stress components is then possible if a reduced integration order with only two integration points in the thickness direction is chosen. A finer mesh sub-division is necessary particularly if 8-noded solid elements are selected. Here, at least four elements are recommended in thickness direction. Modeling of the welds is generally recommended and easily possible as shown in (b) of Figure 3.6.4(3).
- ⑥ For modeling with three dimensional elements the dimensions of the first two or three elements in front of the weld toe are to be chosen as follows. The element length may be selected to correspond to the plate thickness. In the transverse direction, the plate thickness may be chosen again for the breadth of the plate elements. However, the breadth is not to exceed the “attachment width”, i.e. the thickness of the attached plate plus $2 \times$ the weld leg length (in case of type c in Figure 3.6.4(2): the thickness of the web plate behind plus $2 \times$ weld leg length). The length of the elements is to be limited to $2t$.
- ⑦ In cases where three-dimensional elements are used for the FE modeling it is recommended that also the fillet weld is modelled to achieve proper local stiffness and geometry.
- ⑧ In order to capture the properties of bulb sections with respect to St Venant torsion it is recommended to use several three-dimensional elements for modeling of a bulb section. If in addition the weld from stiffeners in the transverse frames is modelled the requirements with respect to element shape will likely govern the FE model at the hot spot region.

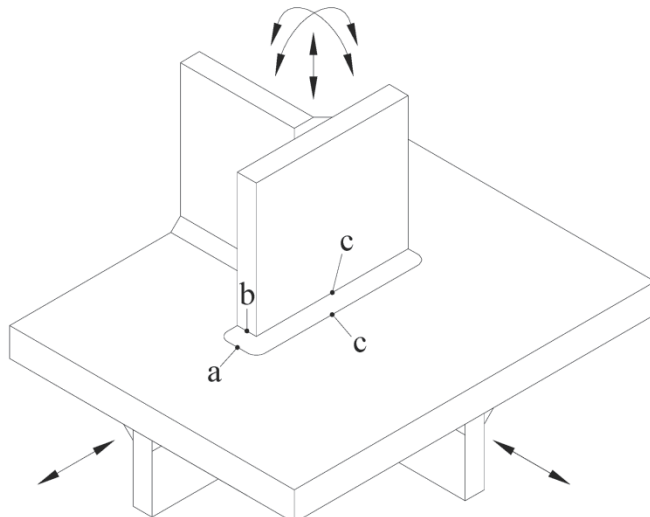


Figure 3.6.4(2) Different Hot Spot Positions

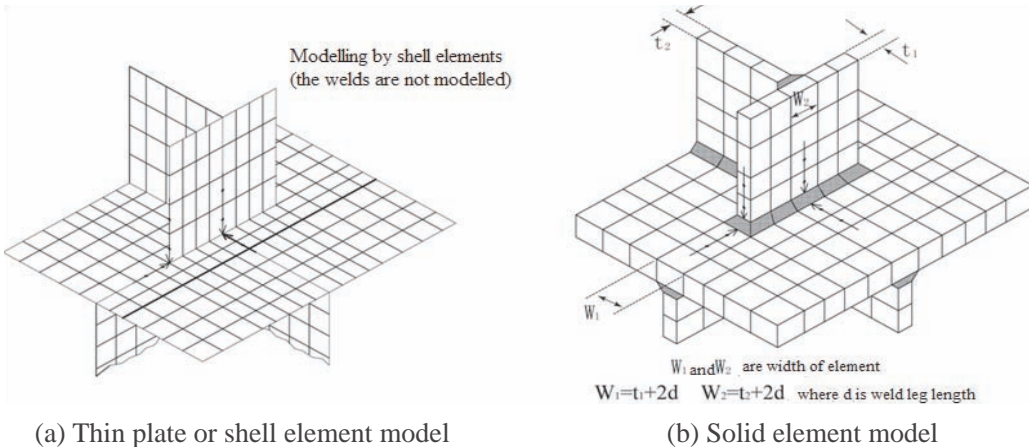


Figure 3.6.4(3) Stress Extrapolation in a Three-dimensional FE Model to the Weld Toe

(3) Derivation of stress at read out points $0.5t$ and $1.5t$

The stress components on the plate surface are to be evaluated along the paths shown in Figure 3.6.4(3) and extrapolated to the hot spot. The average stress components between adjacent elements are used for the extrapolation. Recommended stress evaluation points are located at distances $0.5t$ and $1.5t$ away from the hot spot, where t is the plate thickness at the hot spot for assessment. The extrapolation process is recommended as follows:

- ① For modeling with shell elements without any weld included in the model a linear extrapolation of the stresses to the intersection line from the read out points at $0.5t$ and $1.5t$ from the intersection line can be performed to derive hot spot stress.
- ② For modeling with three-dimensional elements with the weld included in the model a linear extrapolation of the stresses to the weld toe from the read out points at $0.5t$ and $1.5t$ from the weld toe can be performed to derive hot spot stress.
- ③ If the element size at a hot spot region of size $t \times t$ is used, the stresses may be evaluated as follows:
 - a. In case of plate or shell elements the surface stress may be evaluated at the corresponding mid-side points, which may be used directly as stress at read out points as shown in Figure 3.6.4(4).
 - b. In case of solid elements the stress may first be extrapolated from the Gaussian points to the surface. Then these stresses can be interpolated linearly to the surface centre or extrapolated to the edge of the elements if this is the line for hot spot stress derivation.
- ④ For meshes with 4-node shell elements larger than $t \times t$, it is recommended to fit a second order polynomial to the element stresses in the three first elements and derive stresses for extrapolation from the $0.5t$ and $1.5t$ points. An example of this is shown schematically in Figure 3.6.4(5). For 8-node elements a second order polynomial may be fitted to the stress results at the mid-side nodes of the three first elements.

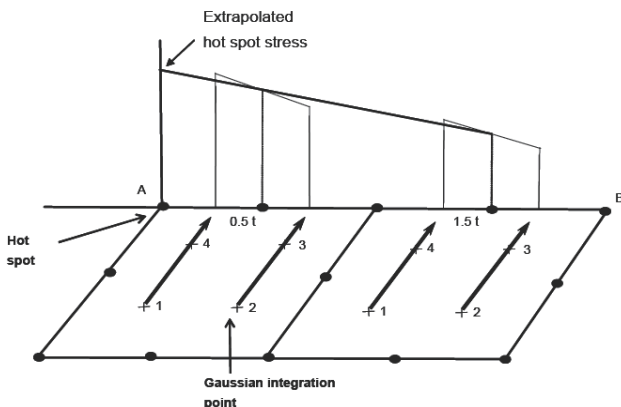


Figure 3.6.4(4) Extrapolation of Stresses at Read Out Points to Derive Hot Spot Stress

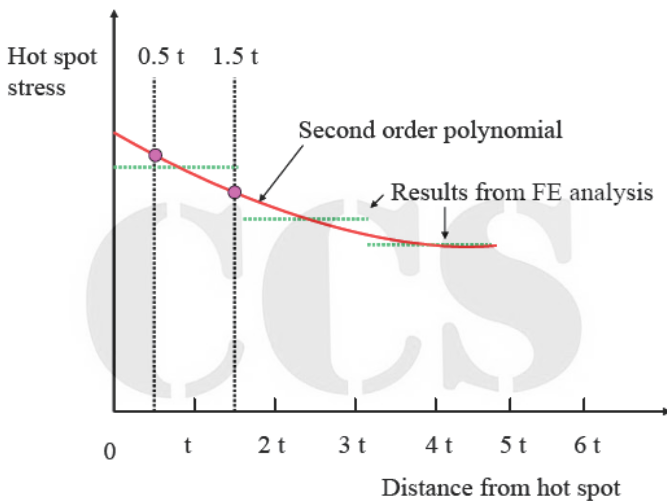


Figure 3.6.4(5) Derivation of Hot Spot Stress for Element Size Larger than $t \times t$

(4) Derivation of hot spot stress in models with significant plate bending

At hot spots with significant plate bending, an effective hot spot stress for fatigue assessment may be derived from the following formula:

$$\Delta\sigma_{e,hot\ spot} = \Delta\sigma_{a,hot\ spot} + 0.60\Delta\sigma_{b,hot\ spot} \quad (3.10)$$

where: $\Delta\sigma_{a,hot\ spot}$ —membrane stress;

$\Delta\sigma_{b,hot\ spot}$ —bending stress.

The reduction factor on the bending stress can be explained by redistribution of loads to other areas during crack growth while the crack tip is growing into a region with reduced stress. The effect is limited to areas with a localised stress concentration. However, in a case where the stress variation along the weld is small, the difference in fatigue life between axial loading and pure bending is much smaller. Therefore it is to be noted that it is not correct to generally reduce the bending part of the stress to 60 percent. This has to be restricted to cases with a pronounced stress concentration (where the stress distribution under fatigue crack development is more similar to a displacement controlled situation than that of a load controlled development, i.e. the constant amplitude test rather than constant load test of fatigue test).

CHAPTER 4 SAFETY FACTOR OF FATIGUE

Section 1 General Provisions

4.1.1 The fatigue failure criteria may be based on the fatigue damage or fatigue life. When based on the fatigue damage, the fatigue strength of the considered point is to comply with:

$$D \leq \frac{1.0}{S_{fg}} \quad (4.1)$$

where: D — fatigue damage ratio;

S_{fg} — safety factor of fatigue, to be taken from Table 4.1.1;

When based on the fatigue life, the fatigue strength of the considered point is to comply with:

$$T_{fg} \geq T_D \cdot S_{fg} \quad (4.2)$$

where: T_{fg} — calculated fatigue life;

T_D — design fatigue life.

Safety Factor of Fatigue S_{fg}

Table 4.1.1

	Safety factor of fatigue	Structural members
Mobile units	1	Internal structures, accessible for survey and without direct welded connections to underwater structures
	1	External structures, accessible for survey and periodic servicing in dry and clean environment
	2	Internal structures, accessible for survey and with direct welded connections to underwater structures
	2	External structures, accessible for survey but not for periodic servicing in dry and clean environment
	3	Areas inaccessible for survey and not intended to be accessible for survey and servicing during operation
Fixed non-floating structures (e.g. jacket, tower, template etc.)	2	Accessible for survey and servicing and without serious failure consequence
	5	Inaccessible for survey and servicing and without serious failure consequence
	5	Accessible for survey and servicing and with serious failure consequence
	10	Inaccessible for survey and servicing and with serious failure consequence
Fixed floating structures (e.g. TLP, SPAR and column stabilized, ship type FPSO etc.)	1	Accessible for survey and servicing in dry environment and without serious failure consequence
	2	Accessible for underwater survey and servicing and without serious failure consequence
	5	Inaccessible for survey and servicing and without serious failure consequence
	2	Accessible for survey and servicing in dry environment and with serious failure consequence
	5	Accessible for underwater survey and servicing and with serious failure consequence
	10	Inaccessible for survey and servicing and with serious failure consequence

Notes: ① For shell envelope plating of mobile units required to be subject to docking survey according to CCS Rules, 1 is to be taken.

- ② For shell envelope plating of mobile units intended to be subject to survey under floating condition in sheltered waters, 1 is to be taken for areas over 1 m above the lowest inspection waterline, 2 for areas below.
- ③ 3 is to be taken for splash zones.
- ④ In case fractures may extend from areas accessible to those inaccessible for survey, the maximum value along the fracture extension is to be taken, e.g. for the welded connections to the inner side of the underwater shell plating (dry hold), the value of similar external connection is to be taken.
- ⑤ Serious consequences mean those consequences likely to give rise to loss of human life, major pollution or major economic loss. For the fatigue failure of connections likely to cause major dangerous accidents and serious consequences, the value is to be specially considered.
- ⑥ The requirements for TLP are to be specially considered. The S-N curve requirements of AWS C1 or API RP 2A-WSD may be applied to circumferential weld of tension cable of TLP unit. But it is to be noted that the AWS standards have restrictions in terms of available geometric shape, material thickness and corrosion condition. AWS C1 curve and S-N curves in API RP 2A-WSD are used depending on high-quality NDT and appropriate corrosion protection, e.g. paint, cathodic protection or both are used.



CHAPTER 5 SIMPLIFIED FATIGUE ANALYSIS METHOD

Section 1 General Provisions

5.1.1 The simplified fatigue assessment method is also sometimes referred to as the permissible stress range method, which can be categorized as an indirect fatigue assessment method because the result of the method's application is not necessarily a value of fatigue damage or a fatigue life value. Often a "pass/fail" answer results depending on whether the acting stress range is below or above the permissible value.

5.1.2 The simplified fatigue assessment method is often used as the basis of a fatigue screening technique of a structural detail. A screening technique is typically a rapid, but usually conservatively biased, check of structural adequacy. If the structure's strength is adequate when checked with the screening criterion, no further analysis may be required. If the structural detail fails the screening criterion, the proof of its adequacy may still be pursued by analysis using more refined techniques. Also, a screening approach is quite useful to identify fatigue sensitive areas of the structure, thus providing a basis to develop fatigue survey planning of the structure.

Section 2 Mathematical Development

5.2.1 General assumptions

In the simplified fatigue analysis, the two-parameter Weibull distribution is used to model the long-term distribution of fatigue stresses. The cumulative distribution function of the stress range can be expressed as:

$$F_s(S) = 1 - \exp\left[-\left(\frac{S}{f_1}\right)^\zeta\right], \quad S > 0 \quad (5.1)$$

where: S — a random variable denoting stress range;

ζ — the Weibull distribution shape parameter;

f_1 — the Weibull distribution scale parameter, to be obtained from the largest stress range S_R in stress cycles N_R , see formula (5.5).

The probability density function of Weibull distribution of stress range is to be taken as:

$$f_s(S) = \frac{\zeta}{f_1} \left(\frac{S}{f_1}\right)^{\zeta-1} \exp\left[-\left(\frac{S}{f_1}\right)^\zeta\right], \quad S > 0 \quad (5.2)$$

The probability of exceedance of stress range is to be taken as:

$$P_s(S) = 1 - \int_0^S f_s(s) ds = \exp\left[-\left(\frac{S}{f_1}\right)^\zeta\right], \quad S > 0 \quad (5.3)$$

Based on the long-term distribution of stress range, a closed form expression for fatigue damage can be derived. A major feature of the simplified method is that appropriate application of experience data can be made to estimate the appropriate Weibull shape parameter, thus avoiding a lengthy spectral analysis.

The other major assumptions underlying the simplified fatigue approach are that the linear cumulative damage (Palmgren-Miner) rule applies, and that fatigue strength is defined by the S-N curves.

5.2.2 Parameters in the Weibull Distribution

- (1) The scale parameter f_1 may be obtained as follows:

Define a reference stress range, S_R , which characterizes the largest stress range anticipated in a reference number of stress cycles, N_R . The probability statement for S_R is:

$$P(S > S_R) = \exp\left[-\left(\frac{S_R}{f_1}\right)^\zeta\right] = \frac{1}{N_R} \quad (5.4)$$

where: N_R — number of cycles in a referenced period of time;

S_R — the largest fatigue stress range once every N_R cycles.

For a particular offshore site, the selection of an N_R and the determination of the corresponding value of S_R may be obtained from empirical data or from long-term wave data (using wave scatter diagram) coupled with appropriate structural analysis.

It follows from formulae (5.3) and (5.4) that:

$$f_1 = \frac{S_R}{(\ln N_R)^{1/\zeta}} \quad (5.5)$$

where: N_R, S_R — the same as 5.4.

- (2) The shape parameter, ζ , can be established from a detailed stress spectral analysis or its value may be assumed based on experience.

The results of the simplified fatigue assessment method can be very sensitive to the values of the Weibull shape parameter. Therefore, where there is a need to refine the accuracy of the selected shape parameters, the performance of even a basic level global response analysis can be very useful in providing more realistic values. Alternatively, it is suggested that when the basis for the selection of a shape factor is not well known, then a range of probable shape factor values are to be employed so that a better appreciation of how selected values affect the fatigue assessment will be obtained.

5.2.3 Fatigue damage calculation for the single segment S-N curve

Consider the bilinear S-N curve of Section 5, Chapter 2. Assume that the left segment is extrapolated into the high number of cycles range down to $S = 0$; i.e., there is no slope change at 10^6 to 10^7 cycles. Such a single segment curve would be used for the case of free corrosion in seawater for tubular and non-tubular details.

For the single segment case, the cumulative fatigue damage can be expressed as:

$$D = \frac{(N_T)}{K} f_1^m \cdot \Gamma\left(\frac{m}{\zeta} + 1\right) \quad (5.6)$$

where: N_T — total number of cycles in the design life, $N_T = T_d / T_z$;

T_d — fatigue design life, in s;

T_z — average zero-crossing period, in s.

$\Gamma(x)$ is the gamma function defined as:

$$\Gamma(x) = \int_0^\infty t^{x-1} e^{-t} dt \quad (5.7)$$

The values of the gamma function for different shape parameters ζ when $m = 3.0$ are given in Table 5.2.3.

Values of the Gamma Function When $m=3.0$

Table 5.2.3

ζ	$m=3.0$	ζ	$m=3.0$	ζ	$m=3.0$
0.60	120.000	0.77	20.548	0.94	7.671
0.61	104.403	0.78	19.087	0.95	7.342
0.62	91.350	0.79	17.772	0.96	7.035
0.63	80.358	0.80	16.586	0.97	6.750
0.64	71.048	0.81	15.514	0.98	6.483
0.65	63.119	0.82	14.542	0.99	6.234
0.66	56.331	0.83	13.658	1.00	6.000
0.67	50.491	0.84	12.853	1.01	5.781
0.68	45.442	0.85	12.118	1.02	5.575
0.69	41.058	0.86	11.446	1.03	5.382
0.70	37.234	0.87	10.829	1.04	5.200
0.71	33.886	0.88	10.263	1.05	5.029
0.72	30.942	0.89	9.741	1.06	4.868
0.73	28.344	0.90	9.261	1.07	4.715
0.74	26.044	0.91	8.816	1.08	4.571
0.75	24.000	0.92	8.405	1.09	4.435
0.76	22.178	0.93	8.024	1.10	4.306

5.2.4 Fatigue damage calculation for the two segment S-N curve

The cumulative fatigue damage for the two-segment S-N curve of Figure 2.5.3 is expressed as:

$$D = \frac{N_T f_1^{m_1}}{K_1} \Gamma\left(\frac{m_1}{\zeta} + 1, Z\right) + \frac{N_T f_1^{m_2}}{K_2} \Gamma_0\left(\frac{m_2}{\zeta} + 1, Z\right) \quad (5.8)$$

where: $\Gamma(a, z)$ —complementary incomplete gamma functions (integrals z to ∞);
 $\Gamma_0(a, z)$ —incomplete gamma functions (integrals 0 to z).

For definitions of other parameters, see Figure 2.5.3 and 5.2.3.

$$\Gamma(a, z) = \int_z^\infty t^{a-1} e^{-t} dt = \Gamma(a) - \Gamma_0(a, z) \quad (5.9)$$

$$\Gamma_0(a, z) = \int_0^z t^{a-1} e^{-t} dt \quad (5.10)$$

$$z = \left(\frac{S_q}{f_1} \right)^\zeta \quad (5.11)$$

where: S_q — stress range at which the slope of the S-N curve changes.

5.2.5 Allowable stress range

An alternative way to characterize fatigue strength is in terms of a maximum allowable stress range. This can be done to include consideration of the safety factor of fatigue defined in Chapter 4. Letting $D = 1/S_{fg}$ in formula (5.8), the maximum allowable stress range, S'_R , at the probability level corresponding to N_R is found as:

$$S'_R = \left[\frac{(\ln N_R)^{m_1/\zeta}}{S_{fg} \cdot N_T \left[\frac{\Gamma\left(\frac{m_1}{\zeta} + 1, Z\right)}{K_1} + \frac{f_1^{m_2-m_1} \Gamma_0\left(\frac{m_2}{\zeta} + 1, Z\right)}{K_2} \right]} \right]^{1/m} \quad (5.12)$$

Note that an iterative method is needed to find S'_R because the scale parameter f_1 also depends on S'_R .

Where the allowable stress range corresponding to number of cycles N_R is known, the following relationship can be used to find the allowable stress range S'_S corresponding to another number of cycles, N_S :

$$S'_S = S'_R \left(\frac{\ln N_S}{\ln N_R} \right)^{1/\zeta} \quad (5.13)$$

5.2.6 Fatigue safety check

When the fatigue damage is determined in accordance with 5.2.3 and 5.2.4, the fatigue safety check is performed according to Section 1, Chapter 4.

When the fatigue is assessed in terms of allowable stress range in accordance with 5.2.5, the safety check expression corresponding to formula (5.12) is:

$$S_R \leq S'_R \quad (5.14)$$

Or if the allowable stress range is modified to reflect a different number of cycles N_S from the formula (5.13), the safety check is:

$$S_S \leq S'_S \quad (5.15)$$

In practice, it is likely that N_R will be based on the design life so that the acting reference stress range and maximum allowable stress range (S_R and S'_R) will refer to N_T .

Section 3 Application of Simplified Fatigue Method to Jacket Type Fixed Offshore Installations

5.3.1 General

The simplified fatigue analysis method is widely used in offshore engineering. For the common steel jacket type platform, and similar structural types that meet the application criteria of API RP 2A-WSD, significant effort has been expended over the years by the industry to calibrate the simplified fatigue analysis method contained in API RP 2A-WSD so that it will serve as an appropriate basis for the fatigue design of such structures. Where relevant conditions given in API RP 2A-WSD are satisfied, CCS recognizes the API RP 2A-WSD simplified method as an acceptable basis to perform the fatigue assessment for a fixed platform.

The use of the API RP 2A-WSD simplified fatigue assessment criteria for a fixed offshore installation at offshore sites where it is shown that the fatigue inducing effects caused by wave loads of the environment are equal to, or less severe than, Bohai Bay sites allows its use in these situations as well. But special consideration is to be given to the ice-induced vibration fatigue which might exist in the northern part of Bohai Bay.

It may not be prudent to use this assessment method as the only basis to judge the acceptability of a design in deeper water, e.g. jackets in oil and gas fields of East and South China Seas because of possibly significant dynamic amplification. In such cases the method can be employed as a screening tool to help identify and prioritize fatigue sensitive areas of the jacket structure. However, it would be expected that the fatigue assessment will ultimately be based on a direct calculation method; and this most likely is to be a spectral-based fatigue assessment. The spectral-based method of fatigue assessment is discussed in the next chapter.



CHAPTER 6 SPECTRAL-BASED FATIGUE ANALYSIS METHOD

Section 1 General Provisions

6.1.1 General

The offshore steel structure produces motion and deformation due to the effect of irregular waves. If it is understood by the concept of energy converter in physics, the irregular waves can be regarded as input, which, by means of the offshore steel structure acting as the energy converter, is converted to the motion and deformation of structure, i.e., the response of structure.

Where the response of system is superimposed and homogenous, the system is referred to as a linear system. Where the superposition and homogeneity of the system do not change with time, the system is referred to as a time constant linear system. Where the input of such system is a stationary and random process, the output is also a stationary and random process.

When solving the issue of the response of offshore steel structures in irregular waves, the structure is used as a time constant linear system by means of various corrections. When assuming that the wind and wave represent a stationary random Gaussian process, the corresponding motion and stress of structural members also represent a random Gaussian process, and the amplitude complies with Rayleigh distribution.

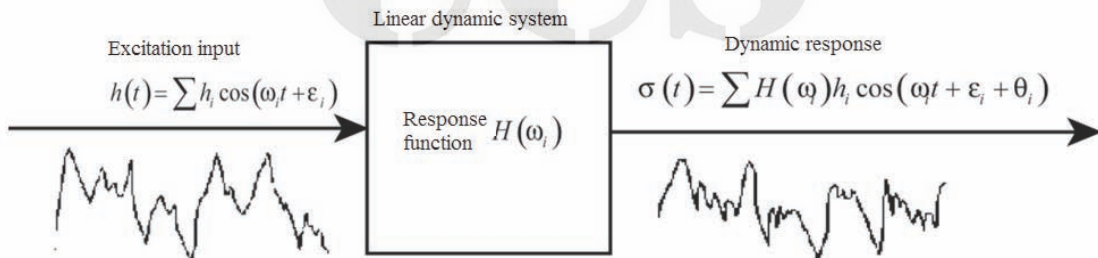


Figure 6.1.1 Linear Dynamic Amplification System

Under the above assumption, the stress response produced by structures due to random waves may be determined by “stress response function”, i.e. the elastic system of structure is regarded as a linear dynamic amplification system where the wave is an input and the stress response of structure is an output. The value is determined by the input wave and output stress response function as shown in Figure 6.1.1. The physical meaning of stress response function is the stress response produced by unit amplitude cosine wave of different frequencies. If the input random wave is expressed by spectrum, the stress spectrum of certain structural point may be obtained in order to calculate the fatigue damage or life of such point.

A spectral-based fatigue assessment produces results in terms of fatigue induced damage or fatigue life, and it is therefore referred to as a direct method. With ocean waves considered the main source of fatigue demand, the fundamental task of a spectral fatigue analysis is the determination of the stress range transfer function, $H_\sigma(\omega|\theta)$, which expresses the relationship between the stress, σ , at a particular structural location per ‘unit wave height,’ and wave of frequency (ω) and heading (θ).

Spectral-based fatigue analysis method is a complex and numerically intensive technique. As such there is more than one variant of the method that can be validly applied in a particular case. The method is most appropriate when there exists a linear relationship between wave height and the wave-induced loads, and the structural response to these loads is linear. Adaptations to the basic method have been developed to account for various non-linearities, but where there is doubt about the use of such methods, recourse can be made to time-domain analysis methods as mentioned in Section 5 of this Chapter.

6.1.2 Floating offshore installations

For column-stabilized and similar offshore engineering structures with large (effective) diameter structural elements, the wave and current induced load components are not dominated by the drag component. Then a linear relationship between wave height and stress range exists. In such a case, the method described in Section 2 of this Chapter applies.

6.1.3 Jacket type fixed platform installations

For a jacket type platform, because the typical sizes of the submerged structural elements are small as compared to wave length (generally the ratio of wave length to pole diameter is greater than 5), the wave and wave with current induced loads are likely to be drag-dominated, thus requiring a structural analysis method that will linearize the hydrodynamic loads. If the dynamic response characteristics of the platform structure make dynamic amplification likely, this effect is also to be included in the spectral analysis method to be employed in the fatigue assessment of the structure. Reference is to be made to API RP 2A-WSD, Commentary Section 5, for information on analysis procedures that are applied in the fatigue analysis of this type of offshore installation.

Section 2 Spectral-based Fatigue Analysis for Offshore Engineering Structures

6.2.1 General

The spectral-based fatigue analysis for offshore engineering structures is based on the following assumptions:

- (1) Ocean waves are the source of the fatigue inducing stress range acting on the structural system being analyzed.
- (2) In order for the frequency domain formulation and the associated probabilistically based analysis to be valid, load analysis and the associated structural analysis are assumed to be linear. Hence the calculation results from unit wave height can be used to derive the calculation results of each wave height, and linear superposition of stress transfer functions are considered valid.
- (3) Non-linearities, brought about by non-linear roll motions and intermittent application of loads such as wetting of the side shell in the splash zone, are to be specially considered.
- (4) Structural dynamic amplification, transient loads and effects such as springing may be linearized equivalently.

Also, for the particular method presented below, it is assumed that the short-term stress variation in a given sea-state is a random narrow banded stationary process. Therefore, the short-term distribution of stress range can be represented by a Rayleigh distribution. Where the bandwidth of short-term stress variation exerts a relatively large influence, Rice distribution may be considered.

6.2.2 Stress transfer function

It is preferred that a structural analysis is carried out at each frequency, heading angle, and loading condition employed in the analysis, and that the resulting stresses are used to generate the stress transfer function directly.

The frequency range and the frequency increment that are used are to be appropriate to establish adequately the stress transfer functions and to meet the needs of the extensive numerical integrations that are required in the spectral-based analysis method. For the wave heading range of 0 to 360 degrees, increments in heading are not to be larger than 30 degrees.

6.2.3 Outline of a closed form spectral-based fatigue analysis procedure

In the ‘short-term closed form’ approach, described below, the stress range is normally expressed in terms of probability density functions for different short-term intervals corresponding to the individual cells (or bins) of the wave scatter diagram. These short-term probability density functions are derived by a spectral approach based on the Rayleigh distribution method whereby it is assumed that the variation of stress is a narrow banded random Gaussian process. When a narrow banded assumption is not valid for the stress process, the number of stress cycles is corrected to reflect the effect of bandwidth in the calculation of short-term fatigue damage, generally by applying a correction factor, e.g. Wirsching’s rainflow correction factor. Having calculated the short-term damage, the total fatigue damage is calculated through their weighted linear summation (using Miner’s rule).

6.2.4 Key steps in closed form damage calculation

The following derivation is only aimed at a specific loading condition and heading. For different loading conditions and headings, weighted fatigue cumulative calculation is to be carried out in accordance with the probability of occurring of each condition and each heading. Weighted method is given in 2.2.4, Chapter 2 of the Guidelines.

- (1) Determine the complex stress transfer function, $H_\sigma(\omega|\theta)$, at a structural location of interest for a particular load condition. This is done in a direct manner where structural analyses are performed for the specified ranges of wave frequencies and headings, and the resulting stresses are used to generate the stress transfer function explicitly at different headings θ .
- (2) Generate a stress energy spectrum, $S_\sigma(\omega|H_s, T_z, \theta)$, by means of stress transfer function $H_\sigma(\omega|\theta)$ and the wave spectrum density function $S_\eta(\omega|H_s, T_z)$ of a short-term sea state in the wave scatter diagram from the following formula:

$$S_\sigma(\omega|H_s, T_z, \theta) = |H_\sigma(\omega|\theta)|^2 \cdot S_\eta(\omega|H_s, T_z) \quad (6.1)$$

where: $S_\sigma(\omega|H_s, T_z, \theta)$ — stress spectrum;

$S_\eta(\omega|H_s, T_z)$ — wave spectrum;

$H_\sigma(\omega|\theta)$ — stress transfer function.

- (3) Calculate the spectral moments. The n^{th} spectral moment, m_n , is calculated as follows:

$$m_n = \int_0^\infty \omega^n S_\sigma(\omega|H_s, T_z, \theta) d\omega \quad (6.2)$$

Most fatigue damage is associated with low or moderate seas, hence confused short-crested sea conditions must be allowed. Confused short-crested seas result in a kinetic energy spread, which is modeled using the cosine-squared function, $(2\pi)\cos^2 \alpha$. Generally, cosine-squared spreading is assumed from +90 to -90 degrees on either side of the selected wave heading. Applying the wave spreading function modifies the spectral moment as follows:

$$m_n = \int_0^\infty \sum_{\alpha=-90}^{\alpha=+90} \left(\frac{2}{\pi} \right) \cos^2 \alpha [\omega^n S_\sigma(\omega | H_s, T_z, \theta)] d\omega \quad (6.3)$$

(4) Using the spectral moments, the Rayleigh probability density function (pdf) describing the short term stress-range distribution, the zero up-crossing frequency of the stress response and the bandwidth parameter are calculated as follows:

Rayleigh probability density function:

$$g(S) = \frac{S}{4\sigma^2} \exp \left[-\left(\frac{S}{2\sqrt{2}\sigma} \right)^2 \right] \quad (6.4)$$

Zero-up crossing frequency, in Hz:

$$f = \frac{1}{2\pi} \sqrt{\frac{m_2}{m_0}} \quad (6.5)$$

Bandwidth parameter:

$$\varepsilon = \sqrt{1 - \frac{m_2^2}{m_0 m_4}} \quad (6.6)$$

where: S — stress range (twice the stress amplitude);

$$\sigma = \sqrt{m_0};$$

m_0 — spectral zero-order moment, see formula (6.2);

m_2 — spectral second-order moment, see formula (6.2);

m_4 — spectral fourth-order moment, see formula (6.2).

(5) Calculate cumulative fatigue damage based on Palmgren-Miner's rule. When the probability density function of the short term stress-range distribution due to a short-term sea state is represented by Rayleigh distribution as shown in formula (6.4), the short term damage incurred in the i -th sea-state assuming a S-N curve of the form $N=Ks^m$ is given by:

$$D_i = \left(\frac{T}{K} \right) \int_0^\infty s^m f_{0i} p_i g_i ds \quad (6.7)$$

where: D_i — damage incurred in the i -th sea-state;

T — design life, in seconds;

f_{0i} — zero-up-crossing frequency of the stress response, i.e. the average operating frequency of stress range, in Hz;

$f_{0i} = \frac{1}{2\pi} \sqrt{\frac{m_{2i}}{m_{0i}}}$, where m_{2i} and m_{0i} are respectively spectral second-order moment and zero-order moment in the i -th sea-state;

p_i — joint probability of significant wave height and zero-up-crossing frequency;

s — specific value of stress range;

g_i — probability density function governing s in the i -th sea state, see formula (6.4).

m and K are physical parameters describing the S-N curve, see Section 5 of Chapter 2.

Summing D_i ($i=1, M$) over all the sea-states (assuming a total of M) in the wave scatter diagram leads to the total cumulative damage, D . Therefore:

$$D = \sum_{i=1}^M D_i = \left(\frac{f_0 T}{K} \right) \int_0^\infty s^m \left[\sum_{i=1}^M f_{0i} p_i g_i / f_0 \right] ds \quad (6.8)$$

where: D — total cumulative damage at calculation point;

f_0 — “average” frequency of s over the lifetime at calculation point, in Hz;

$f_0 = \sum_i f_{0i}$ (where the summation is done from $i = 1$ to M , the number of considered sea-states);

p_i — joint probability of significant wave height and zero-up-crossing frequency;

s — specific value of stress range;

g_i — probability density function governing s in the i -th sea state;

T — design life, in seconds.

Introducing, long-term probability density function, $g(s)$ of the stress range and total number of cycles in design life N_T :

$$g(s) = \frac{\sum_i f_{0i} p_i g_i}{\sum_i f_{0i} p_i}, \quad N_T = f_0 T \quad (6.9)$$

the expression for total cumulative damage, D can be re-written as:

$$D = \frac{N_T}{K} \int_0^\infty s^m g(s) ds \quad (6.10)$$

(6) If the total number of cycles N_T corresponds to the required minimum design life of 20 years, the calculated fatigue life would then be equal to $20/D$. The fatigue safety check is to be done in accordance with Section 1 of Chapter 4.

(7) Closed form damage expression

① For all one-segment linear S-N curves, the closed form expression of damage, D as given by formula (6.8) is as follows:

$$D = \frac{T}{K} \left(2\sqrt{2} \right)^m \Gamma \left(\frac{m}{2} + 1 \right) \sum_{i=1}^M \lambda(m, \varepsilon_i) f_{0i} p_i (\sigma_i)^m \quad (6.11)$$

where: $\sigma_i = \sqrt{m_0}$, square root of spectral zero-order moment for the i -th considered sea state;

Γ — gamma function, see formula (5.7) of Chapter 5;

λ — rain flow factor of Wirsching and is defined as:

$$\lambda(m, \varepsilon_i) = a(m) + [1 - a(m)] [1 - \varepsilon_i]^{b(m)} \quad (6.12)$$

where: $a(m) = 0.926 - 0.033m$;

$b(m) = 1.587m - 2.323$;

ε_i — spectral bandwidth, see formula (6.6).

- ② For bi-linear S-N curves (see Figure 2.5.3) where the negative slope changes at point (N_q, S_q) from m to $r = m + \Delta m (\Delta m > 0)$ and the constant K_1 changes to K_2 , the expression for damage as given in formula (6.11) is as follows:

$$D = \frac{T}{K_1} \left(2\sqrt{2}\right)^m \Gamma\left(\frac{m}{2} + 1\right) \sum_{i=1}^M \lambda(m, \varepsilon_i) \mu_i f_{0i} p_i (\sigma_i)^m \quad (6.13)$$

where: μ_i — endurance factor having its value between 0 and 1 and measuring the contribution of the stress cycle in lower branch of the S-N curve to the fatigue damage. It is defined as:

$$\mu_i = 1 - \frac{\int_0^{S_q} s^m g_i ds - \left(\frac{K_1}{K_2}\right) \int_0^{S_q} s^{m+\Delta m} g_i ds}{\int_0^{\infty} s^m g_i ds} \quad (6.14)$$

If probability density function, $g(s)$ of the stress range is a Rayleigh distribution, then μ_i is:

$$\mu_i = 1 - \frac{\Gamma_0\left(\frac{m}{2} + 1, \nu_i\right) - (1/\nu_i)^{\Delta m/2} \Gamma_0\left(\frac{m + \Delta m}{2} + 1, \nu_i\right)}{\Gamma(m/2 + 1)} \quad (6.15)$$

where: $\nu_i = \frac{1}{8} \left(\frac{S_q}{\sigma_i}\right)^2$;

Γ_0 — incomplete gamma function, see formula (5.8) of Chapter 5.

6.2.5 Fatigue safety check is described in Section 1 of Chapter 4.

Section 3 Combined Method of Low-frequency and Wave-frequency Fatigue Damage

6.3.1 When the process that induces variable stresses in a structural detail contains wave-frequency and low-frequency components, the process is considered to be wide-banded. Although the Wirsching's rainflow counting correction of formula (6.12) can be applied to account for a wide band process, the formulae are calibrated only to a wave frequency process.

6.3.2 When wave-frequency and low-frequency stress responses are obtained separately, simple summation of fatigue damage from the two frequency bands does not count the effects of simultaneous occurrence of the two frequency bands processes. This method is therefore non-conservative.

6.3.3 There is an alternative method, which is both conservative and easy to use, that is known as the combined spectrum method. In this method, the stress spectra for the two frequency bands are combined. The standard deviation and mean zero-up-crossing frequency of the combined stress process are given, respectively, as

$$\begin{aligned} \sigma_c &= (\sigma_w^2 + \sigma_l^2)^{1/2} \\ f_{0c} &= (f_{0w}^2 \sigma_w^2 + f_{0l}^2 \sigma_l^2)^{1/2} / \sigma_c \end{aligned} \quad (6.16)$$

where: σ_w — standard deviation of the wave-frequency stress components, equal to $\sqrt{m_{0w}}$, where m_{0w} is wave-frequency spectral zero-order moment, see formula (6.2);

σ_l — standard deviation of the low-frequency stress components, equal to $\sqrt{m_{0l}}$, where m_{0l} is low-frequency spectral zero-order moment, see formula (6.2);

f_{0w} — mean zero-up-crossing frequency of the wave-frequency stress components; calculation method is given in formula (6.7);

f_{0l} — mean zero-up-crossing frequency of the low-frequency stress components; calculation method is given in formula (6.7).

For each short-term sea state, the fatigue damage for the combined wave-frequency and low-frequency process is obtained by substituting the above σ_c and f_{0c} for the combined process into the calculation formula of spectral fatigue given in Section 2 of this Chapter.

6.3.4 However, if both frequency components of stress range are significant, the above-mentioned combination method of formula (6.16) may be too conservative (for ratio of wave frequency to low frequency greater than 10, the ratio of calculated damage to actual damage might be as large as 2) since the wave-frequency contribution is expected to dominate, thus controlling the mean zero-up-crossing frequency of the combined stress process. To eliminate the conservatism, a correction factor given below can be applied to the calculated fatigue damage of the sea state:

$$\lambda = \frac{f_{op}}{f_{0c}} \left[\lambda_l^{\frac{m}{2}+2} \left(1 - \sqrt{\lambda_w/\lambda_l} \right) + \frac{m\Gamma(m/2+1/2)}{\Gamma(m/2+1)} \left(\sqrt{\pi\lambda_w\lambda_l} \right) \right] + \frac{f_{0w}}{f_{0c}} \lambda_w^{m/2} \quad (6.17)$$

where: $\lambda_l = \sigma_l^2 / \sigma_c^2$;

$= \sigma_w^2 / \sigma_c^2$;

$f_{0p} = (\lambda_l^2 f_{0l}^2 + \lambda_l \lambda_w f_{0w}^2)^{1/2}$;

m — slope parameter of the lower cycle segment of the S-N curve;

Γ — gamma function, see formula (5.7) of 5.2.3 of this Chapter.

Attention is to be given to the following requirements during correction:

- (1) where the ratio of wave frequency to low frequency is less than 4, the above correction factor is not to be used;
- (2) the above correction is based on one-segment linear S-N curves, and therefore one-segment linear curve is to be used during damage calculation, ignoring the change of slope of S-N curves.

6.3.5 An alternative, more accurate method of fatigue damage calculation is to simulate the combined stress process in the time domain, and employ rainflow counting to count the stress cycles for each sea state. The accumulative fatigue damage is the weighted summation of the damages from all sea states considering the probability of occurrence of each sea state, as given in the wave scatter diagram.

Section 4 Fatigue Damage due to Loading and Offloading of Produced Fluids

6.4.1 Where applicable, the fatigue damage due to low-cycle, high-stress-range situations caused by loading/offloading of produced fluids is also to be considered in the total fatigue damage, e.g. fatigue damage of bulkhead and side shell details of FPSO.

6.4.2 The low-cycle loads of loading/offloading of produced fluids may produce large stress range that even exceeds the yield strength of the material used. In this case, ordinary S-N curves are not valid at this level of stress ranges. It is recommended that S-N curve or $\Delta\varepsilon$ -N curve (total strain range vs. cycles to failure) suitable for large stress ranges be used in the computation of damage instead.

6.4.3 Fatigue damage induced by these low-cycle loads is usually estimated with the cycle counting for the stress range and can be added to that induced by wave loads via linear summation. The analysis procedure usually includes:

- (1) selection of structural details for fatigue damage calculation;
- (2) definition of the loading configurations that characterize a typical complete loading and offloading cycle experienced by the vessel in the field;
- (3) calculation of still water stress (including still water bending moment and still water pressure) in each loading condition, generally including full load and empty condition;
- (4) definition of the stress sequence in a complete loading and offloading cycle according to (2) and (3);
- (5) where the stress range does not exceed the yield strength of material, the fatigue damage of a complete loading/offloading cycle is calculated according to ordinary S-N curves;
- (6) calculation of total number of loading/offloading during service life, which is multiplied by fatigue damage obtained in (5) for calculation of total fatigue damage and is not to be less than 1,200 for service life of 20 years.

6.4.4 The standard deviation and mean zero-up-crossing frequency of stress process may also be determined according to the loading manual or observation data (since the crew may deviate from the typical loading cases in the operating manual by using control of loading/offloading by means of direct calculation that keeps the vessel on an even keel without exceeding permissible stress limits). And then the fatigue damage is calculated according to Section 3 of this Chapter. The calculated standard deviation may be combined with the stress process induced by wave and drift loads via the square root of the sum of the squares (SRSQ) method. The analysis procedure usually includes:

- (1) selection of structural details for fatigue damage calculation;
- (2) definition of the loading configurations that characterize a typical complete loading and offloading cycle experienced by the vessel in the field;
- (3) calculation of still water stress in each loading condition;
- (4) definition of the stress sequence in a complete loading and offloading cycle according to (2) and (3) and use of a statistical method to calculate the standard deviation and the mean zero-up-crossing frequency of stress due to loading/offloading.

Section 5 Time-Domain Analysis Fatigue Assessment Methods

6.5.1 Due to the limitations of the spectral method, e.g. linear and hard to predict low-frequency fatigue stresses, the time-domain method along with its associated rainflow counting technique is employed in the fatigue assessment of Tension Leg Platforms and SPAR Platforms to predict the fatigue life of structures.

6.5.2 In the time-domain approach, the long-term wave condition is discretized into representative sea-states of short duration and constant intensity. A time history of the wave kinematics for the short duration is generated from the wave spectrum. Hydrodynamic loads are then calculated based on the wave kinematics and applied to the structural model. Nonlinear effects can be included in the analysis. Structural analyses are performed to estimate stress responses. Rainflow counting technique is applied to estimate the number of stress cycles based on the stress time-history. After the number of stress cycles is obtained, the selected S-N curves can be used for the assessment of the fatigue damage.

6.5.3 The high order load effect may be considered in the time-domain analysis. The response analysis may be carried out by applying the measured load time history to the structure rather than based on assumed spectrum shape, in order to obtain the stress response time history of certain detail.

6.5.4 In areas with severe ice conditions of Bohai Bay, where the ice force spectrum is unavailable, similar time-domain analysis method is recommended for the fatigue assessment of ice-induced vibration of fixed units.



CHAPTER 7 FATIGUE ANALYSIS METHOD BASED ON FRACTURE MECHANICS

Section 1 General

7.1.1 After a crack occurs in any part of structure, whether the crack will grow under alternating loads or the growth rate depends on the stress field of crack tip, i.e. the value and condition of stress.

7.1.2 The S-N curve approach cannot predict the crack growth rate and the remaining fatigue life. Fracture mechanics method is to be used for the assessment of fatigue life of structure after a crack is discovered.

7.1.3 The fatigue life of steel structures of offshore engineering is generally taken as the number of cycles corresponding to the occurrence of through thickness crack, including crack initiation life and crack growth life.

7.1.4 For the assessment of fatigue life of steel structures of offshore engineering, while the S-N curve approach is recommended, fracture mechanics may be used for fatigue life assessment as supplement to the S-N curve approach. The fracture mechanics method may be considered in the following cases:

- (1) When assessing the fitness for purpose of a detail/joint for which a crack is discovered and measured. The crack is difficult and/or expensive to repair and a ‘repair/no-repair’ decision must be made. In accordance with the assessment results of fracture mechanics, one of the three choices might be given: immediate repair, no repair for the moment but with enhanced observation, or no need of repair.
- (2) In a design context when the detail/joint is unusual and is not adequately represented by the standard S-N classification or when a detail/joint is subjected to the influence of multiple, complex stress concentrations. For these special cases, CCS may require additional studies based on fracture mechanics.
- (3) When developing and updating in-service inspection planning programs.
- (4) When assessing the remaining fatigue life of an aging structure.

7.1.5 The objective of this Chapter is to provide basic information on the fatigue assessment method based on fracture mechanics. The specific steps of fatigue life prediction based on the information are given in Section 3 of this Chapter. For more details, reference may be made to relevant internationally recognized standards, e.g. BS 7910 Guide to methods for assessing the acceptability of flaws in metallic structures.

Section 2 Crack Growth Model

7.2.1 Paris law

The fracture mechanics analysis for fatigue strength relies on crack growth data. Strength is characterized by a relationship between the crack growth rate, da/dN , and the stress intensity factor range of crack tip, ΔK (also referred to as Paris law):

$$\frac{da}{dN} = C(\Delta K)^m \quad (7.1)$$

where: N — number of stress cycles;

a — depth of the crack, a function of N ;

C — Paris coefficient, i.e. intercept of $\log(da/dN)$ axis by the logarithm line;

m — exponent as determined from crack growth data (also referred to as the slope of logarithm line);

ΔK — stress intensity factor range, equal to $Y(a)S\sqrt{\pi a}$, where $Y(a)$ is geometry function and S is stress range.

The formula above also applies to the calculation of flat plate crack growth along the length direction, where a is to be taken as half of crack length and C , m and ΔK are to be taken as values corresponding to the crack growth along the length direction.

7.2.2 Determination of the Paris parameters, C and m

The Paris parameters C and m depend on the material and the applied conditions, such as stress ratio, environment, frequency and waveform of test load in the crack growth test. Whenever possible, C and m data relevant to the particular material under service conditions is to be used and where any doubt exists concerning the influence of the environment such data is to be obtained. If the available data are sufficient to define C , the chosen values are to correspond to the mean plus two standard deviation of $\log da/dN$. When such data are not available, suitable values of C and m are to be determined from other relevant published data.

For more details on C and m , reference may be made to relevant internationally recognized standards, e.g. BS 7910 Guide to methods for assessing the acceptability of flaws in metallic structures.

Section 3 Crack Growth Life Prediction

7.3.1 Relationship between stress cycles and crack depth

The analysis objective is number of cycles to failure, or alternatively the crack size associated with a given life. In doing so, it is assumed that the real flaws can be idealized as sharp-tipped cracks.

The number of cycles, N , required for a crack to propagate from an initial size, a_i , to a crack depth a , can be determined from the following formula:

$$NS^m = \frac{1}{C} \int_{a_i}^a \frac{1}{[Y(x)]^m (\pi x)^{m/2}} dx \quad (7.2)$$

When $a = a_c$, the critical crack depth, failure is assumed, and N would be the number of cycles to failure.

Note that this formula (7.2) is identical to the S-N model of Chapter 2, ($NS^m = K$). The fatigue strength coefficient, K , will be equal to the right hand side of formula (7.2). This can be useful for the simplified fatigue assessment method of Chapter 5.

7.3.2 Determination of initial crack size

The fracture mechanics model critically depends upon the value of the initial crack size, whose value is to be determined accounting for the accuracy of the NDE inspection methods, which are used to detect defects during fabrication.

In the context of design, an assumption of initial crack size must be made. The initial crack size to be used in the calculation is to be evaluated in each case, taking into account the initial crack size for various fabrication welds, geometries and the survey accuracy. For surface cracks starting from the transition between weld/base material, a crack depth of 0.5 mm may be assumed if no other reliable data on crack depth are available.

Section 4 Possible Failure Modes of Fatigue Assessment Based on Fracture Mechanics

7.4.1 The analyst must use engineering judgment with regard to the choice of a_c . Each of the following failure modes is to be considered carefully in making this judgment:

- (1) unstable brittle fracture;
- (2) yielding of the remaining section;
- (3) leakage;
- (4) stress corrosion;
- (5) instability;
- (6) creep.

Section 5 Determination of Geometry Function

7.5.1 There are several options for determining $Y(a)$. Direct analysis for $Y(a)$ or the use of applicable, recognized solutions recognized by the industry may be employed. When submitting the fatigue assessment report, the analyst is to submit documentation demonstrating the validity of the analysis method, or of the published geometry function $Y(a)$ obtained from the Fracture Mechanics based analysis. It is generally recommended to select the geometry function in a conservative manner.

CHAPTER 8 IMPROVEMENT METHODS OF FATIGUE LIFE

Section 1 General

8.1.1 It is to be noted that improvement of the toe will not improve the fatigue life of the structural detail if fatigue cracking from the root is the most likely failure mode. The improvement methods of fatigue strength given in this Chapter are for conditions where the root is not considered to be a critical initiation point. Except for weld profiling (section 2 of this Chapter) the effect from different improvement methods as given in Sections 3 to 5 of this Chapter on the fatigue life cannot be added.

8.1.2 Reference is made to IIW Recommendations, on post weld improvement with respect to execution of the improvement.

Section 2 Weld Profiling

8.2.1 By weld profiling in this Section is understood profiling by machining or grinding as profiling by welding only is not considered to be an efficient mean to improve fatigue strength.

8.2.2 In fatigue strength calculations of design stage, the thickness correction exponent in 2.5.9 of Chapter 2 may be reduced to 0.15 (including tubular and non-tubular details) provided that the weld is profiled by either machining or grinding to a radius of approximately half the plate thickness.

8.2.3 When weld profiling is performed by either machining or grinding and complies with the requirements of this Section, a reduced stress for fatigue calculation of the structural detail can be calculated as:

$$\sigma_{reduced} = \sigma_m \cdot \alpha + \sigma_b \cdot \beta \quad (8.1)$$

where: $\sigma_{reduced}$ —reduced stress for fatigue calculation of calculation point;

σ_m —membrane stress component of calculation point;

σ_b —bending stress component of calculation point;

α —reduction factor of membrane stress component, $\alpha=0.47+0.17(\tan\varphi)^{0.25}(T/R)^{0.5}$;

β —reduction factor of bending stress component, $\beta=0.60+0.13(\tan\varphi)^{0.25}(T/R)^{0.5}$.

where T , R and φ are shown in Figure 8.2.3.

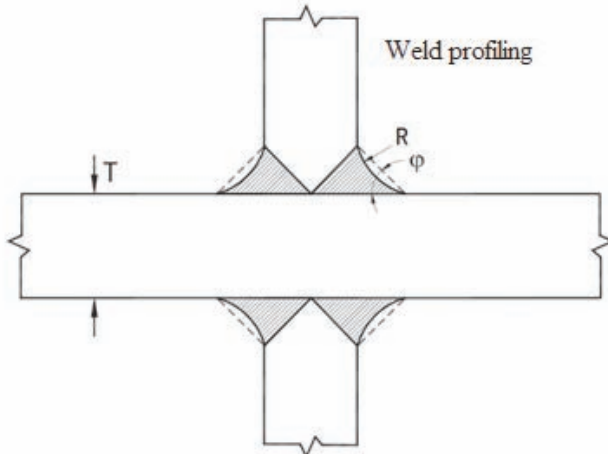


Figure 8.2.3 Parameters of Weld Profiling by Machining or Grinding

8.2.4 The weld profiling of structural detail does not change the classification of the detail, which means the reduced stress $\sigma_{reduced}$ is to be used together with the same S-N curve as the detail is classified for without weld profiling.

8.2.5 In addition the fatigue life can be increased taking account of weld toe grinding, reference is made to Section 3 of this Chapter. However, the maximum improvement factor from weld profiling by grinding and weld toe grinding is then to be limited to a factor 2 on fatigue life.

Section 3 Weld Toe Grinding

8.3.1 Where grinding of the weld toes below any visible undercuts is performed the fatigue life of assessment calculation may be increased by a factor given in Table 8.3.1. In addition the thickness correction exponent in 2.5.9 of Chapter 2 may be reduced to 0.2 (including tubular and non-tubular details), see Figure 8.3.1.

Times of Improvement on Fatigue Life by Different Methods Table 8.3.1

Improvement method	Improvement factor on fatigue life
Grinding	2
TIG dressing	2
Hammer peening	4

Notes: ① The maximum S-N class that can be claimed by fatigue life improvement method is C depending on NDE and different techniques.

- ② The improvement effect is dependent on tool used and workmanship. Therefore, if the fabricator is without experience with respect to hammer peening, it is recommended to perform fatigue testing of relevant detail (with and without hammer peening) before a factor on improvement is decided.
- ③ Improvement of welded connections provides S-N data that shows increased improvement in the high cycle region of the S-N curve as compared with that of low cycle region. Thus the slope of S-N curve changes more slowly (factor m is increased) by improvement. In the high cycle region an alternative way of calculating fatigue life after improvement is by analysis of fatigue damage by using new S-N curves. Such S-N curves are obtained based on improvement of test data of structural detail and subject to agreement of CCS.

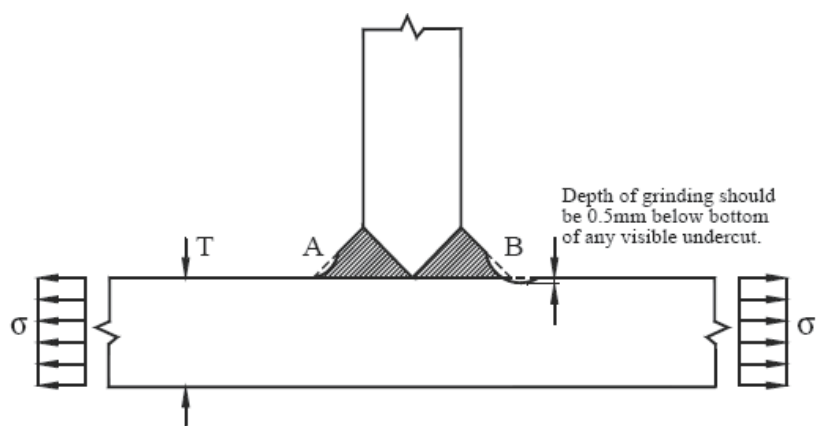


Figure 8.3.1 Grinding of Weld Toe

8.3.2 Grinding a weld toe tangentially to the plate surface, as at A of Figure 8.3.1, will produce only little improvement in fatigue strength. To be efficient, grinding is to extend below the plate surface in order to remove toe defects and provide effective corrosion protection of the grinding area. Grinding is normally carried out by a rotary burr. The treatment is to produce a smooth concave profile at the weld toe with the depth of the depression penetrating into the plate surface to at least 0.5 mm below the bottom of any visible undercut. In general the depth of concave is to be small insofar as practicable with a maximum value of 1 mm. In any case, the grinding depth is not to exceed 2 mm or 7% of the plate thickness, whichever is smaller. The scope of grinding is to extend beyond the high stress area.

8.3.3 It is to be noted that if grinding is required to achieve a specified fatigue life, the hot spot stress is rather high. Due to grinding a larger fraction of the fatigue life is spent during the initiation of fatigue cracks, and the crack grows faster after initiation as compared to structural details without grinding. As a result, due attention is to be given during service life to details without large fatigue life margin after taking into account grinding contribution, in order to detect the cracks before they become dangerous for the integrity of the structure.

8.3.4 In some structures the welds are machined flush to achieve a high S-N class. It has to be documented that weld overfill has been removed by grinding and that the surface has been proven free from defects. The weld overfill may be removed by a coarse grinder tool such as a coarse grit flapper disk, grit size 40-60. The final surface is to be achieved by fine grit grinding below that of weld toe defects. The surface is to show a smooth or polished finish with no visible score marks. The roughness is to correspond to $R_a = 3.2\mu\text{m}$ or better. (It is to be remembered that if the area is planned to be coated, a roughness around $R_a = 3.2\mu\text{m}$ is often recommended). The surface is to be checked by magnetic particle inspection. It is assumed that grinding is performed until all indications of defects are removed. Then possible presence of internal defects in the weld may be a limitation for use of a high S-N class and it is important to perform a reliable non-destructive examination and use acceptance criteria that are in correspondence with the S-N classification that is used.

8.3.5 At design stage, the contribution of weld toe grinding to fatigue life improvement is not considered. The designer is to improve the fatigue strength of structural detail or to reduce the stress range by means of other methods, and keep the possibility of grinding during or after fabrication as a supplementary method. Where grinding is used, the grinding standards of structural details are to include grinding scope, smoothness, final weld shape, grinding techniques and adopted quality standards, which are to be clearly indicated in the applicable drawings and submitted for information together with supporting calculation information. Such information is to indicate recommended fatigue life factor. In general grinding has been considered as an efficient method for reliable fatigue life improvement during fabrication. Grinding also improves the reliability of surveys after construction and during service life.

Section 4 Tungsten Inert Gas (TIG) Dressing

8.4.1 The weld fatigue life may be improved by TIG dressing by a factor given in Table 8.3.1. Due to uncertainties regarding quality assurance of the welding process and TIG dressing, this method may not be recommended for general use at the design stage.

Section 5 Hammer Peening

8.5.1 The weld fatigue life may be improved by means of hammer peening by a factor given in Table 8.3.1. However, the following limitations apply:

- (1) Hammer peening is only to be used on members where failure will be without substantial consequences.
- (2) Overload in compression must be avoided, because the residual stress set up by hammer peening will be destroyed.
- (3) It is recommended to grind a steering groove by means of a rotary burr of a diameter suitable for the hammer head to be used for the peening. The peening tip must be small enough to reach weld toe.

Due to uncertainties regarding workmanship and quality assurance of the process, this method may not be recommendable for general use at the design stage.



CHAPTER 9 EXTENDED FATIGUE LIFE

Section 1 General

9.1.1 An extended fatigue life is considered to be acceptable and within normal design criteria if the calculated fatigue life is longer than the total design life times the safety factor of fatigue. Otherwise an extended life may be based on results from performed surveys throughout the prior service life. Such an evaluation is to be based on:

- (1) Calculated crack growth characteristics, i.e. crack length/depth as function of time/number of cycles (this depends on type of joint, type of loading, and possibility for redistribution of stress).
- (2) Reliability of survey method used (It is recommended to use Eddy Current or Magnetic Particle Inspection for survey of surface cracks starting at hot spots), and elapsed time from last survey performed.

9.1.2 For welded connections that are ground and inspected for fatigue cracks the following procedure may be used for calculation of an elongated fatigue life:

- (1) Provided that grinding below the surface to a depth of approximately 1.0 mm is performed and that fatigue cracks are not found by a detailed Magnetic Particle Inspection of the considered hot spot region at the weld toe, the fatigue damage at this hot spot may be considered to start again at zero. If a fatigue crack is found, a further grinding is to be performed to remove any indication of this crack. If more than 7% of the thickness is removed by grinding, the effect of this on increased stress is to be included when a new fatigue life is assessed. In some cases as much as 30% of the plate thickness may be removed by grinding before a weld repair is resorted to. This depends on type of joint, loading condition and accessibility for a repair.
- (2) It is to be noted that fatigue cracks growing from the weld root of fillet welds can hardly be detected by NDE. Also, the fatigue life of such regions cannot be improved by grinding of the surface.
- (3) It is to be remembered that if renewal of one hot spot area is performed by local grinding, there are likely other areas close to the considered hot spot region that are not ground and that has cumulated certain damage under a significant dynamic loading during past service. The fatigue damage at such area may be reassessed taking into account the correlation with a ground neighbour hot spot region that has not cracked and the reliability of performed in-service surveys.

APPENDIX 1 STRUCTURAL DETAIL CLASSIFICATION CORRESPONDING TO S-N CURVE FATIGUE ASSESSMENT

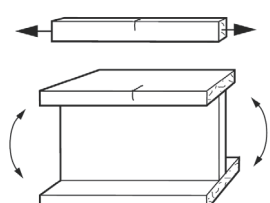
Section 1 Structural Detail Classification Used in This Appendix

A1.1.1 The structural detail classification of this Appendix consists of 7 types;

- (1) Non-welded base material;
- (2) Continuous welds essentially parallel to the direction of applied stress;
- (3) Butt welds essentially perpendicular to the direction of applied stress;
- (4) Welded attachments on the surface or edge of a stressed member;
- (5) Load-carrying fillet and T-butt welds;
- (6) Small attachments on welded girders or tubular members;
- (7) Welded small attachments on tubular members.

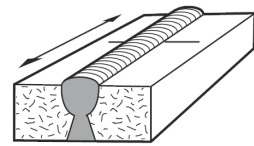
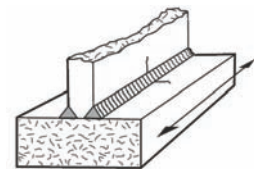
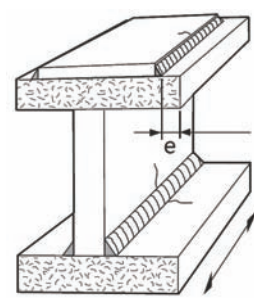
Type 1 Materials Free From Welding

Table A1.1

Type number, description and notes on mode of failure	S-N curve	Joint description	Example and failure mode
1.1 Base material			
(a) Edges of plates and sections without flame-cut and free from cracks and notches.	B	Beware of using Class B for a member which may acquire stress concentrations during its life, e.g. as a result of rust pitting. In such an event Class C would be more appropriate.	
(b) As (a) but with any flame-cut edges subsequently ground or machined to remove all visible sign of the drag lines.	B	Any re-entrant corners in flame-cut edges are to have a radius greater than the plate thickness.	
(c) As (a) but with the edges machine flame-cut by a controlled procedure to ensure that the cut surface is free from cracks.	C	Note, however, that the presence of a re-entrant corner implies the existence of a stress concentration so that the design stress is to be taken as the net stress multiplied by the relevant stress concentration factor.	
Notes on potential modes of failure: In plain steel, fatigue cracks initiate at the surface, usually either at surface irregularities or at corners of the cross-section. In welded construction, fatigue failure will rarely occur in a region of plain material since the fatigue resistance of the welded joints will usually be much lower. In steel with rivet or bolt holes or other stress concentrations arising from the shape of the member, failure will usually initiate at the stress concentration.			

Type 2 Double Side Full Penetration Butt Welds Essentially Parallel to the Direction of Applied Stress

Table A1.2

Type number, description and notes on mode of failure	S-N curve	Joint description	Example and failure mode
2.1 Full or partial penetration butt welds, or fillet welds. Parent or weld metal in members, without attachments, built up of plates or sections, and joined by continuous welds.			
(a) Full penetration butt welds with the weld overfill dressed flush with the surface and finish-machined in the direction of stress, and with the weld proved free from significant defects by nondestructive examination.	B	The significance of defects is to be determined with the aid of specialist advice and/or by the use of fracture mechanics analysis. The NDT technique must be selected with a view to ensuring the detection of such significant defects.	Stress direction as indicated by arrows 
(b) Butt or fillet welds with the welds made by an automatic submerged or open arc process and with no stop-start positions within the length.	C	If an accidental stop-start occurs in a region where Class C is required remedial action is to be taken so that the finished weld has a similar surface and root profile to that intended.	
(c) As (b) but with the weld containing stop-start positions within the length.	D	For situation at the ends of flange cover plates see joint Type 6.4.	 e is edge distance from weld toe to edge of flange, e>10 mm
<p>Notes on potential modes of failure: With the excess weld metal dressed flush, fatigue cracks would be expected to initiate at weld defect locations. In the as-welded condition, cracks might initiate at stop-start positions or, if these are not present, at weld surface ripples.</p> <p>General comments:</p> <ol style="list-style-type: none"> (1) Backing strips If backing strips are used in making these joints: (i) they must be continuous, and (ii) if they are attached by welding those welds must also comply with the relevant rules requirements (note particularly that tack welds, unless subsequently ground out or covered by a continuous weld, would reduce the joint to Class F, see joint 6.5). (2) Edge distance An edge distance criterion exists to limit the possibility of local stress concentrations occurring at unwelded edges as a result, for example, of undercut, weld spatter, or accidental overweave in manual fillet welding (see also notes on joint Type 4). Although an edge distance can be specified only for the 'width' direction of an element, it is equally important to ensure that no accidental undercutting occurs on the unwelded corners of, for example, cover plates or box girder flanges. If it does occur it is subsequently to be ground smooth. 			

Type 3 Double Side Full Penetration Butt Welds Essentially Perpendicular to the Direction of Applied Stress **Table A1.3**

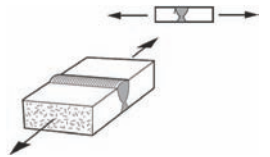
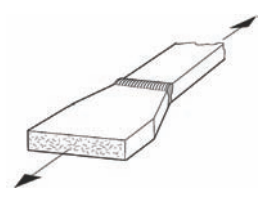
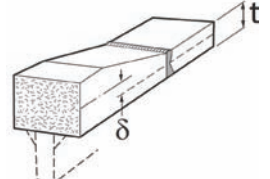
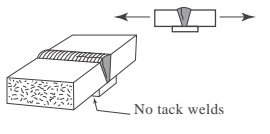
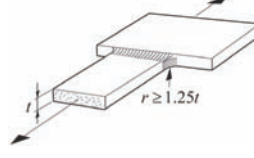
Type number, description and notes on mode of failure	S-N curve	Joint description	Example and failure mode
3.1 Parent metal adjacent to, or weld metal in, full penetration butt joints welded from both sides between plates of equal width and thickness or where differences in width and thickness are machined to a smooth transition not steeper than 1 in 4. Note that this includes butt welds which do not completely traverse the member, such as welds used for inserting infilling plates into temporary holes.			
(a) With the weld overfill dressed flush with the surface and with the weld proved free from significant defects by non-destructive examination.	C	The significance of defects is to be determined with the aid of specialist advice and/or by the use of fracture mechanics analysis. The NDT technique must be selected with a view to ensuring the detection of such significant defects.	
(b) With the welds made, either manually or by an automatic process other than submerged arc, provided all runs are made in the downhand position.	D	In general welds made by the submerged arc process, or in positions other than downhand, tend to have a poor reinforcement shape, from the point of view of fatigue strength. Hence such welds are downgraded from D to E.	
(c) Welds made other than in (a) or (b).	E	In both (b) and (c) of the corners of the cross-section of the stressed element at the weld toes are to be dressed to a smooth profile. Note that step changes in thickness are in general, not permitted under fatigue conditions, but that where the thickness of the thicker member is not greater than $1.15 \times$ the thickness of the thinner member, the change can be accommodated in the weld profile without any machining. Step changes in width lead to large reductions in strength (see joint Type 3.3).	 δ is eccentricity of centerlines
3.2 Parent metal adjacent to, or weld metal in, full penetration butt joints made on a permanent backing strip between plates of equal width and thickness or with differences in width and thickness machined to a smooth transition not steeper than 1 in 4.	F	Note that if the backing strip is fillet welded or tack welded to the member the joint could be reduced to Class G (joint Type 4.2).	 No tack welds

Table A1.3 (continued)

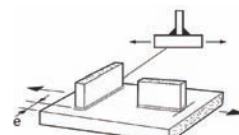
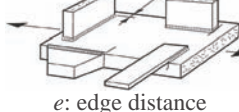
Type number, description and notes on mode of failure	S-N curve	Joint description	Example and failure mode
3.3 Parent metal adjacent to, or weld metal in, full penetration butt welded joints made from both sides between plates of unequal width, with the weld ends ground to a radius not less than 1.25 times the thickness t .	F2	Step changes in width can often be avoided by the use of shaped transition plates, arranged so as to enable butt welds to be made between plates of equal width. Note that for this detail the stress concentration has been taken into account in the structural detail classification.	

Notes on potential modes of failure: With the weld ends machined flush with the plate edges, fatigue cracks in the as-welded condition normally initiate at the weld toe, so that the fatigue strength depends largely upon the shape of the weld overfill. If this is dressed flush the stress concentration caused by it is removed and failure is then associated with weld defects. In welds made on a permanent backing strip, fatigue cracks initiate at the weld metal/strip junction, and in partial penetration welds (which are not to be used under fatigue conditions), at the weld root. Welds made entirely from one side, without a permanent backing, require care to be taken in the making of the root bead in order to ensure a satisfactory profile.

Design stresses: In the design of butt welds of Types 3.1 or 3.2 which are not aligned the stresses must include the effect of any eccentricity. An approximate method of allowing for eccentricity in the thickness direction is to multiply the normal stress by $(1 + 3\delta/t)$, where δ is the distance between centers of thickness of the two abutting members; if one of the members is tapered, the center of the untapered thickness must be used, and t is the thickness of the thinner member. Note that it is equivalent to the use of SCF formulae in Sections 2 and 4 of Chapter 3 where $\delta_0=0$, because a higher class S-N curve is used for welds dressed flush.

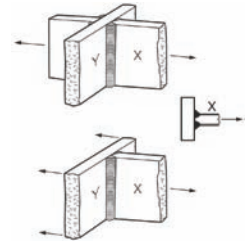
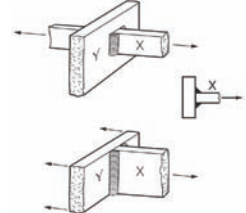
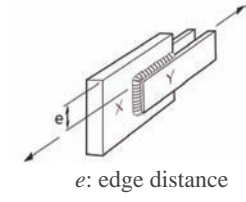
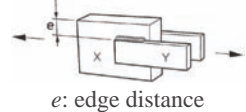
With connections which are supported laterally, e.g. flanges of a beam which are supported by the web, eccentricity may be neglected.

Type 4 Welded Attachments on the Surface or Edge of a Stressed Member Table A1.4

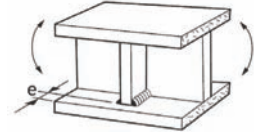
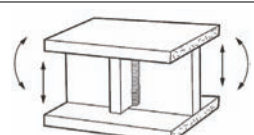
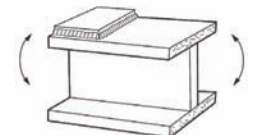
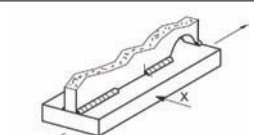
Type number, description and notes on mode of failure	S-N curve	Joint description	Example and failure mode
4.1 Parent metal (of the stressed member) adjacent to toes or ends of bevel-butt or fillet welded attachments, regardless of the orientation of the weld to the direction of applied stress, and whether or not the welds are continuous round the attachment.			
		Butt welded joints are to be made with an additional reinforcing fillet so as to provide a similar toe profile to that which would exist in a fillet welded joint.	
(a) With attachment length (parallel to the direction of the applied stress) ≤ 150 mm and with edge distance ≥ 10 mm.	F	The decrease in fatigue strength with increasing attachment length is because more load is transferred into the longer gusset giving an increase in stress concentration.	 e: edge distance
(b) With attachment length (parallel to the direction of the applied stress) > 150 mm and with edge distance ≥ 10 mm.	F2		
4.2 Parent metal (of the stressed member) at the toes or the ends of butt or fillet welded attachments on or within 10 mm of the edges or corners of a stressed member, and regardless of the shape of the attachment, the orientation of the weld to the direction of applied stress, and whether or not the welds are continuous round the attachment.	G	Note that the classification applies to all sizes of attachment. It would therefore include, for example, the junction of two flanges at right angles. In such situations a low fatigue classification can often be avoided by the use of a transition plate (see also joint Type 3.3).	 e: edge distance
4.3 Parent metal (of the stressed member) at the toe of a butt weld connecting the stressed member to another member slotted through it. Note that this classification does not apply to fillet welded joints (see joint Type 5.1b). However it does apply to loading in either direction (L or T in the sketch).			
(a) With the length of the slotted-through member, parallel to the direction of the applied stress, ≤ 150 mm and edge distance ≥ 10 mm.	F		
(b) With the length of the slotted-through member, parallel to the direction of the applied stress, > 150 mm and edge distance ≥ 10 mm.	F2		
(c) With edge distance < 10 mm.	G		
Notes on potential modes of failure: When the weld is parallel to the direction of the applied stress fatigue cracks normally initiate at the weld ends, but when it is transverse to the direction of stressing they usually initiate at the weld toe; for attachments involving a single, as opposed to a double weld, cracks may also initiate at the weld root. The cracks then propagate into the stressed member. When the welds are on or adjacent to the edge, of the stressed member the stress concentration is increased and the fatigue strength is reduced; this is the reason for specifying an 'edge distance' in some of these joints (see also note on edge distance in joint Type 2).			

Type 5 Load-carrying Fillet and T-butt Welds

Table A1.5

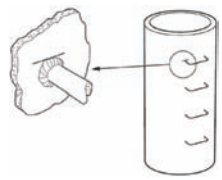
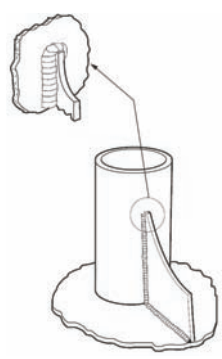
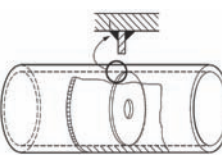
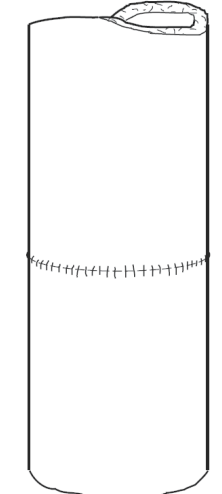
Type number, description and notes on mode of failure	S-N curve	Joint description	Example and failure mode
5.1 Joint description Parent metal adjacent to cruciform joints or T joints (member marked X in sketches).		Member Y can be regarded as one with a non-load-carrying weld (see joint Type 4.1). Note that in this instance the edge distance limitation applies.	
(a) Joint made with full penetration welds and with any undercutting at the corners of the member dressed out by local grinding.	F		
(b) Joint made with partial penetration or fillet welds with any undercutting at the comers of the member dressed out by local grinding.	F2	In this type of joint, failure is likely to occur in the weld throat unless the weld is made sufficiently large (see joint Type 5.4).	
5.2 Parent metal adjacent to the toe of load-carrying fillet welds which are essentially transverse to the direction of applied stress (member Y in sketch).		The relevant stress in member X is to be calculated on the assumption that its effective width is the same as the width of member Y.	
(a) Edge distance $\geq 10\text{mm}$	F2	These classifications also apply to joints with longitudinal welds only.	
(b) Edge distance $< 10\text{mm}$	G		
5.3 Parent metal at the ends of load-carrying fillet welds which are essentially parallel to the direction of applied stress, with the weld end on plate edge (member Y in sketch).	G		
5.4 Weld metal in load-carrying joints made with fillet or partial penetration welds, with the welds either transverse or parallel to the direction of applied stress (based on nominal shear stress on the minimum weld throat area).	W	This includes joints in which a pulsating load may be carried in bearing, such as the connection of bearing stiffeners of flanges. In such examples the welds are to be designed on the assumption that none of the load is carried in bearing.	
Notes on potential modes of failure: Failure in cruciform or T joints with full penetration welds will normally initiate at the weld toe, but in joints made with load-carrying fillet or partial penetration butt welds cracking may initiate either at the weld toe and propagate into the plate or at the weld root and propagate through the weld. In welds parallel to the direction of the applied stress, however, weld failure is uncommon; cracks normally initiate at the weld end and propagate into the plate perpendicular to the direction of applied stress. The stress concentration is increased, and the fatigue strength is therefore reduced, if the weld end is located on or adjacent to the edge of a stressed member rather than on its surface.			

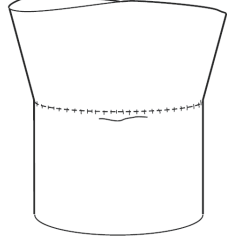
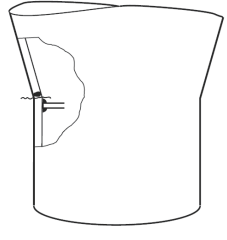
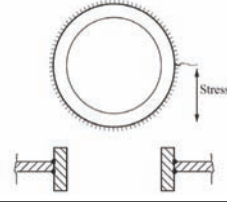
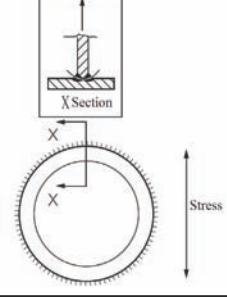
Type 6 Details in Welded Girders (including Small Attachment) Table A1.6

Type number, description and notes on mode of failure	S-N curve	Joint description	Example and failure mode
6.1 Parent metal at the toe of a weld connecting a stiffener, diaphragm, etc. to a girder flange.		Edge distance refers to distance from a free, i.e. unwelded, edge. In this example, therefore, it is not relevant as far as the (welded) edge of the Web plate is concerned. For reason for edge distance see note on joint Type 2.	
(a) Edge distance ≥ 10 mm (see joint Type 4.2).	F		
(b) Edge distance < 10 mm (see joint Type 4.2).	G		
6.2 Parent metal at the end of a weld connecting a stiffener, diaphragm, etc. to a girder web in a region of combined bending and shear.	E	This classification includes all attachments to girder webs.	
6.3 Parent metal adjacent to welded shear connectors.			
(a) Edge distance ≥ 10 mm (see joint Type 4.2).	F		
(b) Edge distance < 10 mm (see joint Type 4.2).	G		
6.4 Parent metal at the end of a partial length welded cover plate, regardless of whether the plate has square or tapered ends and whether or not there are welds across the ends.	G	This Class includes cover plates which are wider than the flange. However, such a detail is not recommended because it will almost inevitably result in undercutting of the flange edge where the transverse weld crosses it, as well as involving a longitudinal weld terminating on the flange edge and causing a high stress concentration.	
6.5 Parent metal adjacent to the ends of discontinuous welds, e.g. intermittent web/flange welds, tack welds unless subsequently buried in continuous runs.	E	This also includes tack welds which are not subsequently buried in a continuous weld. This may be particularly relevant in tack welded backing strips. Note that the existence of the cope hole is allowed for in the structural detail classification.	 <p>The relevant stress is the nominal stress in the member marked X in the sketch. If the weld is load-carrying, it is to be checked with joint type 5.4.</p>
6.5b Ditto. Adjacent to cope holes.	F	It is not to be regarded as an additional stress concentration.	

Notes on potential modes of failure: Fatigue cracks generally initiate at weld toes and are especially associated with local stress concentrations at weld ends, short lengths of return welds, and changes of direction. Concentrations are enhanced when these features occur at or near an edge of a part (see notes on joint Type 4). General comment: Most of the joints in this section are also shown, in a more general form, in joint Type 4; they are included here for convenience as being the joints which occur most frequently in welded girders. Where edge distance is mentioned in the joint type 6, it refers to the distance from a free (unwelded) edge.

Type 7 Details Relating to Tubular Members (including Small Attachment) Table A1.7

Type number, description and notes on mode of failure	S-N curve	Joint description	Example and failure mode
7.1 Parent material adjacent to the toes of full penetration welded nodal joints.	T	In this situation, design is to be based on the hot spot stress as defined in Chapter 3 of the Guidelines.	
7.2 Parent metal at the toes of welds associated with small (≤ 150 mm in the direction parallel to the applied stress) attachments to the tubular member.	F		
Ditto, but with attachment length > 150 mm.	F2		
7.3 Gusseted connections made with full penetration or fillet welds. (But note that full penetration welds are normally required).	F	Note that the design stress must include any local bending stress adjacent to the weld end.	
	W	For failure in the weld throat of fillet welded joints.	
7.4 Parent material at the toe of a weld attaching a diaphragm or stiffener to a tubular member.	F	Stress is to include the stress concentration factor due to overall shape of adjoining structure.	
7.5 Parent material adjacent to the toes of circumferential butt welds between tubes.		In this type of joint the stress is to include the stress concentration factor to allow for any thickness change and for fabrication tolerances.	
(a) Weld made from both sides with the weld overfill dressed flush with the surface and with the weld proved free from significant defects by non-destructive examination.	C	The significance of defects is to be determined with the aid of specialist advice and/or by the use of fracture mechanics analysis. The NDT technique is to be selected with a view to ensuring the detection of such significant defects.	
(b) Weld made from both sides.	E		
(c) Weld made from one side on a permanent backing strip.	F		
(d) Weld made from one side without a backing strip provided that full penetration is achieved.	F2	Note that step changes in thickness are in general, not permitted under fatigue conditions, but that where the thickness of the thicker member is not greater than $1.15 \times$ the thickness of the thinner member, the change can be accommodated in the weld profile without any machining.	

Type number, description and notes on mode of failure	S-N curve	Joint description	Example and failure mode
7.6 Parent material at the toes of circumferential butt welds between tubular and conical sections.	C E F F2	Class and stress are to be those corresponding to the joint type as indicated in 7.5, but the stress must also include the stress concentration factor due to overall form of the joint.	
7.7 Parent material (of the stressed member) adjacent to the toes of bevel butt or fillet welded attachments in a region of stress concentration.	F F2	Class depends on attachment length (see Type 4.1) but stress is to include the stress concentration factor due to the overall shape of adjoining structure.	
7.8 Parent metal adjacent to, or weld metal in, welds around a penetration through the wall of a member (on a plane essentially perpendicular to the direction of stress). Note that full penetration welds are normally required in this situation.	D	In this situation the relevant stress is to include the stress concentration factor due to the overall geometry of the detail.	
7.9 Weld metal in partial penetration or fillet welded joints around a penetration through the wall of a member (on a plane essentially parallel to the direction of stress).	W	The stress in the weld is to include an appropriate stress concentration factor to allow for the overall joint geometry.	

APPENDIX 2 PARAMETRIC FORMULAE OF STRESS CONCENTRATION FACTORS OF TUBULAR JOINTS

Section 1 General

2.1.1 Several parametric formulae have been produced for the prediction of SCFs for tubular joints, based on data from both physical and FE models^[1-6].

Section 2 Simple Tubular Joints

2.2.1 For simple tubular joints, the performance of the various sets of SCF equations in terms of accuracy, degree of conservatism and range of applicability has been assessed in a number of recent studies, notably in a study by Edison Welding Institute (EWI) funded by API^[7] and a study by Lloyd's Register funded by Health and Safety Executive (HSE)^[8].

2.2.2 The main conclusion from the EWI study was that the Efthymiou equations^[2] and the Lloyd's design equations^[8] have considerable advantages in consistency and coverage in comparison with other available equations. When discussing the Lloyd's SCF equations it is important to clarify that two modern sets of Lloyd's SCF equations exist, namely:

- (1) mean SCF equations created from the database of acrylic test results that were available in 1988;
- (2) design SCF equations defined as mean-plus-one standard deviation from the same database in (1).

When assessed by EWI against the latest SCF database, the Lloyd's mean SCF equations are found to generally under-predict SCFs and fail the HSE assessment criteria. The mean SCF equations are not recommended for design. A second conclusion from the EWI study was that the option of mixing-and-matching equations from different sets would lead to inconsistencies and is not recommended. An inconsistency of this type is already present in the Lloyd's design SCF equations, due to the variable partial factor used, but it is not very significant.

2.2.3 For the Alpha-Kellogg equations^[9] that are given in previous editions of API RP 2A-WSD, some research concluded that they generally predict lower SCF than the Efthymiou equations and Lloyd's equations over the range of common design cases. Perhaps the most significant weakness of the Alpha-Kellogg equations is that the predicted SCFs for all joint types are independent of β . While reasonable for K-joints and multi-planar nodes, this is clearly not the case for isolated T, Y, and X-joints, as evidenced from test data and FE results. Further, the equations imply that chord SCFs are proportional to $\sqrt{\gamma}$, as opposed to observations which indicate that they increase linearly with γ . However, one advantage of the Alpha-Kellogg equations is their simplicity.

2.2.4 In the comparison studies by Lloyd's Register, the Efthymiou SCF equations were found to provide a good fit to the screened SCF database, with a bias of about 10–25% on the conservative side. They generally pass the HSE criteria for goodness of fit and conservatism, except for the important case of K-joints under balanced axial load. A closer examination of this specific case revealed that these equations are to be considered satisfactory for both the chord and the brace side. For the chord side in particular, the Efthymiou equation provides the best fit to the database (COV = 19%) and has a bias of 19% on the conservative side. The 'second best' equation (Lloyd's) has a COV of 21% and a bias of 41% on the conservative side. The HSE criteria were deliberately concocted to favor those equations that over-predict SCFs and to penalize under-predictions. This is why the Efthymiou equations for K joints marginally failed the criteria, even though they provide a good fit and also are biased on the safe side^[10].

2.2.5 The Lloyd's design SCF equations generally pass the HSE criteria, except for T/Y-joints under axial force and ipb on the brace crown side. The reason for this is that there seems to be a systematic difference between the acrylic results and steel results for T/Y-joints at the brace crown^[10].

2.2.6 For simple tubular joints, use of the Efthymiou SCF equations is recommended because this set of equations is considered to offer the best option for all joint types and types brace forces. In addition, they are also recommended in API RP 2A-WSD (2007)^[11-12].

Section 3 Multi Planar Tubular Joints

2.3.1 For multi planar tubular joints SCFs are usually determined assuming there is no interaction between joints in different planes so that they are treated as simple tubular joints. However, in certain load cases, significant interaction can occur between joints in different planes. These effects, which can result in significantly different SCFs, are to be assessed using appropriate methods, e.g. expressions used in Efthymiou^[2].

Section 4 Overlapped Tubular Joints

2.4.1 Parametric formulae for the prediction of SCFs in overlapped tubular joints have been published in Efthymiou^[2]. They have not been validated because of the limited database available.

Section 5 Stiffened Tubular Joints

2.5.1 Parametric SCF formulae for ring-stiffened tubular joints have been developed from acrylic model test data^[13-14], which give the brace/chord intersection SCFs in terms of the equivalent, unstiffened joint SCFs. Equations to predict the SCF at the ring inner edge have also been given^[13-14].

Section 6 Efthymiou Equations and Validity Ranges

2.6.1 The Efthymiou equations are given in Tables A2.1 to A2.4. The validity ranges for the Efthymiou equations are as follows:

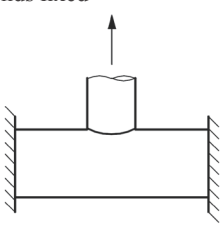
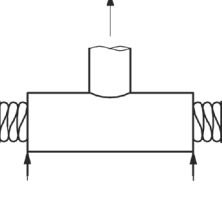
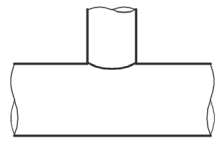
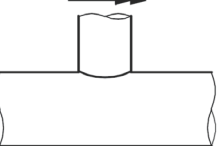
$$\begin{aligned} 0.2 &\leq \beta \leq 1.0 \\ 0.2 &\leq \tau \leq 1.0 \\ 8.0 &\leq \gamma \leq 32 \\ 4.0 &\leq \alpha \leq 40 \\ 20^\circ &\leq \theta \leq 90^\circ \\ -\frac{0.6\beta}{\sin\theta} &\leq \zeta \leq 1.0 \end{aligned} \tag{A2.1}$$

For cases where one or more parameters fall outside this range, the following procedure is to be adopted:

- (1) evaluate SCFs using the actual values of geometric parameters;
- (2) evaluate SCFs using the limit values of geometric parameters in formula (A2.1);
- (3) use the maximum of (1) or (2) above in the fatigue analysis.

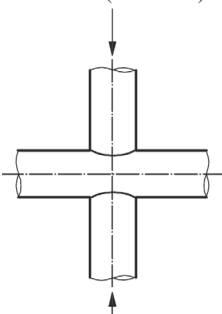
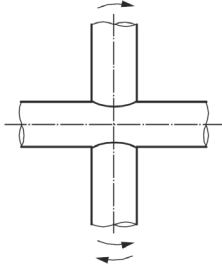
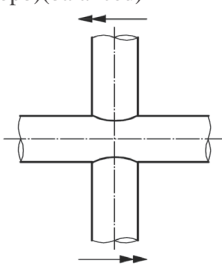
Equations for SCFs in T/Y-joints

Table A2.1

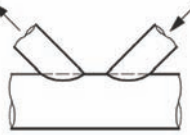
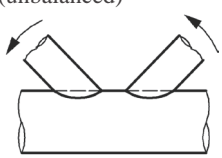
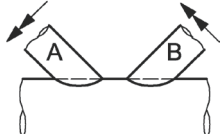
Type of brace force and fixity conditions	SCF equation
Axial brace force, chord ends fixed 	Chord saddle: $C_{CS} = F_1 C_{T1} \quad C_{T1} = \gamma \tau^{1.1} [1.11 - 3(\beta - 0.52)^2] \sin^{1.6} \theta$ Chord crown: $C_{CC} = C_{T2} \quad C_{T2} = \gamma^{0.2} \tau [2.65 + 5(\beta - 0.65)^2] + \tau \beta (0.25\alpha - 3) \sin \theta$ Brace saddle: $C_{BS} = F_1 C_{T3} \quad C_{T3} = 1.3 + \gamma \tau^{0.52} \alpha^{0.1} [0.187 - 1.25 \beta^{1.1} (\beta - 0.96)] \sin^{(2.7-0.01\alpha)} \theta$ Brace crown: $C_{BC} = C_{T4} \quad C_{T4} = 3 + \gamma^{1.2} [0.12 \exp(-4\beta) + 0.011 \beta^2 - 0.045] + \beta \tau (0.1\alpha - 1.2)$
Axial brace force, general chord fixity 	Chord saddle: $C_{CS} = F_2 C_{T5} \quad C_{T5} = C_{T1} + C_1 (0.8\alpha - 6) \tau \beta^2 (1 - \beta^2)^{0.5} \sin^2 2\theta$ Chord crown: $C_{CC} = C_{T6} \quad C_{T6} = \gamma^{0.2} \tau [2.65 + 5(\beta - 0.65)^2] + \tau \beta (C_2 \alpha - 3) \sin \theta$ Brace saddle: $C_{BS} = F_2 C_{T3}$ See above Brace crown: $C_{BC} = C_{T7} \quad C_{T7} = 3 + \gamma^{1.2} [0.12 \exp(-4\beta) + 0.011 \beta^2 - 0.045] + \beta \tau (C_3 \alpha - 1.2)$
In-plane bending (ipb) 	Chord crown: $C_{CC} = C_{T8} \quad C_{T8} = 1.45 \beta \tau^{0.85} \gamma^{(1-0.68\beta)} \sin^{0.7} \theta$ Brace crown: $C_{BC} = C_{T9} \quad C_{T9} = 1 + 0.65 \beta \tau^{0.4} \gamma^{(1.09-0.77\beta)} \sin^{(0.06\gamma-1.16)} \theta$
Out-of-plane bending (opb) 	Chord saddle: $C_{CS} = F_3 C_{T10} \quad C_{T10} = \gamma \tau \beta (1.7 - 1.05 \beta^3) \sin^{1.6} \theta$ Brace saddle: $C_{BS} = F_3 C_{T11} \quad C_{T11} = \tau^{-0.54} \gamma^{-0.05} (0.99 - 0.47 \beta + 0.08 \beta^4) \times C_{T10}$
	Short chord correction factors ($\alpha < 12$): $F_1 = 1 - (0.83\beta - 0.56\beta^2 - 0.02) \gamma^{0.23} \exp(-0.21\gamma^{-1.16} \alpha^{2.5})$ $F_2 = 1 - (1.43\beta - 0.97\beta^2 - 0.03) \gamma^{0.04} \exp(-0.71\gamma^{-1.38} \alpha^{2.5})$ $F_3 = 1 - 0.55 \beta^{1.8} \gamma^{0.16} \exp(-0.49 \gamma^{-0.89} \alpha^{1.8})$ where $\exp(x) = e^x$
	Chord-end fixity parameter: C $0.5 \leq C \leq 1.0$ (Typically $C = 0.7$) $C_1 = 2(C - 0.5); \quad C_2 = C/2; \quad C_3 = C/5$

Equations for SCFs in X-joints

Table A2.2

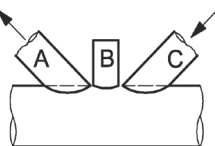
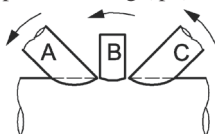
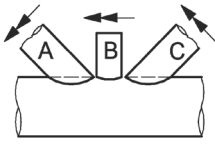
Type of brace force	SCF equation
 <p>Axial force (balanced)</p>	<p>Chord saddle:</p> $C_{CS} = C_{X1} \quad C_{X1} = 3.87\gamma\tau\beta(1.10 - \beta^{1.8})\sin^{1.7}\theta$ <p>Chord crown:</p> $C_{CC} = C_{X2} \quad C_{X2} = \gamma^{0.2}\tau[2.65 + 5(\beta - 0.65)^2] - 3\tau\beta\sin\theta$ <p>Brace saddle:</p> $C_{BS} = C_{X3} \quad C_{X3} = 1 + 1.9\gamma\tau^{0.5}\beta^{0.9}(1.09 - \beta^{1.7})\sin^{2.5}\theta$ <p>Brace crown:</p> $C_{BC} = C_{X4} \quad C_{X4} = 3 + \gamma^{1.2}[0.12\exp(-4\beta) + 0.011\beta^2 - 0.045]$
<p>In joints with short chords, $\alpha < 12$, which have stiffened ends, both the chord saddle and the brace saddle SCF may be reduced by multiplying them by the short chord factor, F_1 or F_2. Factor F_1 can be used for stiff end reinforcements preventing ovalization as well as rotation of the chord wall while factor F_2 can be used for end reinforcements partially preventing ovalization only.</p> <p>If the chord ends are completely free, both the chord saddle and the brace saddle SCF can increase significantly. An approximation may be obtained by increasing them by the ratio $1/F_2$, but FEA is recommended.</p> <p>F_1 and F_2 are given in Table A2.1.</p>	
 <p>In-plane bending (ipb) (balanced or unbalanced)</p>	<p>Chord crown:</p> $C_{CC} = C_{T8} \quad \text{see Table A2.1}$ <p>Brace crown:</p> $C_{BC} = C_{T9} \quad \text{see Table A2.1}$
 <p>Out-of-plane bending (opb)(balanced)</p>	<p>Chord saddle:</p> $C_{CS} = C_{X5} \quad C_{X5} = \gamma\tau\beta(1.56 - 1.34\beta^4)\sin^{1.6}\theta$ <p>Brace saddle:</p> $C_{BS} = C_{X6} \quad C_{X6} = \tau^{-0.54}\gamma^{-0.05}(0.99 - 0.47\beta + 0.08\beta^4) \times C_{X5}$
<p>In joints with short chords, $\alpha < 12$, which have ends stiffened with a diaphragm or ring stiffener, both the chord saddle and the brace saddle SCF may be reduced by multiplying them by the short chord factor F_3; see Table A2.1.</p> <p>If the chord ends are completely free, saddle SCFs can increase significantly. An approximation may be obtained by increasing them by the ratio $1/F_3$, but FEA is recommended.</p>	

Equations for SCFs in overlapping or non-overlapping K-joints Table A2.3

Type of brace force	SCF equation
Axial forces (balanced) 	<p>Chord:</p> $C_C = C_{K1}$ $C_{K1} = \left[\tau^{0.9} \gamma^{0.5} (0.67 - \beta^2 + 1.16\beta) \sin \theta \right] \left[\frac{\sin \theta_{\max}}{\sin \theta_{\min}} \right]^{0.30} \times \left(\frac{\beta_{\max}}{\beta_{\min}} \right)^{0.30}$ $\times [1.64 + 0.29\beta^{-0.38} \arctan(8\zeta)]$ <p>Brace:</p> $C_B = C_{K2}$ $C_{K2} = 1 + C_{K1} (1.97 - 1.57\beta^{0.25}) (\tau^{-0.14} \sin^{0.7} \theta)$ $+ [K\beta^{1.5} \gamma^{0.5} \tau^{-1.22} \sin^{1.8} (\theta_{\max} + \theta_{\min})] \times [0.131 - 0.084 \arctan(14\zeta + 4.2\beta)]$ <p>where:</p> <p>$C=0$ for gap joints; $C=1$ for the through brace; $C=0.5$ for the overlapping brace; the arctangents are evaluated in radians; τ, β, θ and the nominal stress relate to the brace being considered.</p>
In-plane bending (ipb) (unbalanced) 	<p>Chord crown:</p> <ol style="list-style-type: none"> ① non-overlapping joint or overlap $\leq 30\%$ of contact length: $C_{CC} = C_{T8}$ see Table A2.1 ② overlap $> 30\%$ of contact length: $C_{CC} = 1.2C_{T8}$ see Table A2.1 <p>Brace crown:</p> <ol style="list-style-type: none"> ① non-overlapping joint: $C_{BC} = C_{T9}$ see Table A2.1 ② overlapping joint: $C_{BC} = C_{T9} \times (0.9 + 0.4\beta)$ see Table A2.1
Out-of-plane bending (opb) (unbalanced)  (The designation of braces A and B is not geometry dependent. It is nominated by the user)	<p>Chord saddle adjacent to brace A:</p> $C_{CS} = F_4 C_{K4}$ $C_{K4} = C_{T10,A} \left[1 - 0.08(\beta_B \gamma)^{0.5} \exp(-0.8x) \right]$ $+ C_{T10,B} \left[1 - 0.08(\beta_A \gamma)^{0.5} \exp(-0.8x) \right] \times [2.05\beta_{\max}^{0.5} \exp(-1.3x)]$ <p>where:</p> $x = 1 + \frac{\zeta \sin \theta_A}{\beta_A}$ <p>$C_{T10,A}$ and $C_{T10,B}$ (see Table A2.1) are calculated with the parameters for braces A and B respectively.</p> <p>Brace saddle adjacent to brace A:</p> $C_{BS} = F_4 C_{K5} \quad C_{K5} = \tau^{-0.54} \gamma^{-0.05} (0.99 - 0.47\beta + 0.08\beta^4) \times C_{K4}$
	<p>Short chord correction factor ($\alpha < 12$):</p> $F_4 = 1 - 1.07\beta^{1.88} \exp[-0.16\gamma^{-1.06}\alpha^{2.4}]$ <p>where: $\exp(x) = e^x$</p>

Equations for SCFs in KT-joints

Table A2.4

Type of brace force	SCF equation
Axial force (balanced)	<p>Chord: $C_C = C_{K1}$ see Table A2.3</p> <p>Brace: $C_B = C_{K2}$ see Table A2.3</p> <p>where: $\zeta = \zeta_{AB} + \zeta_{BC} + \beta_B$ for the diagonal braces A and C; $\zeta = \max(\zeta_{AB}, \zeta_{BC})$ for the central brace B</p> 
In-plane bending (ipb)	<p>Chord crown: $C_{CC} = C_{T8}$ see Table A2.1</p> <p>Brace crown: $C_{BC} = C_{T9}$ see Table A2.1</p> 
Out-of-plane bending (opb) (unbalanced)	<p>Chord saddle at diagonal brace A: $C_{CS} = C_{KT1}$</p> $C_{KT1} = C_{T10,A} \left[1 - 0.08(\beta_B \gamma)^{0.5} \exp(-0.8x_{AB}) \right] \times \left[1 - 0.08(\beta_C \gamma)^{0.5} \exp(-0.8x_{AC}) \right]$ $+ C_{T10,B} \left[1 - 0.08(\beta_A \gamma)^{0.5} \exp(-0.8x_{AB}) \right] \times \left[2.05\beta_{\max}^{0.5} \exp(-1.3x_{AB}) \right]$ $+ C_{T10,C} \left[1 - 0.08(\beta_A \gamma)^{0.5} \exp(-0.8x_{AC}) \right] \times \left[2.05\beta_{\max}^{0.5} \exp(-1.3x_{AC}) \right]$ <p>where: $x_{AB} = 1 + \frac{\zeta_{AB} \sin \theta_A}{\beta_A}$; $x_{AC} = 1 + \frac{(\zeta_{AB} + \zeta_{BC} + \beta_B) \sin \theta_A}{\beta_A}$</p> <p>Chord saddle at central brace B: $C_{CS} = C_{KT2}$</p> $C_{KT2} = C_{T10,B} \left[1 - 0.08(\beta_A \gamma)^{0.5} \exp(-0.8x_{AB}) \right]^{(\beta_A/\beta_B)^2}$ $\times \left[1 - 0.08(\beta_C \gamma)^{0.5} \exp(-0.8x_{BC}) \right]^{(\beta_C/\beta_B)^2}$ $+ C_{T10,A} \left[1 - 0.08(\beta_B \gamma)^{0.5} \exp(-0.8x_{AB}) \right] \times \left[2.05\beta_{\max}^{0.5} \exp(-1.3x_{AB}) \right]$ $+ C_{T10,C} \left[1 - 0.08(\beta_B \gamma)^{0.5} \exp(-0.8x_{BC}) \right] \times \left[2.05\beta_{\max}^{0.5} \exp(-1.3x_{BC}) \right]$ <p>where: $x_{AB} = 1 + \frac{\zeta_{AB} \sin \theta_B}{\beta_B}$; $x_{BC} = 1 + \frac{\zeta_{BC} \sin \theta_B}{\beta_B}$</p> <p>Brace saddle (based on SCF of adjacent chord): $C_{BS} = C_{KTB}$</p> $C_{KTB} = \tau^{-0.54} \gamma^{-0.05} (0.99 - 0.47\beta + 0.08\beta^4) \times C_{CS}$ <p>where: C_{CS} is obtained from SCF equation of adjacent chord</p> 

References:

- [1] HEALY, B.E. and BUITRAGO, J. Extrapolation procedures for determining SCFs in mid-surface tubular joint models. 6th Intl. Symp. on Tubular Structures, Monash University, Melbourne, Australia, 1994.
- [2] EFTHYMIOU, M. Development of SCF formulae and generalised influence functions for use in fatigue analysis. Recent Developments in Tubular Joint Technology, Proceedings of Offshore Tubular Joints Conference- OTJ'88, October 1988, London, plus updates.
- [3] SMEDLEY, P.A. and FISHER, P. Stress concentration factors for simple tubular joints. Offshore and Polar Engineering Conf., ISOPE-1, Edinburgh, UK, 1991.
- [4] POTVIN, A.B. et al. Stress concentration in tubular joints. SPE Journal, August 1977.
- [5] WORDSWORTH, A.C. Stress concentration factors at K and KT joints. Fatigue in Offshore Structural Steels, ICE, London, 1981.
- [6] MARSHALL, P.W. and LUYTIES, W.H. Allowable stress for fatigue design. Proc. 3rd Intl. Conf on the Behaviour of Offshore Structures, BOSS 1982, Paper S1, 2, MIT Cambridge, Massachusetts, 1982, pp. 3-25.
- [7] Edison Welding Institute, Stress Concentration Factors for Tubular Connections. EWI Project No. J7266, March 1995.
- [8] Lloyd's Register of Shipping, Stress concentration factors for simple tubular joints. Report OTH 354, Health and Safety Executive, 1997.
- [9] KINRA, R.K. and MARSHALL, P.W. Fatigue Analysis of the Cognac Platform. J. Petroleum Technology, Paper SPE 8600, March 1980
- [10] ISO 19902, Petroleum and natural gas industries —Fixed steel offshore structures, 2007.
- [11] MARSHALL, P.W., BUCKNELL, J. and MOHR, W.C. Background to New API fatigue provisions. Proc. 38th Offshore Technology Conf. Paper OTC 17295, Houston, May, 2005.
- [12] API, Recommended Practice for Planning, Designing and Constructing Fixed Offshore Platforms—Working Stress Design (with ERRATA AND SUPPLEMENT 3, OCTOBER 2007).
- [13] SMEDLEY, P.A. and FISHER, P. A Review of Stress Concentration Factors for Complex Tubular Joints, Integrity of Offshore Structures Conference, Glasgow, 1990.
- [14] SMEDLEY, P.A. and FISHER, P. Stress Concentration Factors for Ring stiffened Tubular Joints, Fourth International Symposium on Tubular Structures, Delft, 1991.

APPENDIX 3 STRESS CONCENTRATION FACTORS FOR PENETRATIONS WITH REINFORCEMENTS

Section 1 Stress Concentration Factors for Circular Penetrations with Reinforcements

3.1.1 General

- (1) Stress concentration factors at holes in plates with inserted tubulars are given in Figures A3.1 to A3.15.
- (2) Stress concentration factors at holes in plates with ring reinforcement are given in Figures A3.16 to A3.20.
- (3) Stress concentration factors at holes in plates with double ring reinforcement given in Figures A3.21 to A3.24.
- (4) The SCFs in the figures of this Appendix may also be used for fatigue assessments of the welds. Stresses in the plate normal to the weld σ_n and shear stresses parallel to the weld $\tau_{\parallel p}$, in formula (3.4) of 3.2.5, Chapter 3 of the Guidelines may be derived from the stresses in the plate and corresponding SCF. The total stress range, S, from formula (3.4) is then used together with the W curve to calculate the fatigue damage.

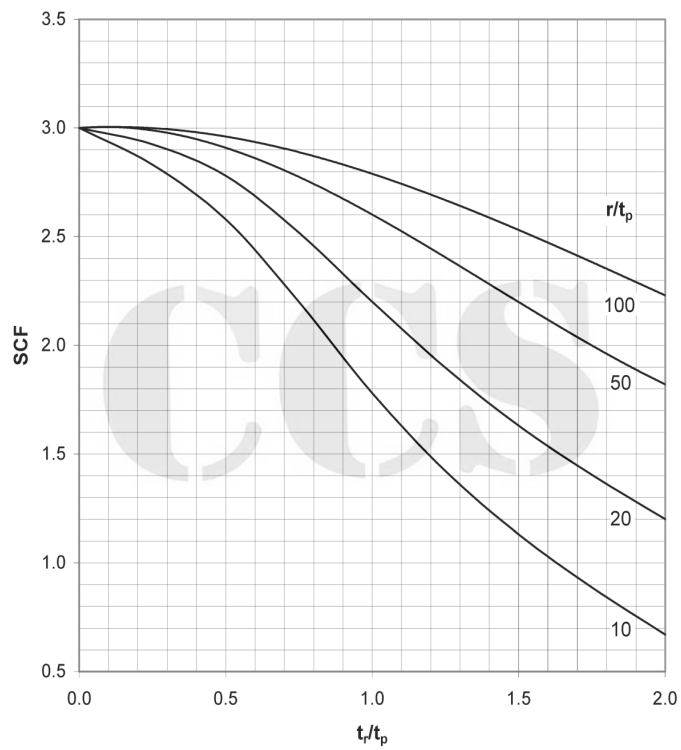
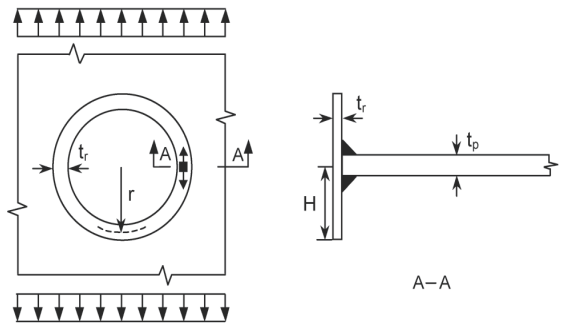


Figure A3.1 SCF at hole with inserted tubular. Stress at outer surface of tubular, parallel with weld. $H/t_r = 2$

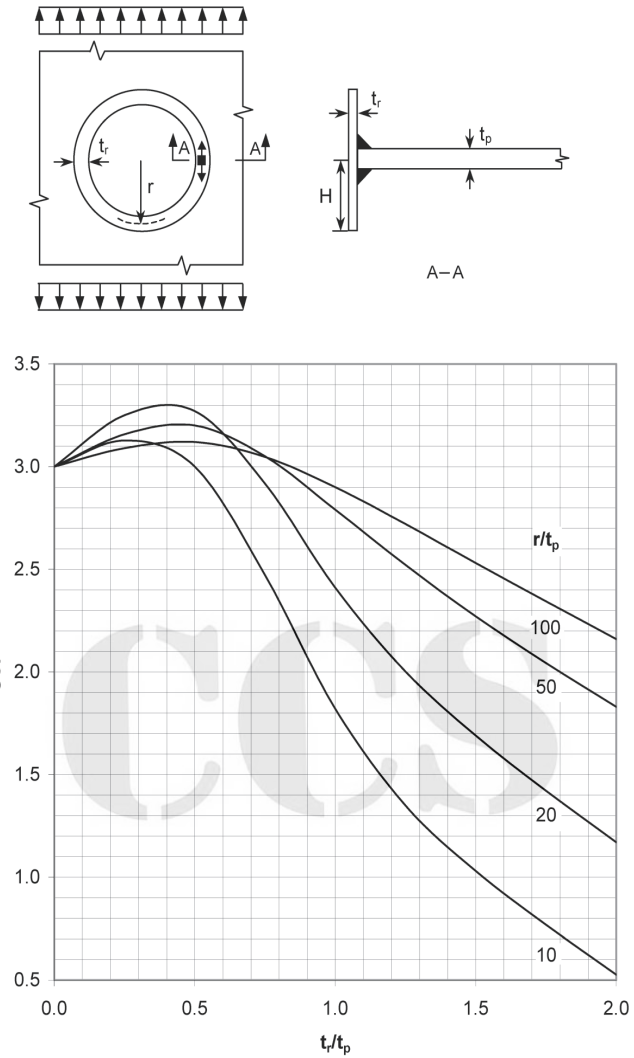


Figure A3.2 SCF at hole with inserted tubular. Stress at outer surface of tubular, parallel with weld. $H/t_r = 5$

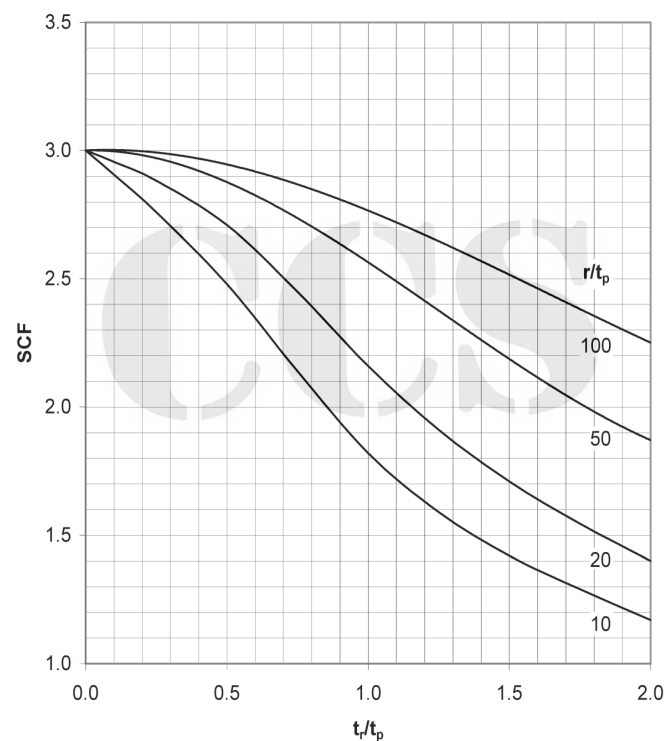
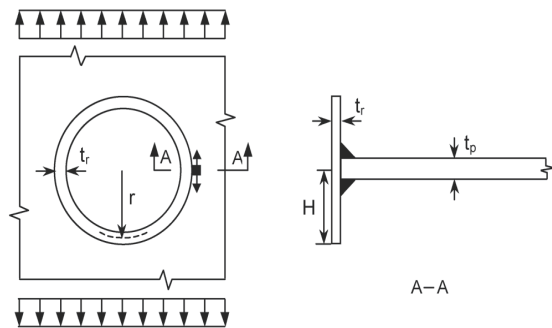


Figure A3.3 SCF at hole with inserted tubular. Stress in plate, parallel with weld. $H/t_r = 2$

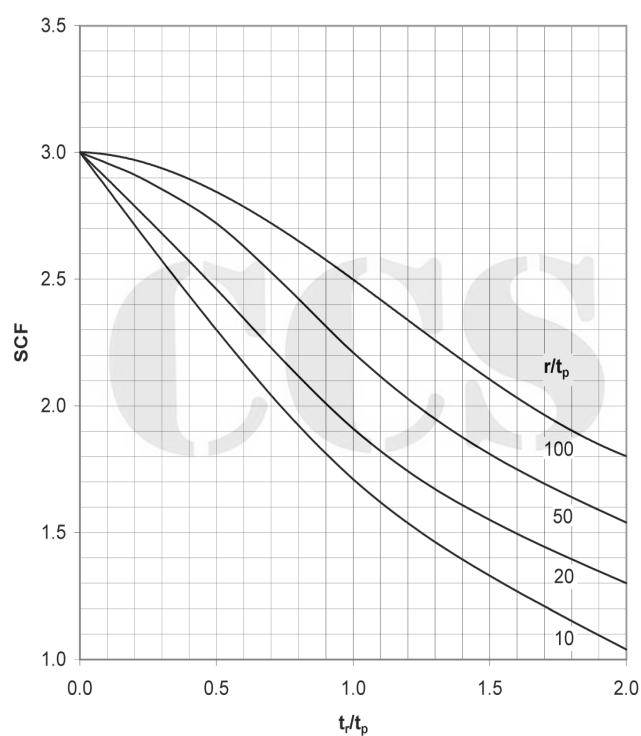
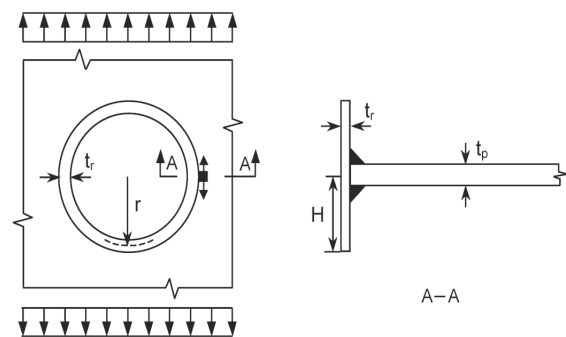


Figure A3.4 SCF at hole with inserted tubular. Stress in plate, parallel with weld. $H/t_r=5$

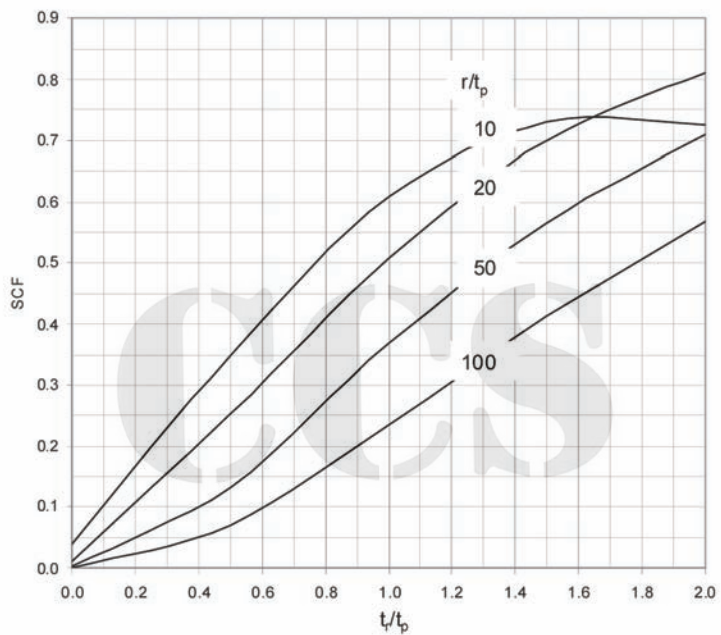
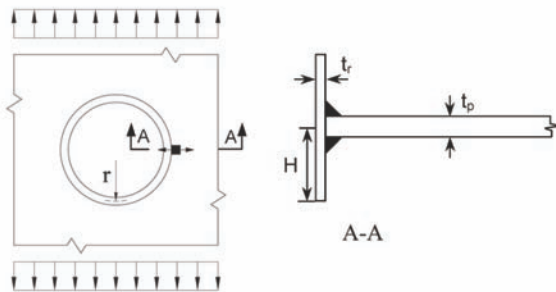


Figure A3.5 SCF at hole with inserted tubular. Stress in plate normal to the weld. $H/t_r=5$

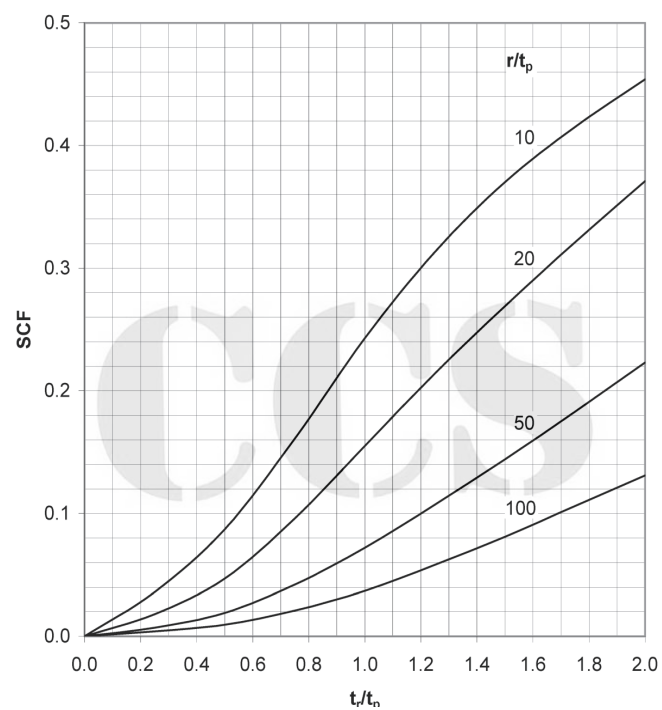
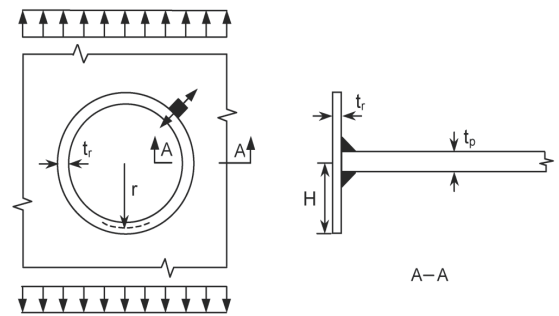


Figure A3.6 SCF at hole with inserted tubular. Stress in plate normal to the weld. $H/t_r=2$

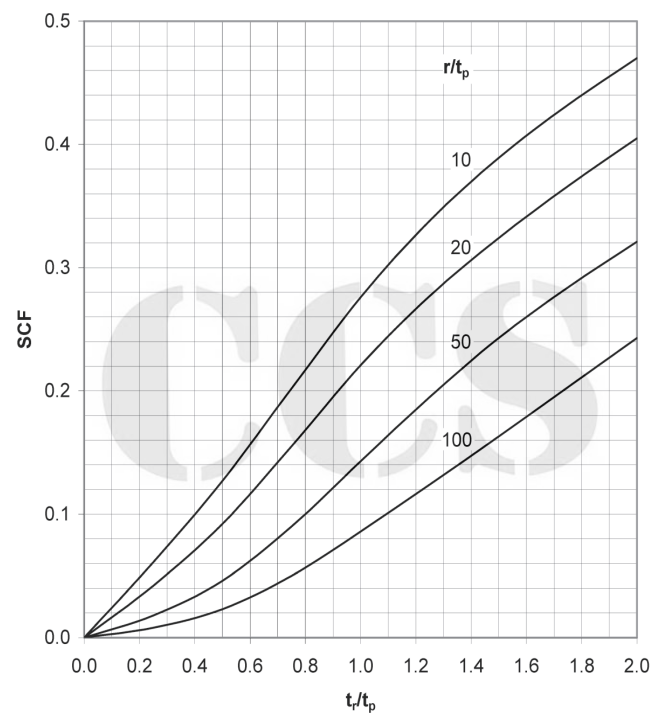
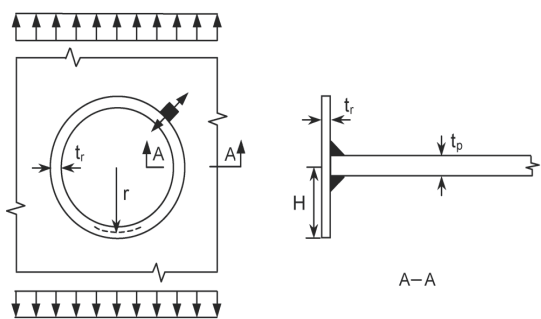


Figure A3.7 SCF at hole with inserted tubular. Stress in plate normal to the weld. $H/t_r=5$

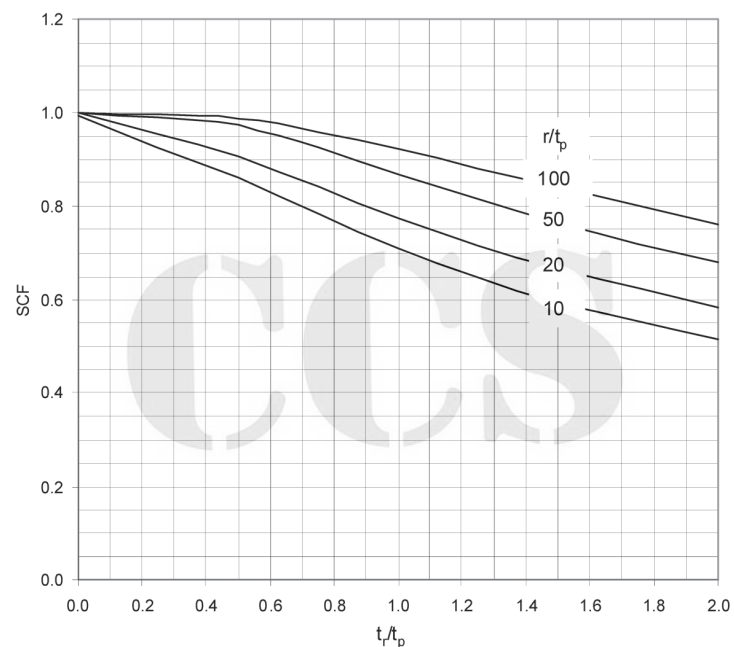
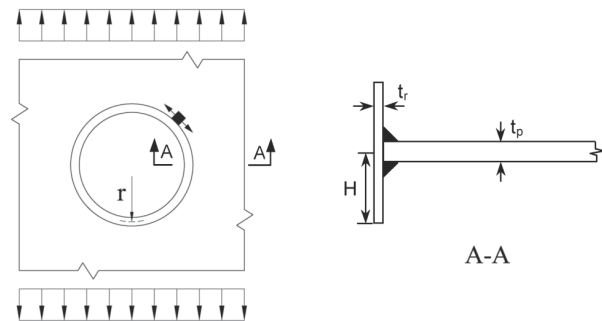
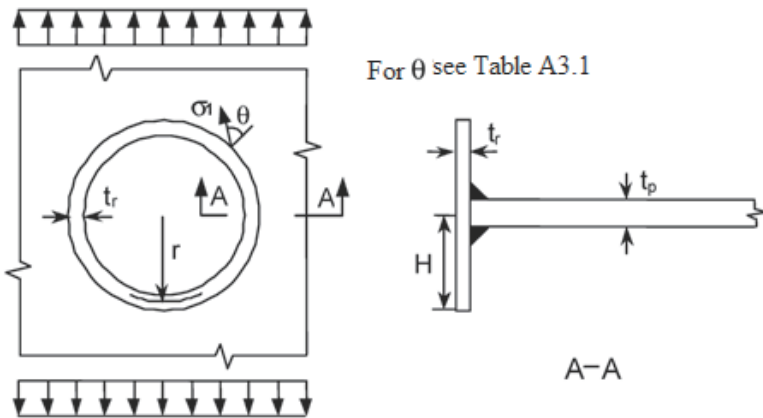


Figure A3.8 SCF at hole with inserted tubular. Stress in plate parallel with weld. $H/t_r=5$



$\theta = \text{angle to principal stress } (H/t_r=2)$

Table A3.1

t_r/t_p	$r/t_p=10$	$r/t_p=20$	$r/t_p=50$	$r/t_p=100$
0.0	90	90	90	90
0.5	72	80	86	88
1.0	56	63	75	82
1.5	50	54	64	73
2.0	46	50	57	66

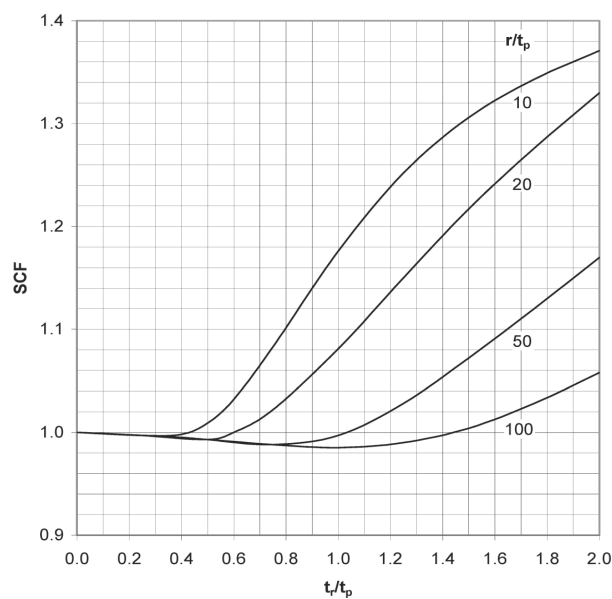
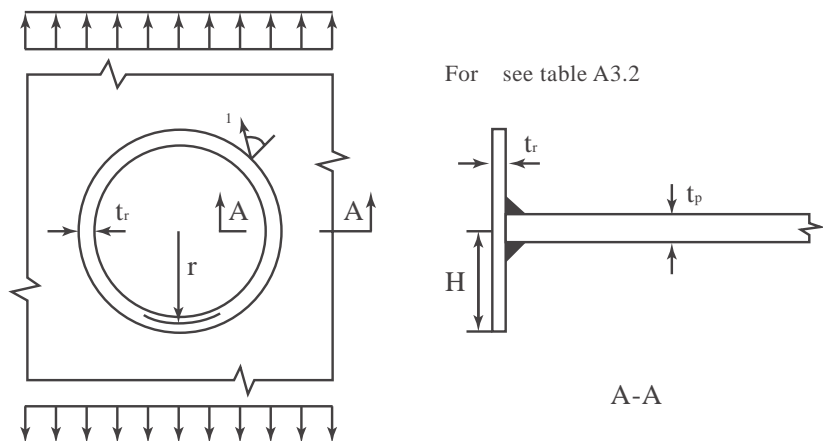


Figure A3.9 SCF at hole with inserted tubular. Principal stress in plate. $H/t_r = 2$



$\theta = \text{angle to principal stress } (H/t_r=5)$

Table A3.2

t_r/t_p	$r/t_p=10$	$r/t_p=20$	$r/t_p=50$	$r/t_p=100$
0.0	90	90	90	90
0.5	66	72	80	85
1.0	54	58	65	72
1.5	49	52	56	62
2.0	46	48	52	56

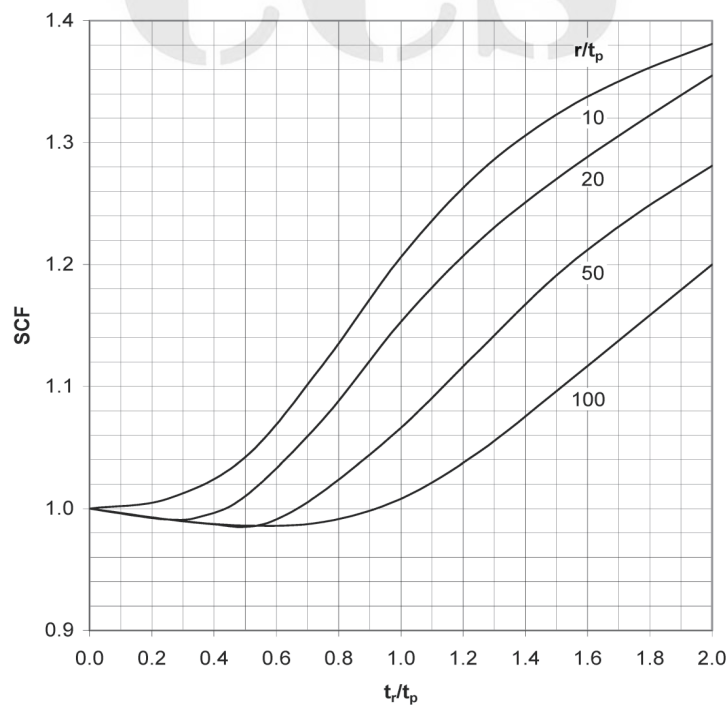


Figure A3.10 SCF at hole with inserted tubular. Principal stress in plate. $H/t_r = 5$

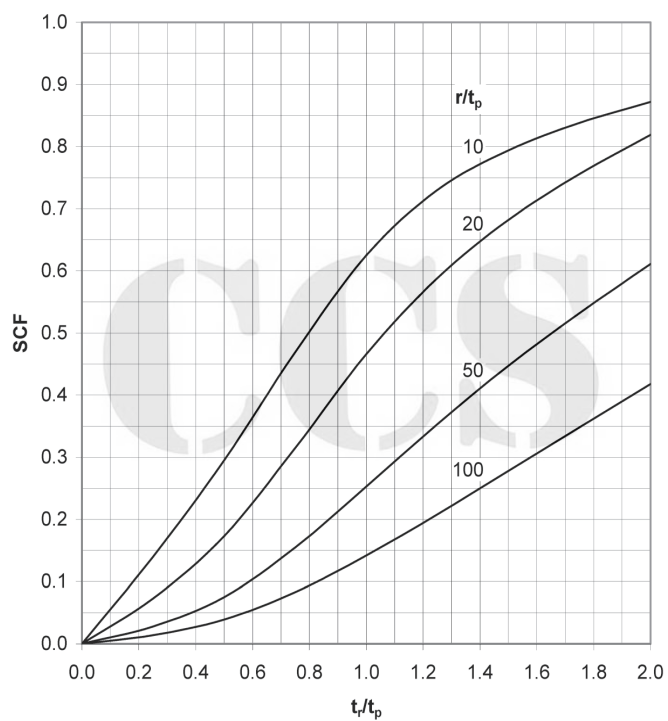
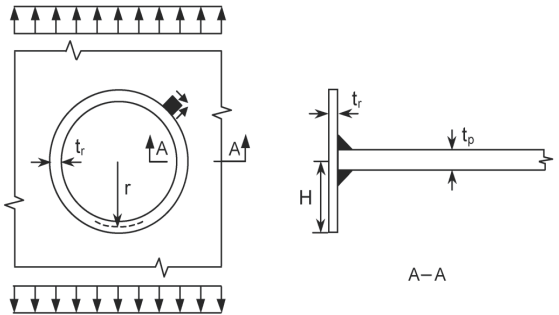


Figure A3.11 SCF at hole with inserted tubular. Shear stress in plate. $H/t_r = 2$

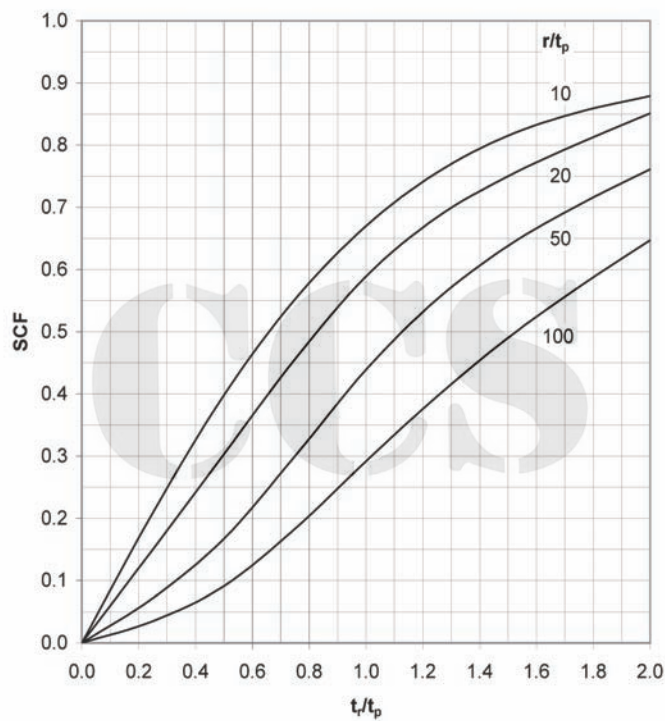
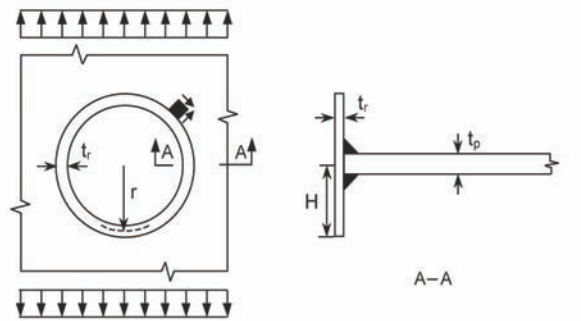


Figure A3.12 SCF at hole with inserted tubular. Shear stress in plate. $H/t_r = 5$

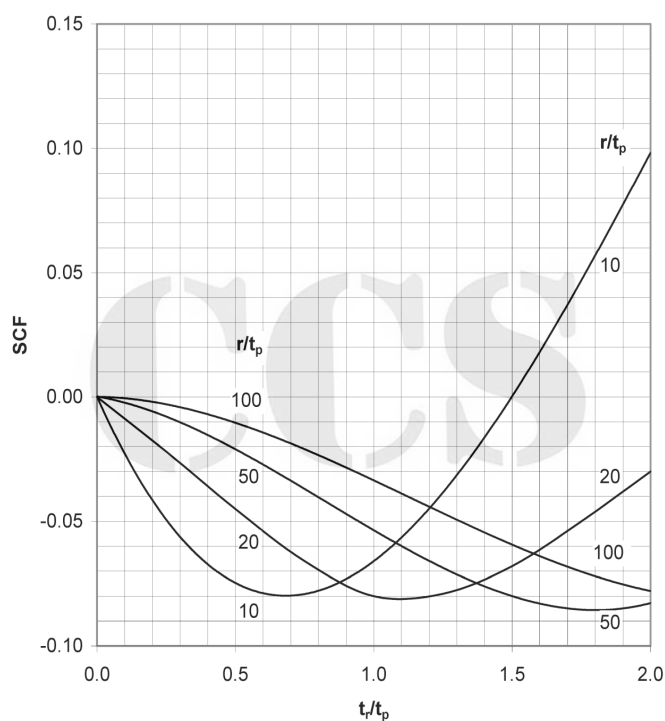
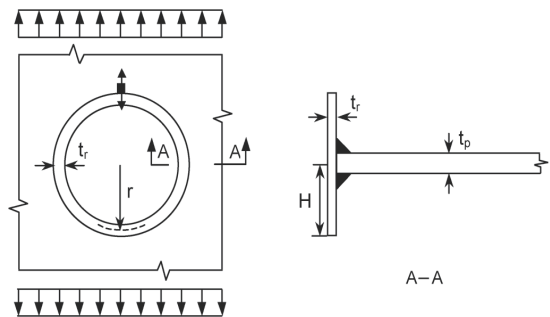


Figure A3.13 SCF at hole with inserted tubular. Stress in plate, normal to weld. $H/t_r = 2$

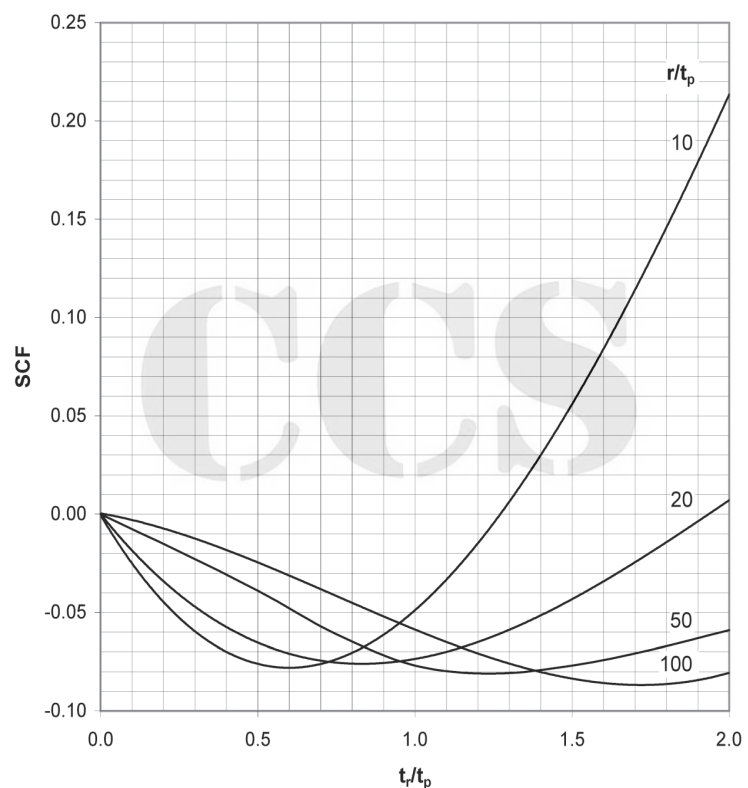
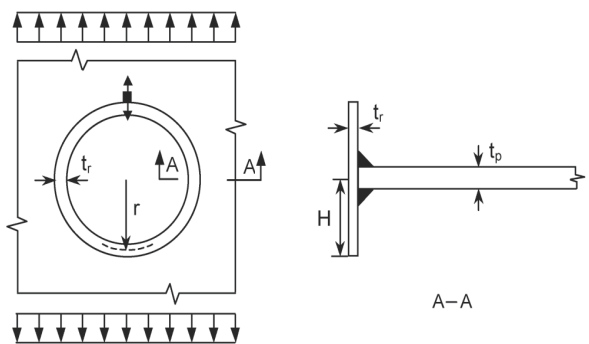


Figure A3.14 SCF at hole with inserted tubular. Stress in plate, normal to weld. $H/t_r = 5$

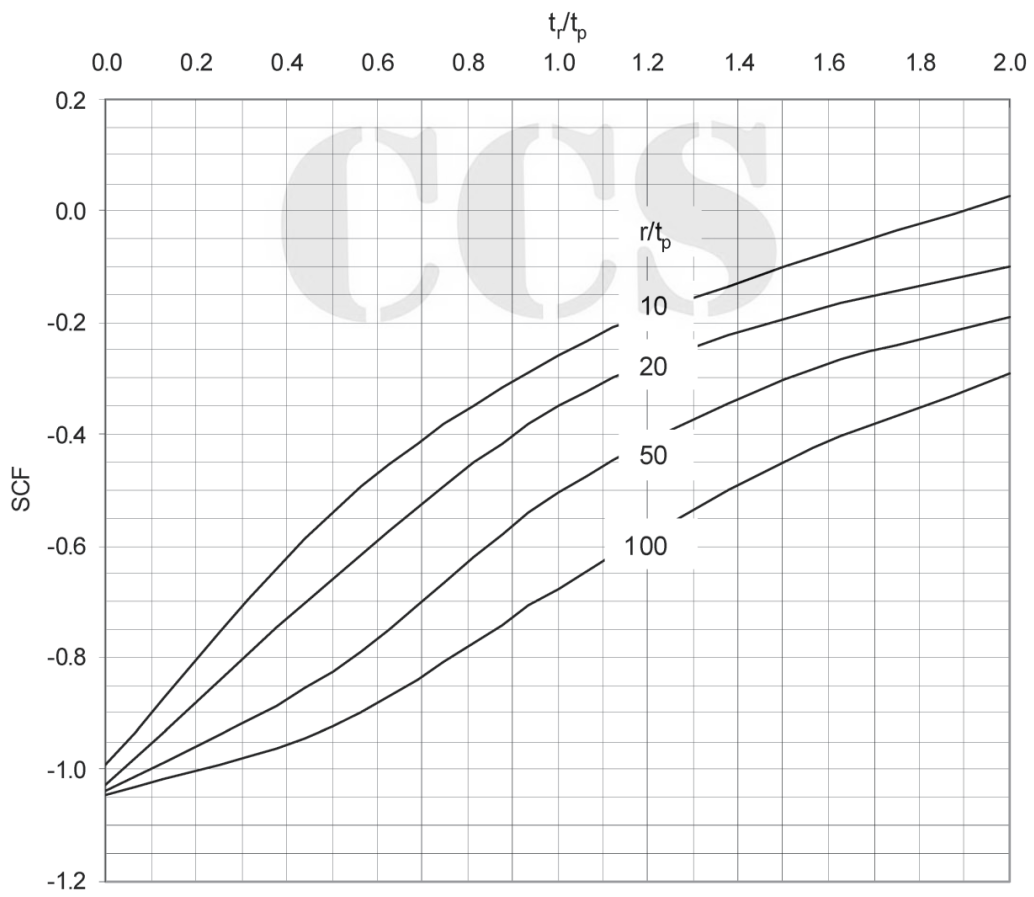
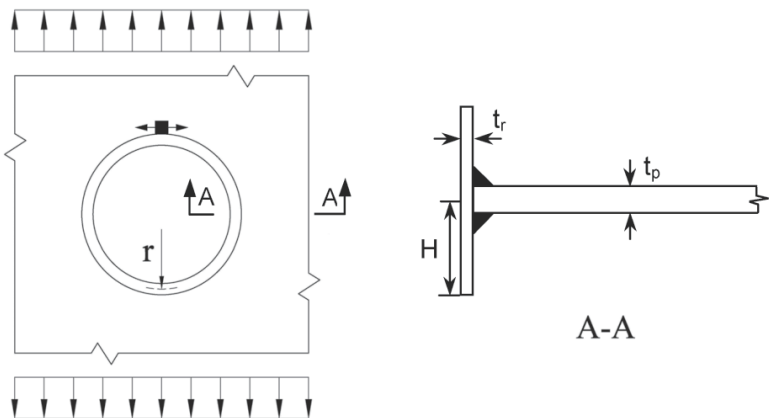


Figure A3.15 SCF at hole with inserted tubular. Stress in plate, parallel with weld. $H/t_r = 5$

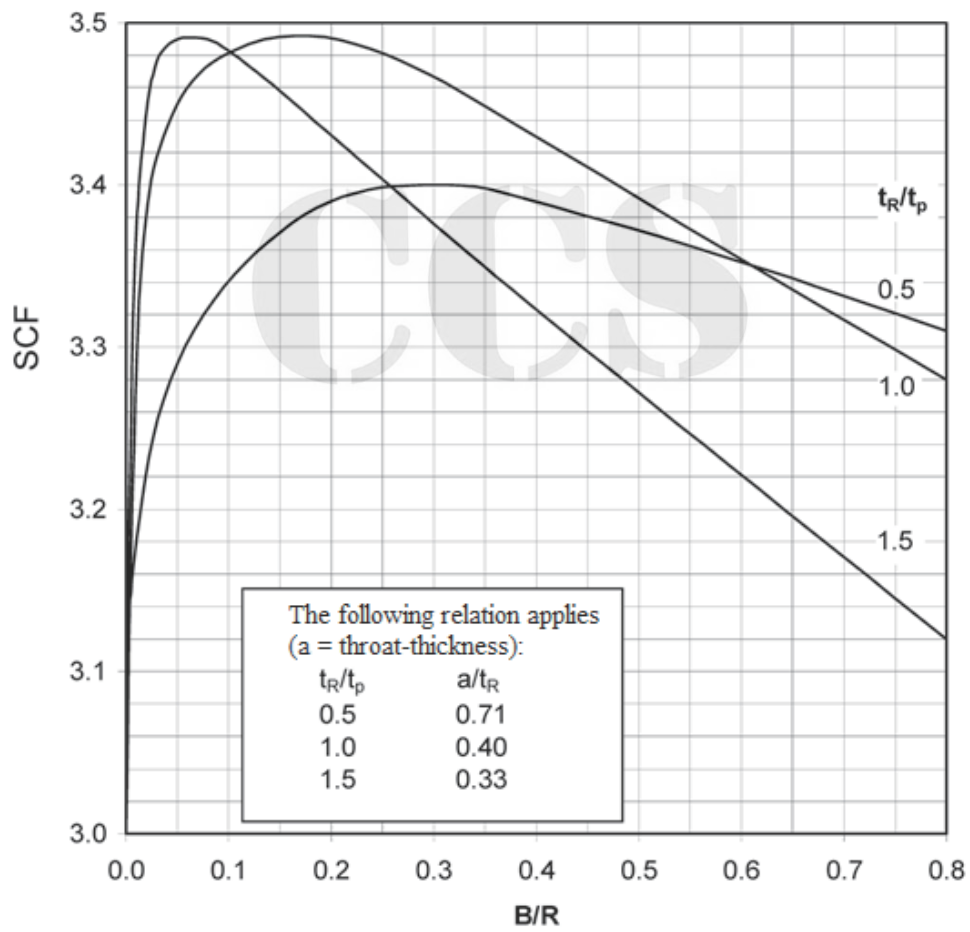
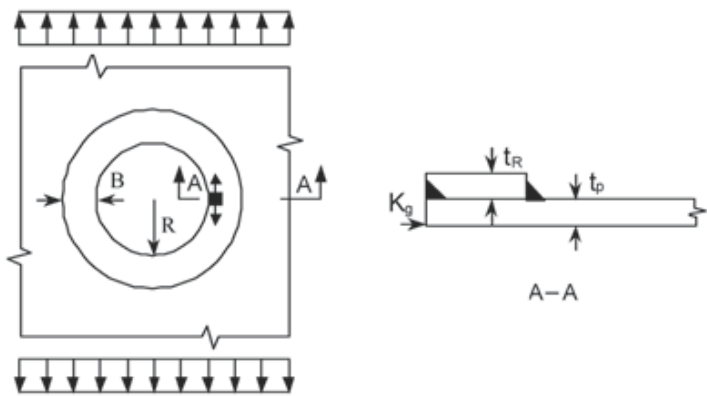


Figure A3.16 SCF at hole with ring reinforcement. Max stress concentration

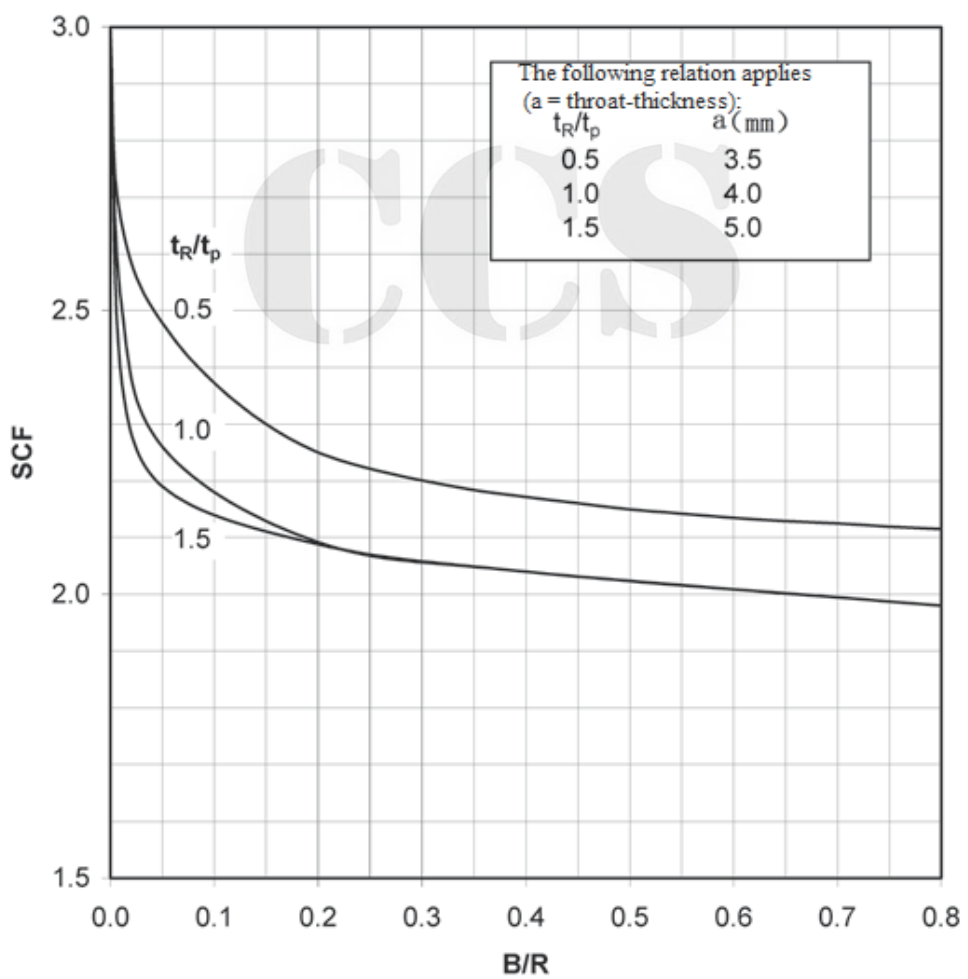
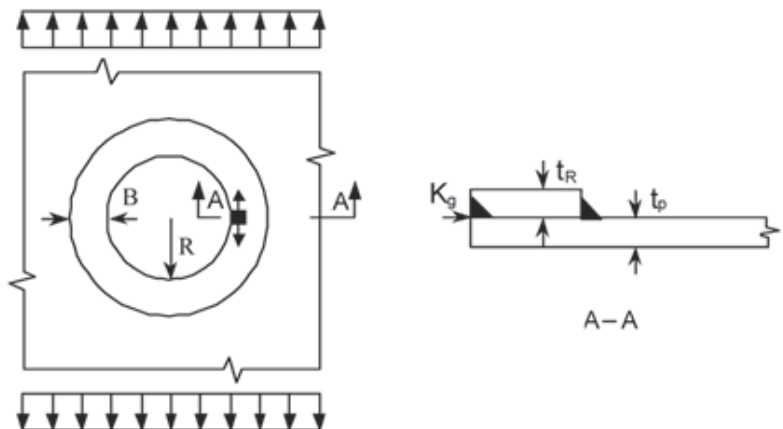


Figure A3.17 SCF at hole with ring reinforcement. Stress at inner edge of ring

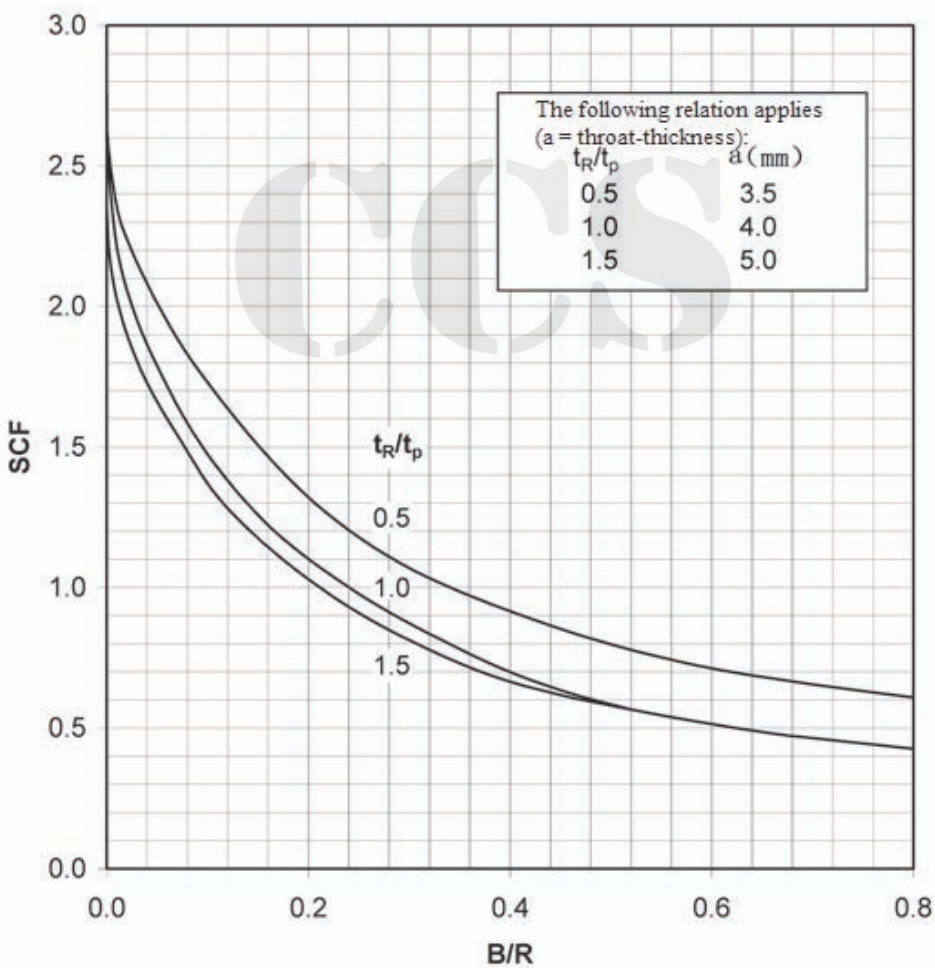
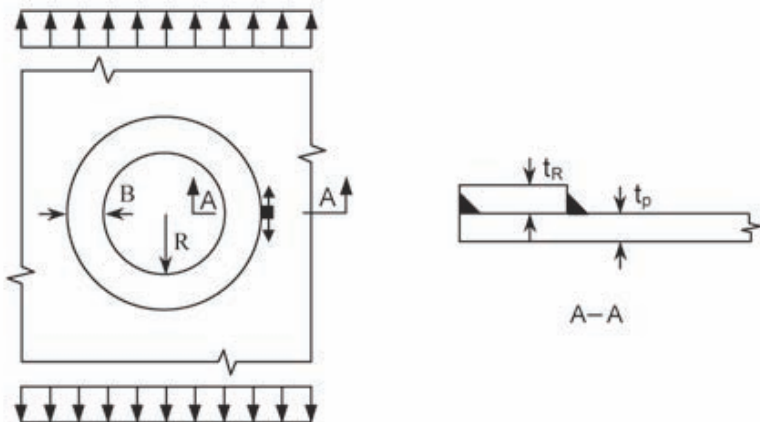


Figure A3.18 SCF at hole with ring reinforcement. Stress in plate, parallel with weld

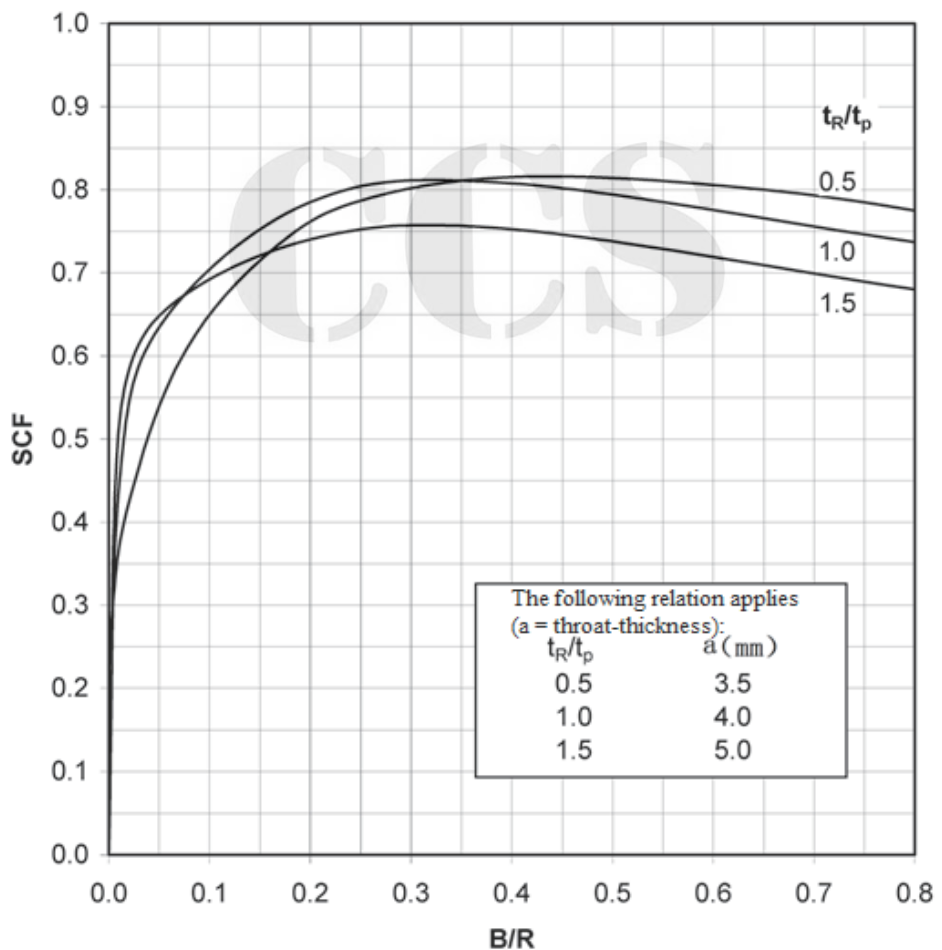
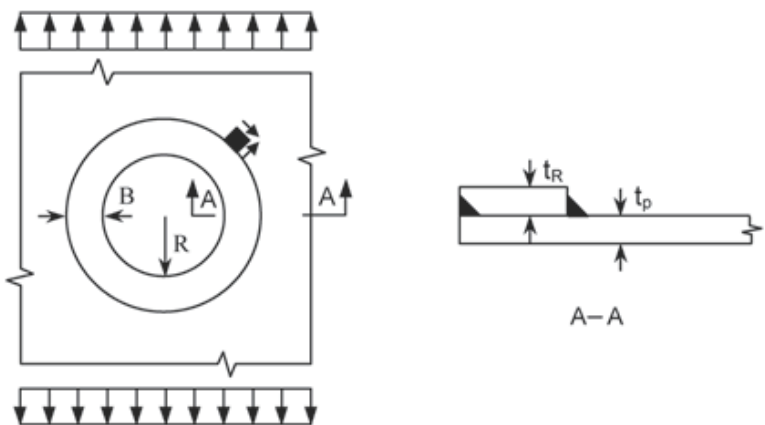


Figure A3.19 SCF at hole with ring reinforcement. Shear stress in plate at weld toe

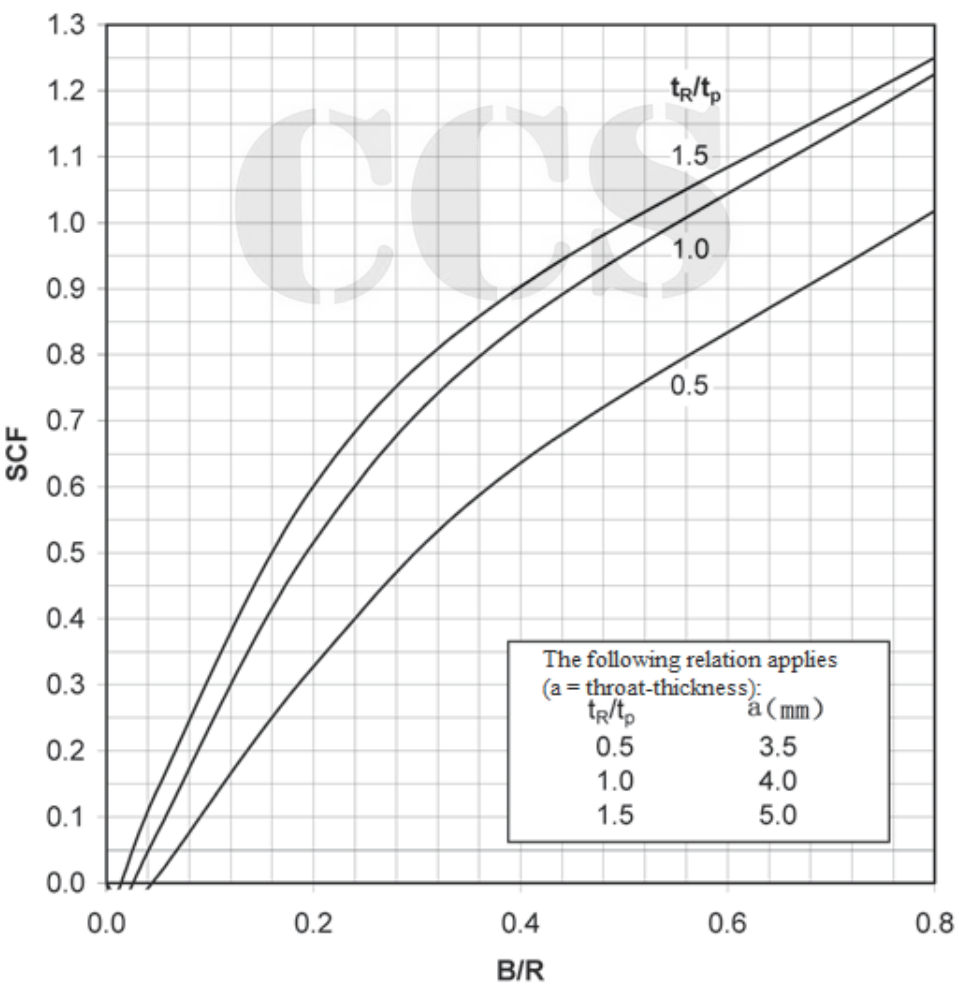
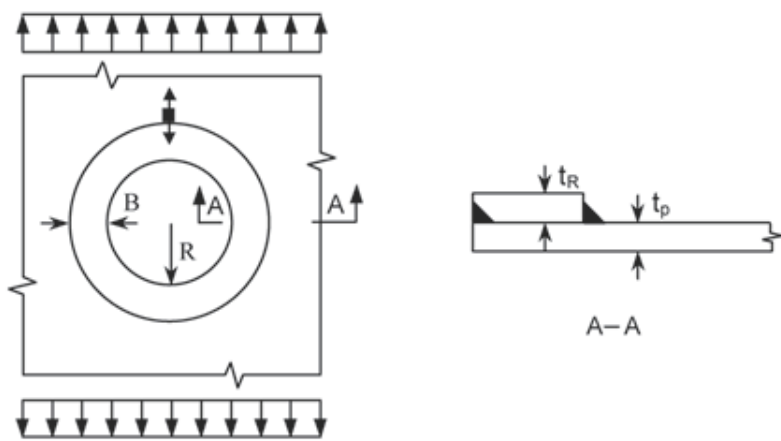


Figure A3.20 SCF at hole with ring reinforcement. Stress in plate, normal to weld

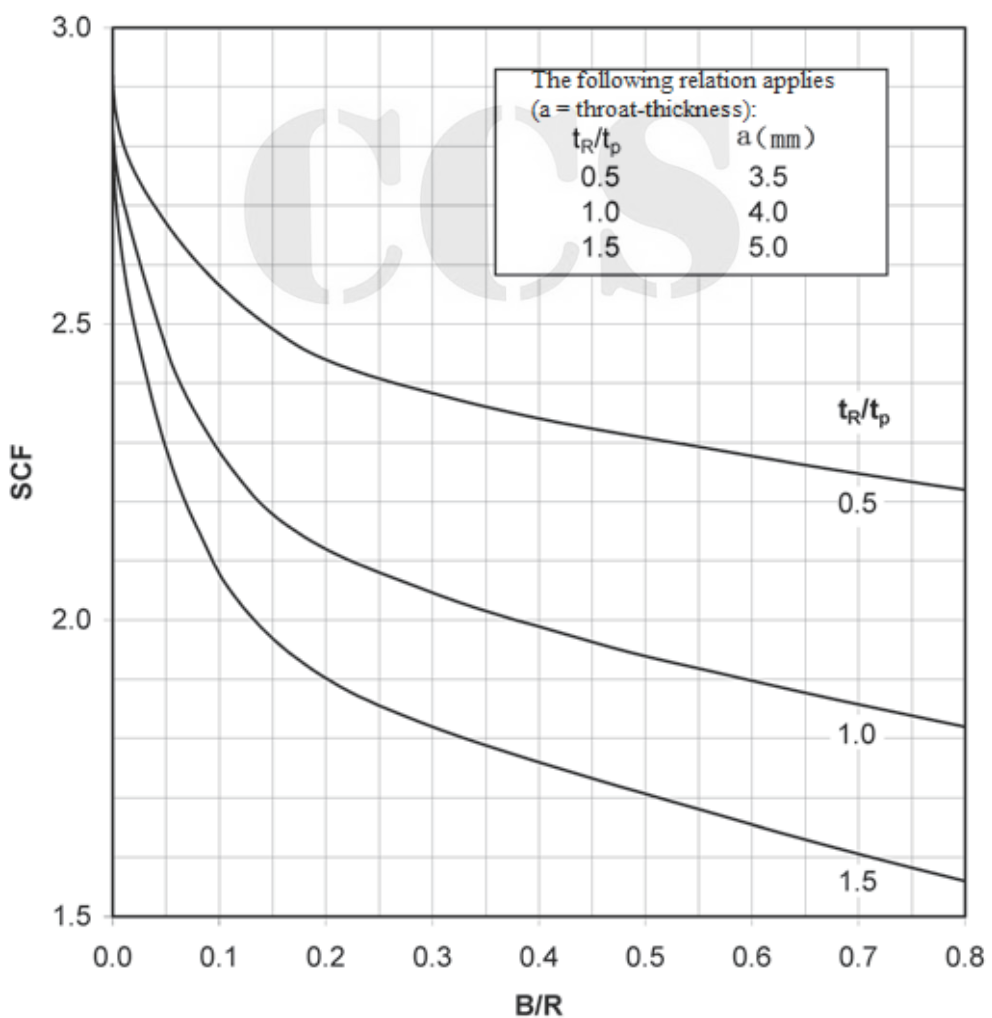
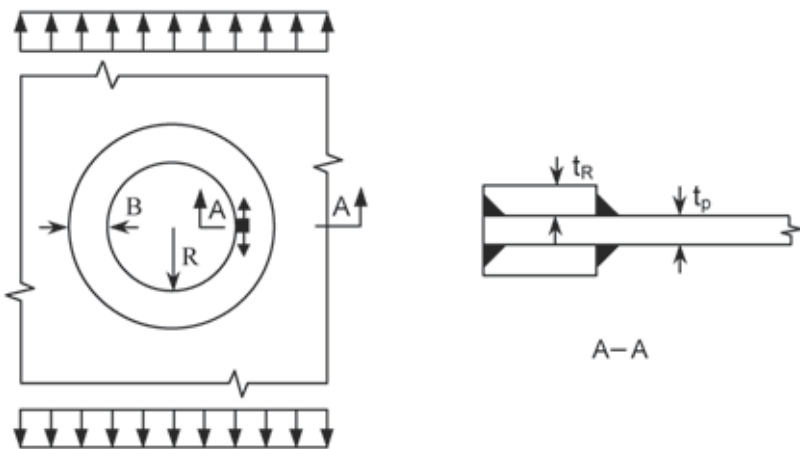


Figure A3.21 SCF at hole with double ring reinforcement. Stress at inner edge of ring

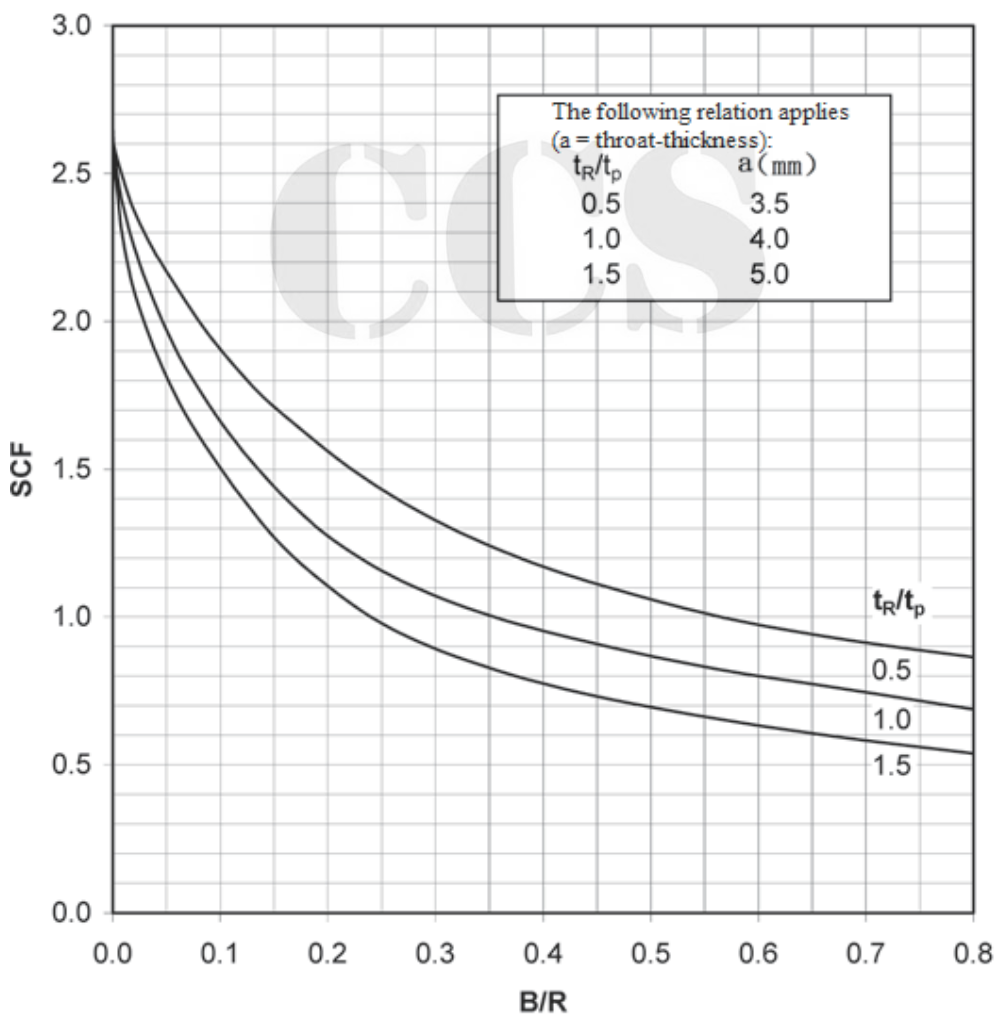
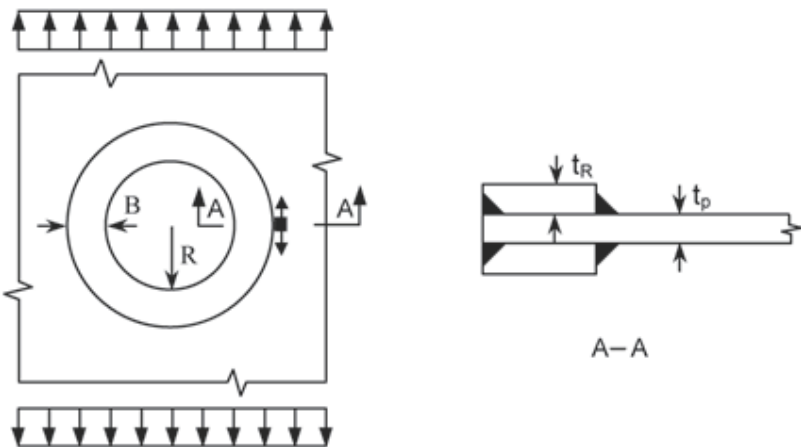


Figure A3.22 SCF at hole with double ring reinforcement. Stress in plate, parallel with weld

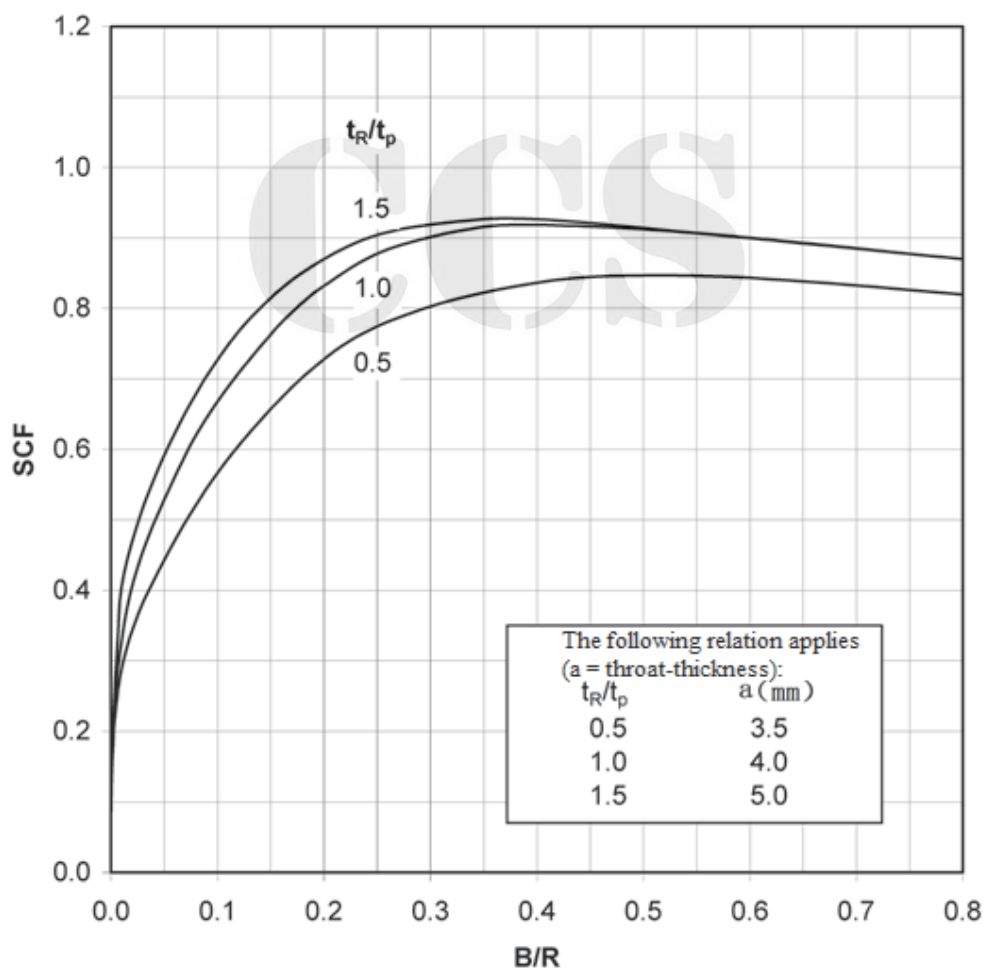
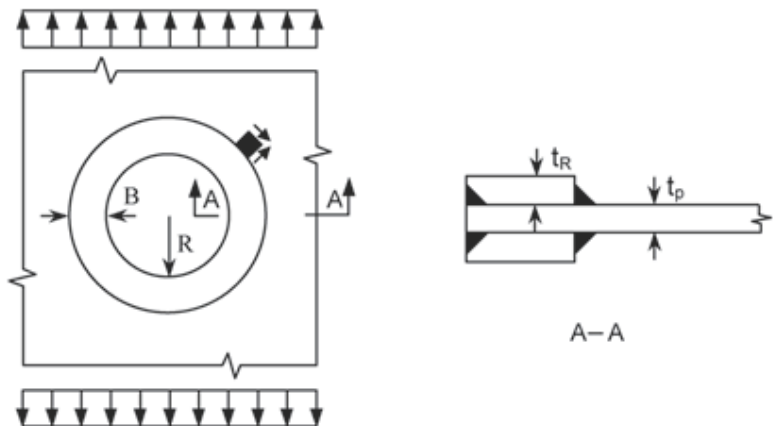


Figure A3.23 SCF at hole with double ring reinforcement. Shear stress in plate at weld toe

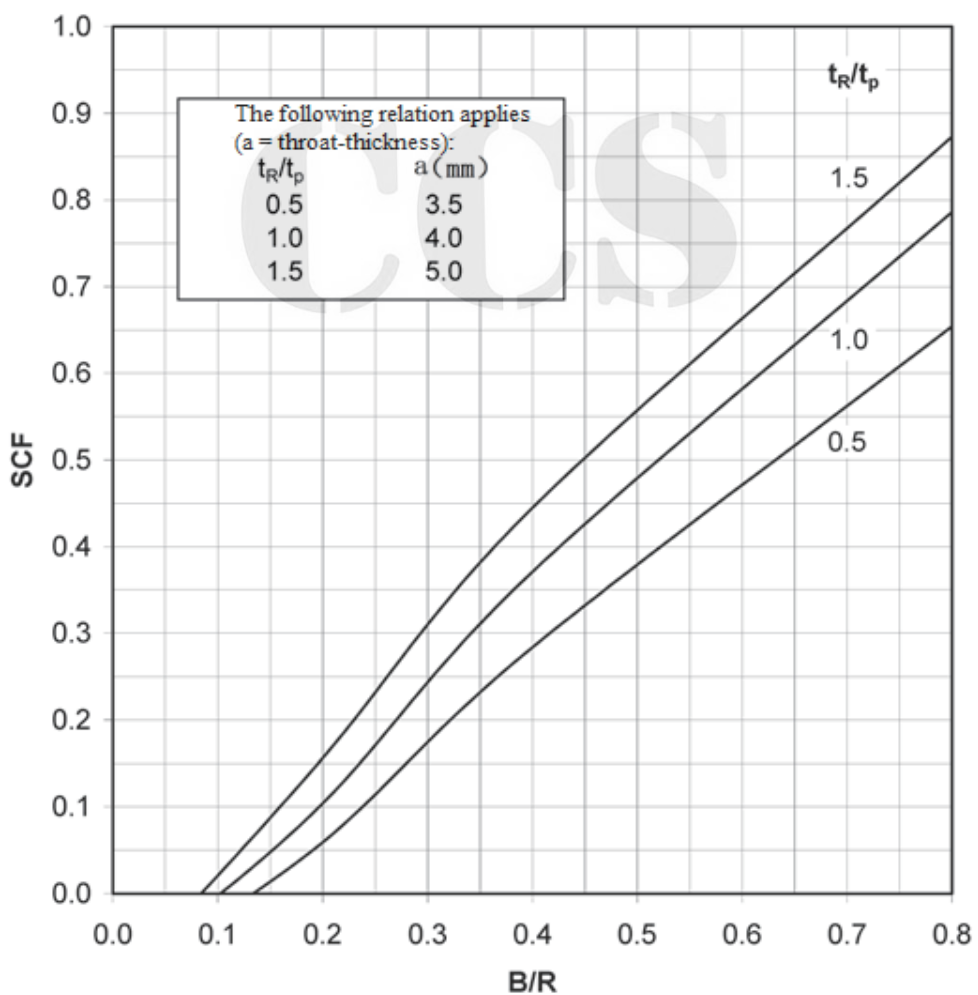
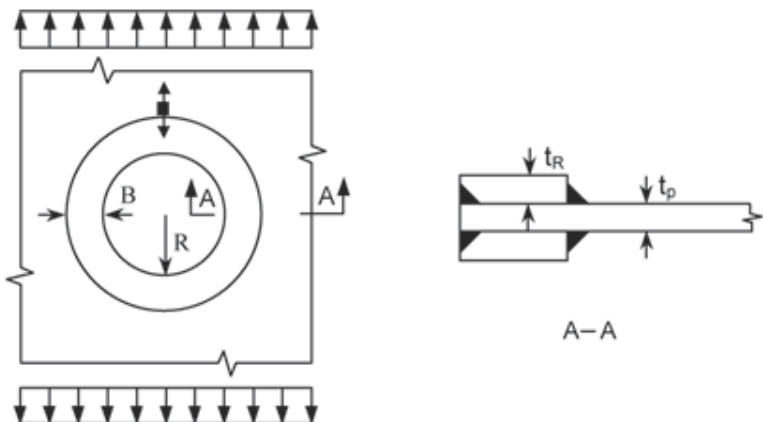


Figure A3.24 SCF at hole with double ring reinforcement. Stress in plate, normal to weld

References:

- [1] HEALY, B.E. and BUITRAGO, J. Extrapolation procedures for determining SCFs in mid-surface tubular joint models. 6th Intl. Symp. on Tubular Structures, Monash University, Melbourne, Australia, 1994.
- [2] EFTHYMIOU, M. Development of SCF formulae and generalised influence functions for use in fatigue analysis. Recent Developments in Tubular Joint Technology, Proceedings of Offshore Tubular Joints Conference- OTJ'88, October 1988, London, plus updates.
- [3] SMEDLEY, P.A. and FISHER, P. Stress concentration factors for simple tubular joints. Offshore and Polar Engineering Conf., ISOPE-1, Edinburgh, UK, 1991.
- [4] POTVIN, A.B. et al. Stress concentration in tubular joints. SPE Journal, August 1977.
- [5] WORDSWORTH, A.C. Stress concentration factors at K and KT joints. Fatigue in Offshore Structural Steels, ICE, London, 1981.
- [6] MARSHALL, P.W. and LUYTIES, W.H. Allowable stress for fatigue design. Proc. 3rd Intl. Conf on the Behaviour of Offshore Structures, BOSS 1982, Paper S1, 2, MIT Cambridge, Massachusetts, 1982, pp. 3-25.
- [7] Edison Welding Institute, Stress Concentration Factors for Tubular Connections. EWI Project No. J7266, March 1995.
- [8] Lloyd's Register of Shipping, Stress concentration factors for simple tubular joints. Report OTH 354, Health and Safety Executive, 1997.
- [9] KINRA, R.K. and MARSHALL, P.W. Fatigue Analysis of the Cognac Platform. J. Petroleum Technology, Paper SPE 8600, March 1980.
- [10] ISO 19902, Petroleum and natural gas industries —Fixed steel offshore structures, 2007.
- [11] MARSHALL, P.W., BUCKNELL, J. and MOHR, W.C. Background to New API fatigue provisions. Proc. 38th Offshore Technology Conf. Paper OTC 17295, Houston, May 2005.
- [12] API, Recommended Practice for Planning, Designing and Constructing Fixed Offshore Platforms—Working Stress Design (with ERRATA AND SUPPLEMENT 3, OCTOBER 2007).
- [13] SMEDLEY, P.A. and FISHER, P. A Review of Stress Concentration Factors for Complex Tubular Joints, Integrity of Offshore Structures Conference, Glasgow, 1990.
- [14] SMEDLEY, P.A. and FISHER, P. Stress Concentration Factors for Ring stiffened Tubular Joints, Fourth International Symposium on Tubular Structures, Delft, 1991.
- [15] Niemi E. Recommendations concerning stress determination for fatigue analysis of welded components. Cambridge: Abington Publishers, 1995.
- [16] “Comparison of fatigue provisions in codes and standards”, Prepared by Bomel Limited for the Health and Safety Executive, (OFFSHORE TECHNOLOGY REPORT 2001/083).

- [17] "Fatigue Life Implications for Design and Inspection for Single Sided Welds at Tubular Joints", Prepared by MSL Engineering Limited MSL House, OFFSHORE TECHNOLOGY REPORT (OTO 1999/022).
- [18] "Fatigue Design Curves for Welded Joints in Air & Sea Water Under Variable Amplitude Loading", Prepared by Failure Control Engineering & Materials Consultants, OFFSHORE TECHNOLOGY REPORT (OTO 1999/058).
- [19] MARSHALL, P.W., BUCKNELL, J. and MOHR, W.C. Background to New API fatigue provisions. Proc. 38th Offshore Technology Conf. Paper OTC 17295, Houston, May 2005.
- [20] "Background to New Fatigue Guidance for Steel Joints and Connections in Offshore Structures", OFFSHORE TECHNOLOGY REPORT OTH 1992/390.
- [21] "Stress Concentration factors for simple tubular joints-Assessment of existing and development of new parametric formulae", prepared by Lloyd's Register of Shipping (OTH 354), 1997.
- [22] Kang SW, Kim WS, Paik YM. Fatigue strength of fillet welded steel structure under out-of-plane bending load, Int. J. Korean Welding Soc.,6; pp33-39, 2002.
- [23] Kim WS, Lotsberg I. Fatigue test data for welded connections in ship-shaped structures, J. of Offshore Mechanics and Arctic Engineering 127; pp359-365, 2005.
- [24] Maddox SJ. Recommended hot-spot stress design S-N curves for fatigue assessment of FPSOs, Proc. of the 11th Int. Offshore and Polar Engineering Conference 2001.
- [25] Lotsberg I., Background for revision of DNV RP C203 fatigue analysis of offshore steel structures, the 24th International Conference on Offshore Mechanics and Arctic Engineering (OMAE2005-67549).
- [26] Dong P.A structural stress definition and numerical implementation for fatigue analyses. International Journal of Fatigue; 23, pp865-876, 2001.
- [27] Fricke W. Petershagen H. Detail Design of Welded Ship Structures based on Hot Spot Stresses. PRADS, Newcastle, 1992.
- [28] Fricke W. Recommended Hot Spot Analysis Procedure for Structural Details of FPSOs and Ships Based on Round-Robin FE Analyses. Proceedings of the Eleventh International Offshore and Polar Engineering Conference 2001; June17-22, Stavanger, Norway.
- [29] Hobbacher A. Fatigue design of welded joints and components. IIW Doc XIII-1539-96/XV-845-96, International Institute of Welding, 1996.
- [30] Bergan PG, Lotsberg I, Fricke W, Francois M, and Pisarski H. (2002). Overview of Phase II of the FPSO Fatigue Capacity JIP. OMAE2002-28538, Oslo.
- [31] Choo YS, Zahidul Hasan M. Hot Spot Stress Evaluation for Selected Connection Details. Proceedings of the OMAE Specialty Symposium on Integrity of Floating Production, Storage and Offloading (FPSO) Systems, August 30-September 2, Houston, 2004.
- [32] Niemi E. Recommendations concerning stress determination for fatigue analysis of welded components. IIW Doc. XIII-1458-92/XV-797-92, International Institute of Welding, 1992.

- [33] Niemi E. Stress determination for fatigue analysis of welded components. IIW Doc. IIS/IIW-1221-93, International Institute of Welding, 1993.
- [34] Niemi E. Recommendations concerning stress determination for fatigue analysis of welded components. Cambridge: Abington Publishers, 1995.
- [35] Niemi E, Marquis G. Introduction to the structural stress approach to fatigue analysis of plate structures. Proceedings of the IIW Fatigue Seminar, Tokyo Institute of Technology 2002, Tokyo. 73-90.
- [36] Niemi E, Fricke W, Maddox SJ. Fatigue Analysis of Welded Components, Designer's guide to the structural hot-spot stress approach (IIW-1430-00), Cambridge: Woodhead Publishing Limited, 2000.
- [37] Lotsberg I., Assessment of fatigue capacity in the new bulk carrier and tanker rules, *Marine Structures* 19, pp83–96, 2006.
- [38] Lotsberg I., Sigurdsson G., Hot spot stress S-N curve for fatigue analysis of plated structures, *Journal of Offshore Mechanics and Arctic Engineering*, Vol. 128, pp330-336, 2006.
- [39] Xiaozhi Wang, Haihong Sun, Zhan Cheng, Methods for fatigue assessment of critical ship details, 23rd International Conference on Offshore Mechanics and Arctic Engineering, Vancouver, Canada, OMAE 2004 – 51630.
- [40] Xiaozhi Wang, Zhan Cheng, Paul H. Wirsching, Haihong Sun, Fatigue design factors and safety level implied in fatigue design of offshore structures, 24th International Conference on Offshore Mechanics and Arctic Engineering, June 12-17, 2005, Halkidiki, Greece, OMAE2005-67488.
- [41] Myung Hyun Kim, Sung Won Kang, Jeong Hwan Kim, Kwang Seok Kim, Joong Kyoo Kang, Joo Ho Heo, An experimental study on the fatigue strength assessment of longi-web connections in ship structures using structural stress, *International Journal of Fatigue* 32, pp318–329, 2010.
- [42] Wolfgang Fricke, Adrian Kahl, Comparison of different structural stress approaches for fatigue assessment of welded ship structures, *Marine Structures* 18, pp 473–488, 2005.
- [43] Fricke W, Doerk O, Grunitz L. Fatigue strength investigation and assessment of fillet welds around stiffener and bracket toes. Proceedings of the OMAE Specialty Conference on FPSO systems, OMAE-FPSO'04-0010, Houston, TX, ASME International Petroleum Technical Institute, 2004.
- [44] Wolfgang Fricke, Hans Paetzold, Full-scale fatigue tests of ship structures to validate the S-N approaches for fatigue strength assessment, *Marine Structures* 23, pp115–130, 2010.
- [45] Fricke W. Fatigue of welded joints: state of development. *Marine Structures* 16, pp185–200, 2003.
- [46] Fricke W. Guideline for the fatigue assessment by notch stress analysis for welded structures. International Institute of Welding; 2008. IIW-Doc. XIII-2240r1-08/XV-1289r1-08.
- [47] Fricke W, Kahl A. Local stress analysis and fatigue assessment of bracket toes based on measured weld profile. International Institute of Welding; 2007. IIW-doc. XIII-2166-07/XV-1253-07.
- [48] IACS Common Structural Rules for Oil Tankers, 2012.

- [49] ABS Guide for the Fatigue Assessment of Offshore Structures. American Bureau of Shipping, Houston, 2012.
- [50] ABS Commentary On The Guide For The Fatigue Assessment Of Offshore Structures American Bureau of Shipping, Houston, 2012.
- [51] Guidance Notes On Spectral-Based Fatigue Analysis For Floating Offshore Structures, American Bureau of Shipping, Houston, 2012.
- [52] DNV Classification Note No.30.7. Fatigue Assessment of Ship Structures. Det Norske Veritas, Oslo, 2003.
- [53] DNV-RP-C203 Fatigue Strength Analysis of Offshore Steel Structures. Det Norske Veritas, Oslo, 2011.
- [54] ISSC In: Proceedings of the 15th international ship and offshore structures congress. San Diego: August 11-15, 2003, San Diego, USA.
- [55] ISSC. In: Proceedings of the 16th international ship and offshore structures congress, 20-25 August 2006, Southampton, UK.
- [56] ISSC. In: Proceedings of the 18th international ship and offshore structures congress, 09-13 Sep. 2012, Rostock, Germany.
- [57] A. Almar-Næss. Fatigue Handbook (Offshore Steel Structure). Tapir. 1985.
- [58] S. Suresh 著. 材料的疲劳. 国防工业出版社. 第二版, 1999.
- [59] 郑学祥. 船舶及海洋工程结构的断裂与疲劳分析. 海洋出版社, 1988.
- [60] Miner, M.A. Cumulative damage in fatigue. Jourinal of Applied Mechanics 67, pp159-164 (1945)
- [61] 方华灿, 海洋石油钢结构的疲劳寿命:模糊概率断裂与损伤力学的应用. 石油大学出版社, 1990.
- [62] 徐 瀚, 疲劳强度. 高等教育出版社, 1988.
- [63] 胡毓仁, 陈伯真. 船舶及海洋工程结构疲劳可靠性分析. 人民交通出版社, 1997.
- [64] Bai Yong, Bai Qiang, "Marine Structural Design" Part 4 chapter 5, Elsevier Science, 2003.
- [65] Walter D. Pilkey, Deborah F. Pilkey, "Peterson's Stress Concentration Factors", Third edition, John Wiley& Sons, Inc. 2008.
- [66] C. R. A. Schneider, S. J. Maddox, Granta Park, Great Abington, Best Practice Guide On Statistical Analysis Of Fatigue Data, International Institute of Welding; IIW-Doc. IIW-XIII-WG1-114 - 03, 2003.
- [67] British Standard, Guide to methods for assessing the acceptability of flaws in metallic structures, BS 7910, 2005.
- [68] Bureau Veritas, Spectral Fatigue Analysis Methodology for Ships and Offshore Units, Guidance Note NI 539, 2008.